VOLUME 34 / NUMBER 2 / 1992

Radiocarbon

An International Journal of Cosmogenic Isotope Research

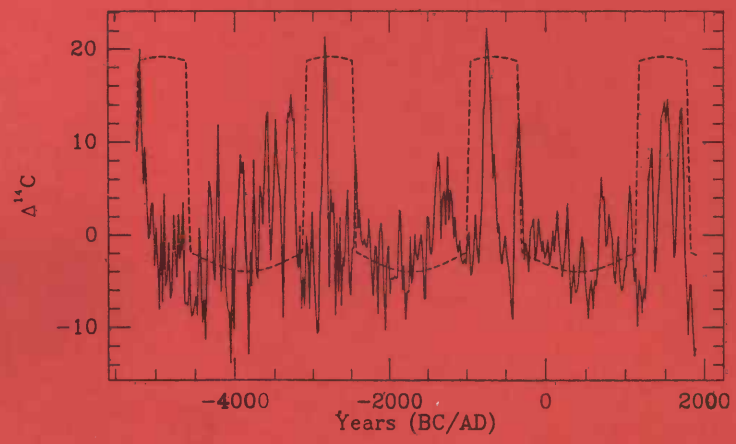

PALEOASTROPHYSICS, PALEOGEOPHYSICS

Proceedings of the Workshop, Paleoastrophysics and Natural Variations of Cosmogenic Isotopes

Edited by Paul E. Damon, Austin Long and Renee S. Kra

Assistant Editor – Frances D. Moskovitz

ent of Geosciences
versity of Arizona
4717 East Ft. Lowell Road
Tucson, Arizona 85712 USA

ISSN: 0033-8222

RADIOCARBON
An International Journal of Cosmogenic Isotope Research

Editor: AUSTIN LONG
Managing Editor: RENEE S. KRA
Assistant Editor: FRANCES D. MOSKOVITZ
Published by
Department of Geosciences
The University of Arizona

Published three times a year at The University of Arizona, Tucson, AZ 85712 USA.

Subscription rate $105.00 (for institutions), $73.50 (for individuals), $36.75 (for students with proper identification). Foreign postage is extra. A complete price list, including Proceedings of International Conferences, appears in the back of this issue.

Back issues and price lists may be obtained from the office of *RADIOCARBON*.

All correspondence and manuscripts should be addressed to the Managing Editor, *RADIOCARBON*, Department of Geosciences, The University of Arizona, 4717 East Ft. Lowell Road, Tucson, AZ 85712 USA. Tel: (602) 881-0857; **Please note our new BITNET address: C14@ARIZVMS**; Fax: (602) 881-0554.

Offprints. The minimum offprint order for each article will be 100 copies without covers. *No offprints will be furnished free of charge unless page charges are paid.* The cost of additional copies will, of course, be greater if the article is accompanied by plates involving unusual expense. Copies will be furnished with a printed cover giving the title, author, volume, page and year, when specially ordered.

Page charges. Each institution sponsoring research reported in a technical paper or a date list, will be asked to pay a charge of $80.00 per printed page. Institutions or authors paying such charges will be entitled to 100 free offprints without covers. *No charges will be made if the author indicates that the author's institution is unable to pay, and payment of page charges on an article will not in any case be a condition for its acceptance. Reduced rates will be in effect for some special issues.*

Missing issues will be replaced without charge only if claim is made within three months (six months for India and Australia) after the publication date. Claims for missing issues will not be honored if absence results from failure by the subscriber to notify the Journal of an address change.

Illustrations should include explanation of symbols used. Copy that cannot be reproduced cannot be accepted. Whenever possible, reduce figures for direct publication. Line drawings should be in black India ink on white drawing board, tracing cloth, or coordinate paper printed in blue and should be accompanied by clear ozalids or reduced photographs for use by the reviewers. Photographs should be positive prints. *Figures* (photographs and line drawings) should be numbered consecutively through each article, using Arabic numerals. **All measurements should be given in SI (metric units).** Tables may be accepted as camera-ready copy.

Citations. A number of radiocarbon dates appear in publications without laboratory citation or reference to published date lists. We ask that laboratories remind submitters and users of radiocarbon dates to include proper citation (laboratory number and date-list citation) in all publications in which radiocarbon dates appear.

Radiocarbon Measurements: Comprehensive Index, 1950–1965. This index covers all published ^{14}C measurements through Volume 7 of *RADIOCARBON*, and incorporates revisions made by all laboratories. It is available at $25.00 per copy.

List of laboratories. Our comprehensive list of laboratories is available upon request. We are expanding the list to include additional laboratories and scientific agencies with whom we have established contacts. The editors welcome more information on these or other scientific organizations. We ask all laboratory directors to provide their telephone, telex and fax numbers as well as their E-mail addresses. Changes in names or addresses, additions or deletions should also be reported to the Managing Editor.

VOLUME 34 / NUMBER 2 / 1992

Radiocarbon

An International Journal of Cosmogenic Isotope Research

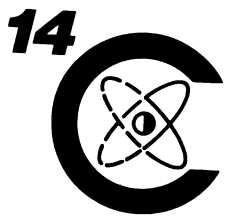

Paleoastrophysics, Paleogeophysics

Proceedings of the Workshop, Paleoastrophysics and Natural Variations of Cosmogenic Isotopes

Department of Geosciences
The University of Arizona
4717 East Ft. Lowell Road
Tucson, Arizona 85712 USA

ISSN: 0033-8222

ASSOCIATE EDITORS

VOL. 34, NO. 2 **RADIOCARBON** 1992

CONTENTS

ACKNOWLEDGMENTS

This Special Issue comprises papers presented at a Workshop on "Paleoastrophysics and Natural Variations of Cosmogenic Isotopes," convened at the 14th International Radiocarbon Conference, 24 May 1991, Tucson, Arizona. The Editors of this issue and the Organizing Committee of "14C14" gratefully acknowledge the support of the US-USSR Cooperation in the Field of Basic Scientific Research Program, Directorate for Scientific, Technological, and International Affairs, Division of International Programs, Natural Science Foundation, Grant no. INT 9105264.

[RADIOCARBON, VOL. 34, NO. 2, 1992, P. v–vi]

PARTICIPANTS

Marisa Alessio
Universita di Roma "La Sapienza"
Istituto di Fisica G. Marconi
Piazzale Aldo Moro 2
I-00185 Roma, Italy

A. V. Blinov
Department of Cosmic Research
St. Petersburg State Technical University
Polytechnicheskaya 29
St. Petersburg 195251 Russia

Thomas F. Braziunas
Quaternary Isotope Research Laboratory
Department of Geosciences
University of Washington
Seattle, Washington 98195 USA

Fr. William F. Cain
Chemistry Department
Loyola Marymount University
7101 West 80th Street
Los Angeles, California 90045 USA

Paul E. Damon
Department of Geosciences
The University of Arizona
Tucson, Arizona 85721 USA

John Eddy
Consortium for International Earth Science
Information Network (CIESIN)
Saginaw Valley State University
2250 Pierce Street
University Center, MI 48710 USA

Menotti Galli
Dipartimento di Fisica
Universitá degli Studi Bologna
Via Irnerio 46
I-40126 Bologna, Italy

Pieter Grootes
Quaternary Isotope Laboratory
Department of Geosciences
University of Washington
Seattle, Washington 98195 USA

Salvatore Improta
Universita di Roma "La Sapienza"
Istituto di Fisica G. Marconi
Piazzale Aldo Moro 2
I-00185 Roma, Italy

John L. Jirikowic
Department of Geosciences
The University of Arizona
Tucson, Arizona 85721 USA

J. R. Jokipii
Department of Planetary Sciences
Lunar and Planetary Laboratory
The University of Arizona
Tucson, Arizona 85721 USA

A. J. T. Jull
NSF-Arizona Accelerator Facility
for Radioisotope Analysis
Department of Physics
The University of Arizona
Tucson, Arizona 85721 USA

G. E. Kocharov
Ioffe Physico-Technical Institute
Polytechnicheskaya 26
St. Petersburg 194021 Russia

A. N. Konstantinov
St. Petersburg State Technical University
Polytechnicheskaya 29
St. Petersburg 195251 Russia

Devendra Lal
Scripps Institution of Oceanography
University of California, San Diego
La Jolla, California 92093-0220 USA

Richard E. Lingenfelter
Center of Astrophysics Space Science
University of California, San Diego
La Jolla, CA 92093 USA

Teresa Nanni
Istituto FISBAT-CNR
Via Castagnoli 1
I-40126 Bologna, Italy

Elizabeth Nesme-Ribes
Section D'Astrophysique
Ministere de L'Education Nationale
Observatoire de Paris
5, Place Jules Janssen
92195 Meudon Principal Cedex, France

A. N. Peristykh
Ioffe Physico-Technical Institute
Polytechnicheskaya 26
St. Petersburg 194021 Russia

Elisabetta Pierazzo
Universita di Padova
Dipartimento di Fisica "Galileo Galilei"
Via Marzolo 8
I-35131 Padova, Italy

Pavel Povinec
Department of Nuclear Physics
Comenius University
Mlynska Dolina F1
CS-842 15 Bratislava, Czecho-Slovakia

Agostino Salomoni
ENEA-TIB
Universitá degli Studi
I-40136 Bologna, Italy

M. A. Shea
Space Physics Division
Geophysics Directorate/Phillips Laboratory
Hanscom Air Force Base
Bedford, Massachusetts 01731-5000 USA

Charles Sonett
Department of Planetary Sciences
Lunar and Planetary Laboratory
The University of Arizona
Tucson, Arizona 85721 USA

Robert S. Sternberg
Department of Geosciences
Franklin & Marshall College
P. O. Box 3003
Lancaster, Pennsylvania 17604-3003 USA

Minze Stuiver
Quaternary Isotope Laboratory
Department of Geosciences
University of Washington
Seattle, Washington 98195 USA

[RADIOCARBON, VOL. 34, NO. 2, 1992, P. vii–viii]

PREFACE

COSMOGENIC ISOTOPE PALEOGEOPHYSICS – PALEOASTROPHYSICS AND NATURAL VARIATION OF COSMOGENIC ISOTOPES

In order to confirm the radiocarbon half-life of 5568 ± 30 years, based upon then available measurements, Willard Libby (1955) produced the first calibration of the radiocarbon time scale, using samples of known age dating back to 5000 BC. He concluded that this half-life was valid and that the $^{14}C/^{12}C$ ratio of atmospheric CO_2 was sufficiently constant to permit accurate dating of paleoevents. A few years later, this assumption was brought into question by Hessel de Vries' (1958) discovery of fluctuations of the $^{14}C/^{12}C$ atmospheric ratio of up to 2% during the Little Ice Age, involving an inaccuracy of the time scale of 160 years. Shortly afterward, workers in the United States demonstrated that the de Vries effect 'wiggles' were superimposed upon longer-term trends (Ralph & Stuckenrath 1960; Suess 1961; Damon, Long & Sigalove 1963). At the International Radiocarbon Conference in Cambridge (Godwin 1962a), accurate measurements were available to designate a new half-life (5730 ± 40 years) (Godwin 1962b) for geophysical-geochemical purposes, and it was then apparent to all attendants that systematic calibration of the radiocarbon time scale was essential (see Damon 1987, for a history of the calibration of the radiocarbon time scale).

Willis, Tauber and Münnich (1960) showed that the de Vries-effect secular variations extended back over the past 1300 years, and appeared to be cyclical, with a period of about 200 years. Shortly thereafter, Stuiver (1961, 1965) demonstrated that the de Vries effect was the result of modulation of radiocarbon production by solar activity. At an earlier date, Suess (1955) had demonstrated a rapid decrease in atmospheric ^{14}C activity resulting from injection of ^{14}C-depleted CO_2 into the atmosphere from combustion of fossil fuels (the Suess effect). It then became apparent that there were generally three categories of possible causes for secular variation of atmospheric ^{14}C: 1) variations in the global rate of ^{14}C production; 2) variation in the rate of exchange between geochemical reservoirs accompanied by changes in the inventory of the various geochemical reservoirs of CO_2; and 3) variations in the total C content of all reservoirs that contain significant amounts of ^{14}C (atmosphere, biosphere, hydrosphere and sediments).

By the time of the 12th Nobel Symposium on "Radiocarbon Variations and Absolute Chronology" held in Uppsala during the summer of 1969, the most significant causes of secular variation of atmospheric ^{14}C had been identified (Olsson 1970): changes in the Earth's dipole moment, changes in solar activity and changes in climate. Attention had also been drawn to possible changes in the galactic cosmic-ray flux entering the solar system, such as those caused by supernovae explosions (Konstantinov & Kocharov 1965; Lingenfelter & Ramaty 1970) or possible intrusion of antimatter into the solar system (Libby 1965). Thus, the 12th Nobel Symposium was a 'watershed' dividing the earlier exploratory research and the subsequent developments in ^{14}C research. The results of 1200 intermediate-precision ^{14}C measurements on tree rings provided the basis for subsequent paleogeophysical-paleoastrophysical studies (Damon *et al.* 1980), until high-precision calibrated dates back through the 8th millennium BC were published following the 12th International Radiocarbon Conference held in Trondheim in June 1985 (Stuiver & Kra 1986). A new set of data will shortly become available with the publication of the new Calibration Issue 1993 (Stuiver, Long & Kra 1993).

Most early research was based on decadal or bidecadal tree-ring samples. The study of solar variations additionally requires annual data to examine the solar activity in both its harmonic

and chaotic phases. It is important to extend available data beyond the last 10,000 years and into the last glacial age. The use of other isotopes in other natural archives, such as ^{10}Be in polar ice, is an essential adjunct to complement ^{14}C and, more importantly, to extend our paleogeophysical-paleoastrophysical work back over hundreds of thousands and even millions of years. New instrumental concepts are evolving (Pavlov, Kogan & Gladkov 1992), as well as a new understanding of solar physics (Nesme-Ribes & Mangeney 1992).

It is important to recall that instrumental measurements of geophysical fields and astrophysical phenomena extend back only a few centuries. The use of cosmogenic isotopes opens a window into the much more distant past. The diligent reader of this issue will be rewarded with an overview of the advances and future directions of a relatively new field.

I wish to thank my colleague, Grant E. Kocharov, for co-chairing this Paleoastrophysics Workshop, and for invaluable help in editing the manuscripts.

Paul E. Damon

REFERENCES

Cowan, C., Atluri, C. R. and Libby, W. F. 1965 Possible anti-matter content of the tunguska meteor of 1908. *Nature* 206: 861–865.

Damon, P. E. 1987 The history of the calibration of radiocarbon dates by dendrochronology. *In* Aurenche, O., Evin, J. and Hourst, F., eds., Relative Chronologies and Absolute Chronology 16,000–4,000 BP. *BAR International Series* 379: 61–104.

Damon, P. E., Lerman, J. C., Long, A., Bannister, B., Klein, J. and Linick, T. W. 1980 Report on the workshop on calibration of the radiocarbon time scale. *In* Stuiver, M. and Kra, R. S., eds., Proceedings of the 10th International ^{14}C Conference. *Radiocarbon* 22(3): 947–949.

Damon, P. E., Long, A. and Sigalove, J. J. 1963 Arizona radiocarbon dates IV. *Radiocarbon* 5: 283–301.

de Vries, H. 1958 Variation in concentration of radiocarbon with time and location on earth. *Koninklijke Nederlandse Akademie van Wetenschappen.* Proceedings Series B 61: 94–102.

Godwin, H. 1962a Radiocarbon dating. *Nature* 195: 984.

_____1962b Half-life of radiocarbon. *Nature* 195: 984.

Konstantinov, B. P. and Kocharov, G. E. 1965 Astrophysical phenomena and radiocarbon. *Doklady Akademii Nauk SSSR* 165: 63–64.

Libby, W. F. 1955 *Radiocarbon Dating.* Second Edition. Chicago, University of Chicago Press: 175 p.

Lingenfelter, R. E. and Ramaty, R. 1970 Astrophysical and geophysical variations in ^{14}C production. *In* Olsson, I., ed., *Radiocarbon Variations and Absolute Chronology.* Proceedings of the 12th Nobel Symposium. New York, John Wiley & Sons: 513–537.

Nesme-Ribes, E. and Mangeney, A. 1992 On a plausible physical mechanism linking the Maunder Minimum to the Little Ice Age. *Radiocarbon,* this issue.

Olsson, I., ed. 1970 *Radiocarbon Variations and Absolute Chronology.* Proceedings of the 12th Nobel Symposium. New York, John Wiley & Sons: 652 p.

Pavlov, A. K., Kogan, V. T. and Gladkov, G. Y. 1992 A tandem mass-spectrometric method of cosmogenic isotope analysis. *Radiocarbon,* this issue.

Ralph, E. K. and Stuckenrath, R. 1960 Carbon-14 measurements of known age samples. *Nature* 188: 185–187.

Stuiver, M. 1961 Variations in radiocarbon concentration and sunspot activity. *Journal of Geophysical Research* 66: 273–276.

_____1965 Carbon-14 content of 18th- and 19th-century wood, variations correlated with sunspot activity. *Science* 149: 533–535.

Stuiver, M. and Kra, R. S., eds. 1986 Calibration Issue. Proceedings of the 12th International Radiocarbon conference. *Radiocarbon* 28(2B): 1030 p.

Stuiver, M., Long, A. and Kra, R. S., eds. 1993 Calibration Issue 1993. *Radiocarbon* 35(1), in press.

Suess, H. E. 1955 Radiocarbon concentration in modern wood. *Science* 122: 415–417.

_____1961 Secular variations in the concentration of atmospheric radiocarbon. In *Proceedings of a Conference on Problems Related to Interplanetary Matter. NAS-NRC Publication* 845: 90–95.

Willis, E. H., Tauber, H. and Münnich, K. O. 1960 Variations in the atmospheric radiocarbon concentration over the past 1300 years. *Radiocarbon* 3: 1–4.

[RADIOCARBON, VOL. 34, NO. 2, 1992, P. 189–198]

Radiocarbon

1992

IMPLICATIONS OF DIPOLE MOMENT SECULAR VARIATION FROM 50,000–10,000 YEARS FOR THE RADIOCARBON RECORD

R. S. STERNBERG

Department of Geosciences, Franklin & Marshall College, Lancaster, Pennsylvania 17604-3003 USA

and

P. E. DAMON

Department of Geosciences, The University of Arizona, Tucson, Arizona 85721 USA

ABSTRACT. Sparse paleointensity data from 10–50 ka suggest that the average dipole moment (DM) was 50–75% of the average of 8.67×10^{22} A m^2 for the past 5 Ma, and 8.75×10^{22} for the past 12 ka. A linear ramp function, increasing the DM from 4 to 8.75×10^{22} A m^2 between 50–10 ka BP, generates a total ^{14}C inventory of 126 dpm/cm$_e^2$, agreeing very well with an inventory assay of 128 dpm/cm$_e^2$, which includes ^{14}C in sediments. With the Lingenfelter and Ramaty (1970) production function and a model DC gain of about 100, this DM function would give a $\Delta^{14}C$ of 500‰ at 20 ka BP, consistent with the Barbados coral record, and also gives a good match to the Holocene record. A Laschamp geomagnetic event at about 45 ka BP, with a DM of 25% of its average value and lasting 5 ka, would only increase the present inventory by 0.3–1.2 dpm/cm$_e^2$, and would probably have only a small effect on $\Delta^{14}C$ at 20 ka BP, but could produce a short-lived ^{14}C spike of over 500‰.

INTRODUCTION

Until recently, discussion of radiocarbon activity fluctuations (Olsson 1970; Damon, Lerman & Long 1978) has focused on the Holocene (Stuiver & Kra 1986). In general, the "long-term" fluctuation with a quasi-periodicity of 10 ka has been attributed to changes in the geomagnetic dipole moment (DM) and the resulting modulation of ^{14}C production (Damon & Sonett 1991; Sternberg 1992; Stuiver *et al.* 1991). Shorter-term fluctuations are attributed to changes in solar activity and its modulation of ^{14}C production (Damon, Cheng & Linick 1989; Stuiver *et al.* 1991).

The research of Bard *et al.* (1990a, b) has revived interest in the late Pleistocene ^{14}C record. Their initial ^{14}C and mass spectrometric U-Th ages on Barbados corals suggested that $\Delta^{14}C$ may have been as high as 500‰ at 20 ka BP (Bard *et al.* 1990a). Subsequent analysis of these coral samples with AMS ^{14}C dates on leached samples suggest that $\Delta^{14}C$ was about 350‰ at 20 ka BP (Bard *et al.* 1990b). Bard *et al.* (1991) further report that corals from French Polynesia also indicate a $\Delta^{14}C$ of 340‰ at 17.6 ka BP. If we accept these results, atmospheric activity was considerably higher than in the tree-ring record. Phillips, Sharma and Wigand (1991) found corroborative evidence in high $^{36}Cl/Cl$ ratios in fossil packrat urine from western Nevada: 410‰ and 280‰ (relative to a sample from 3 ka BP) at 21 ka and 12 ka, respectively. The question naturally arises as to a cause, and one possibility is geomagnetic modulation of ^{14}C production.

We examine here the relationship between the ^{14}C record and DM behavior in the Late Pleistocene. We assume that the long-term ^{14}C fluctuations are primarily due to geomagnetic modulation. Our analysis consists of three components. First, we look at the ^{14}C inventory, which integrates Q over

time, and is independent of the details of the geochemical system. Second, we model atmospheric activity fluctuations. Third, we consider the effects that a "Laschamp" event would have had on ^{14}C activities. We hope to demonstrate that the high activities suggested by the Barbados coral records are consistent with geomagnetic modulation of ^{14}C production by a low DM in the Late Pleistocene.

INVENTORY

Method of Calculation

We use the term, "inventory," as the total amount of ^{14}C in all geochemical reservoirs combined. The equation for inventory is

$$I = \frac{\int_0^\infty Q(t)e^{-\lambda t}dt}{\int_0^\infty e^{-\lambda t}dt} \tag{1}$$

$$= \lambda \int_0^\infty Q(t)e^{-\lambda t}dt \tag{2}$$

where I is the inventory in dpm/cm$_e^2$, t is time in years BP, Q is the production in atoms/cm$_e^2$/min, and λ is the ^{14}C decay constant (Elsasser, Ney & Winckler 1956; Houtermans 1966; Libby 1967; Ramaty 1967; Lingenfelter & Ramaty 1970; Sternberg & Damon 1979; Damon & Sternberg 1989). We get the present inventory by integrating Q back in time. Inventory is a useful parameter for geomagnetic history, because it depends only on Q, and is independent of the ^{14}C geochemical system.

We have calculated the inventory for a number of DM models and production functions. Figure 1 shows our "standard" DM model and corresponding "standard" Q function. The DM model for the last 12 ka is based on the compilation of McElhinny & Senanayake (1982), using their 0.5 ka global averages back to 2 ka BC, and 1 ka averages from 2–10 ka BC. The standard DM model for the period before 12 ka BP is based on data from McElhinny and Senanayake (1982: Fig. 5). We let the DM linearly decrease from 8.36×10^{22} A m^2 at 11.5 ka BP (midpoint for the last 1 ka average) to 4.0×10^{22} A m^2 at 20 ka BP, and remain constant at that value farther into the past.

The standard production function uses the relationship

$$\frac{Q}{Q_0} = \left(\frac{M}{M_0}\right)^{-0.5} \tag{3}$$

where M is the DM, and Q_0 and M_0 are corresponding reference values of the production and DM (Elsasser, Ney & Winckler 1956; Wada & Inoue 1966; Ramaty 1967; Lingenfelter & Ramaty 1970; O'Brien 1979; Blinov 1988; Lal 1988). For reference values, we used Q_0 = 132 atoms/cm$_e^2$/min, averaged over three recent solar cycles (Lingenfelter & Ramaty 1970), for the present DM of 8.0×10^{22} A m^2.

Inventory Assay

The calculated value for inventory is compared with an estimate for the ^{14}C contained in all geochemical reservoirs. We take our estimate of 142 ± 19 (2σ) dpm/cm$_e^2$ from Damon and Stern-

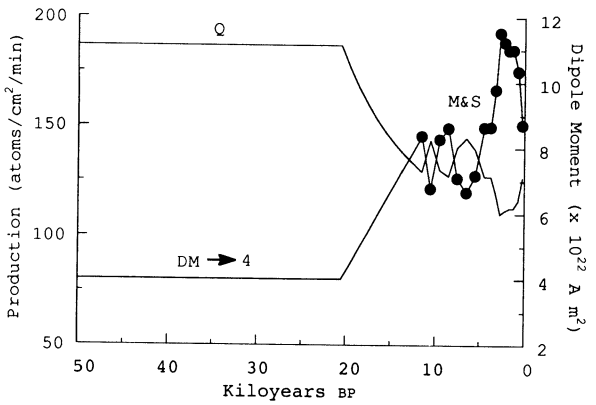

Fig. 1. The standard DM model and corresponding ^{14}C production function. M&S = McElhinny & Senanyake (1982)

berg (1989). We estimated that 10% of this amount is produced by solar flares, which will not be subject to the same rules of geomagnetic modulation; thus, we estimate that geomagnetically modulated production is responsible for 128 ± 17 (2σ) dpm/cm$_e^2$.

Results of Inventory Calculations

Figure 2 shows the results of the inventory calculation for the standard DM and Q functions. Integration is from the present to 50 ka BP, so the inventory value shown at that time is actually the present inventory. The result is 126 dpm/cm$_e^2$, almost exactly the same as the geomagnetically modulated inventory value given above.

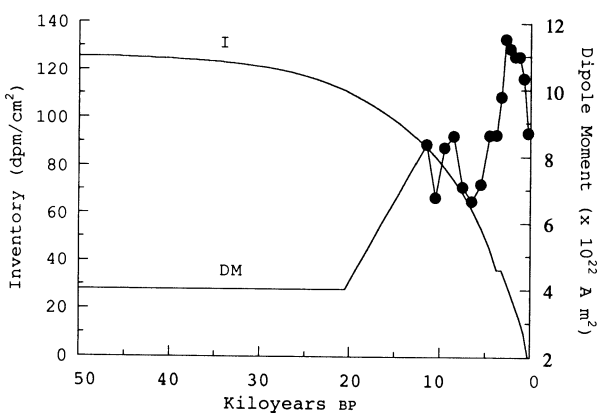

Fig. 2. The standard DM model and the resulting global ^{14}C inventory, calculated by integrating back in time, so the value at 50 ka BP is actually the present inventory

Table 1 presents inventory calculations for other cases. The standard (std) DM model represents a "slow" drop spanning 8 ka to the lower DM at 20 ka BP (Case 1); in contrast, the "fast" drop lasts just 1 ka (Case 2). Paleointensities for Hawaii (Coe, Grommé & Mankinen 1978), the western USA (Champion 1980), Iceland (Schweitzer & Soffel 1980), Europe (Salis, Bonhommet & Levi 1989), and Japan (Tanaka 1990) suggest that the DM could have been as low as 5–6 × 10^{22} A m^2 by 11–12 ka BP.

The next two cases (3 and 4) in Table 1 increase and decrease, respectively, all values in the standard DM model by 1 σ, using the standard deviation values given by McElhinny and Senanayake (1982) back to 12 ka BP, and then relative standard deviations of 17.5%, representative of

TABLE 1. Global ^{14}C Inventory Calculations

Case	DM*	Production**	Inventory (dpm/cm_e^2)
1	M&S to 4, slow (std)	L&R	126
2	M&S to 4, fast	L&R	132
3	M&S + 1 σ to 4, slow	L&R	114
4	M&S − 1 σ to 4, slow	L&R	143
5	M&S to 8.67	L&R	118
6	Std	OBr	104
7	Std	C&L	146
8	Std + "Laschamp"	L&R	127

*DM model for the past 12 ka based on: M&S = McElhinny & Senanayake (1982). See text for additional details.
**Production functions from: L&R = Lingenfelter & Ramaty (1970); OBr = O'Brien (1979); C&L = Castagnoli & Lal (1980).

the present field (McElhinny & Senanayake 1982), for earlier values. These generate inventories of 114 and 143 dpm/cm_e^2, respectively, which are both within 1σ of the assay value.

We have considered a DM model (Table 1, Case 5) that switches from the McElhinny and Senanayake (1982) data to a value of 8.67×10^{22} A m^2, which is the average DM during the past 5 Ma, according to McFadden and McElhinny (1982). The resulting inventory is 118 dpm/cm_e^2.

We also tried different production functions (Damon 1988; Damon & Sternberg 1989) with the standard DM model. The lowest production function is O'Brien's (1979), which is 26% lower than that of Lingenfelter and Ramaty (1970). Consequently, this gives a low inventory of 104 dpm/cm_e^2 (Case 6), which is not consistent with the assay value. The highest production function of Castagnoli and Lal (1980) gives an inventory of 146 dpm/cm_e^2 (Case 7), still within the error of the assay.

Finally, we considered the effects of a "Laschamp" (in quotes because of the inconclusive evidence regarding this event) event on the inventory. Bonhommet and Babkine (1967) first detected anomalous paleomagnetic directions in the Laschamp flows. Marshall, Chauvin and Bonhommet (1988), Roperch, Bonhommet and Levi (1988) and Levi *et al.* (1990) have correlated anomalous paleomagnetic directions at Laschamp and Iceland that have similar dates of 45 ka BP and paleointensities about 15% of the present field strength. The Laschamp event was not originally observed in the high-fidelity sedimentary paleomagnetic record of Lac du Bouchet (Thouveny, Creer & Blunk 1990), very close to the type locality for the Laschamp lavas. More recently, Thouveny and Creer (1991) observed low relative paleointensities in Lac du Bouchet from 28–60 ka BP, with a minimum at 33 ka (Thouveny & Creer 1991). On the other hand, anomalous magnetic directions have not been observed in all paleomagnetic records during the time of Laschamp. Heller and Petersen (1982) have even suggested that the rocks of Laschamp may be self-reversing.

To calculate the inventory, we modeled an extreme case for the Laschamp event, with a DM decreasing to 1.0×10^{22} A m^2, about 12% of the present value, from 40-50 ka BP (Table 1, Case 7). Although production doubles to 373 $atoms/cm_e^2/min$, this is old enough to add only a negligible 1 dpm/cm_e^2 to the inventory calculation.

We have not considered the relative paleointensity data derived from marine sediments by Tauxe and Valet (1989), as was done by Stuiver *et al.* (1991). This is an intriguing data set, in that it

tends to corroborate the general pattern in the McElhinny and Senanayake (1982) compilation. However, these paleointensities are only relative, not absolute, and coming from a single locality, would include a non-dipole as well as a dipole component.

Our conclusions from the inventory analysis are: 1) the standard DM model, including low DM prior to 20 ka BP, yields an inventory concordant with the assayed value; 2) O'Brien's production function appears to be too low; 3) a Laschamp event is not ruled out, although it is certainly not necessary.

FLUCTUATIONS

We next examine the effects of late Pleistocene DM behavior on atmospheric ^{14}C activity. Barbetti and Flude (1979) and Barbetti (1980) used simpler modeling in previous research. Although the Barbados coral record was not yet available, it is noteworthy that Barbetti (1980: Fig. 1) inferred the possibility of such high activities from the low DM during the late Pleistocene.

The Model

To model atmospheric fluctuations, we used a three-box first-order exchange model with a sedimentary sink. We did our modeling using the STELLA program (Richmond, Peterson & Vescuso 1987) on the Apple Macintosh computer. The boxes represent, respectively, the ambient reservoir (Box 1 = atmosphere), the mixed layer reservoir (Box 2 = biosphere, humus, surface water, and mixed layer of the oceans), and the deep-sea reservoir (Box 3 = deep sea and saprosphere). Sediments are transported from deep sea to sedimentary sink (Box s), but are not returned. The frequency response of this model is similar to that of other suitably parameterized models, including the box-diffusion model, for the longer periods associated with geomagnetic modulation (Damon, Sternberg & Radnell 1983: Fig. 1). It is important to include the sedimentary sink, because it significantly decreases the DC gain. We have emphasized this by keeping many of our results in terms of ^{14}C activity rather than converting them to $\Delta^{14}C$. This conversion is commonly done by calculating the $\Delta^{14}C$ relative to a reference activity determined by the model for a given year, *e.g.*, AD 1890. This makes the modeler's work too easy, by effectively adding one degree of freedom, and can lead to error if the DC gain is not balanced (Lazear, Damon & Sternberg 1980).

To initially parameterize the model, we took reservoir contents (n1, n2, n3, and ns) from Damon (1988). Two exchange rates remained fixed in the analysis: k_{12}, from the ambient reservoir to mixed layer, and k_{23}, from the mixed layer to deep sea. Values were $k_{12} = 1/10\ a^{-1}$ and $k_{23} = 1/30\ a^{-1}$, consistent with values used by previous investigators. We calculated exchange rates, k_{21}, k_{32} and k_{3s} from steady-state equations.

Earlier models (*e.g.*, Sternberg & Damon 1979) assumed continuously oscillating DMs, but in all our DM models (other than Laschamp models), we assume a constant DM prior to 20 ka BP. To renormalize the model to initial conditions for the Pleistocene, we made runs with constant production corresponding to the pre-20 ka BP value. From the resulting steady-state equilibrium values, we generated new initial values for n1, n2, n3 and ns, which we used with the fixed values for k12 and k23 to calculate values for the other exchange rates. Although n1, n2, n3, and ns change during the course of a run, the exchange rates were held constant.

Results

Figure 3 shows the results of several model calculations. For comparison, we show the tree-ring record back to 9.6 ka BP (Stuiver & Kra 1986), and the earlier Barbados coral data (Bard *et al.*

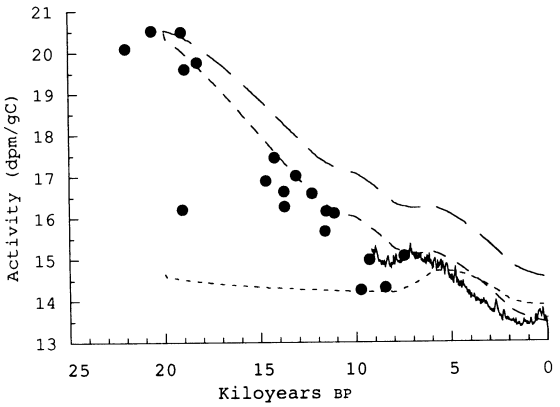

Fig. 3. The atmospheric ^{14}C activity record from tree rings (continuous curve) and Barbados corals (•), and modeled results for: the standard DM and box models (— —); the standard models with lowered DC gain (DC100)(- - -); and the DM model with a late Pleistocene value corresponding to the average field strength for the past 5 Ma (- - - -).

1990a). The revised coral AMS ^{14}C dates lower the activities at 20 ka BP by about 10% (Bard *et al.* 1990b), but do not substantively affect the implications herein. We converted the $\Delta^{14}C$ data for these records to activities by using a reference activity of 13.56 dpm/gC (Karlén *et al.* 1964). The results of the standard run give a model fluctuation curve that has the general shape of the data, but is, overall, too high. One can adjust for this by lowering the DC gain. Thus, we increased the initial ^{14}C content of the sedimentary sink from 34 to 50 dpm/cm$_e^2$, thereby reducing the DC gain from 108 to 100. This lowered the model curve (Fig. 3) to agree very well with the data. The model result still lags behind the data, a problem first noted by Damon (1970). This can be ameliorated by using a longer atmospheric residence time or a relatively smaller atmospheric reservoir (Sternberg & Damon 1979: Fig. 6). Of course, the problem could be due also to changes in heliomagnetic modulation or reservoir parameters.

According to the adjusted standard model, final reservoir decay rates for the present are n1 = 1.55, n2 = 8.72, n3 = 86.7 and ns = 37.8 dpm/cm$_e^2$. These compare favorably to reservoir estimates of n1 = 1.64, n2 = 9.19, n3 = 91.2, n4 = 41.2 (Damon 1988).

As an alternative model, the fast decrease to a lower DM before 12 ka BP generates an activity too high and too close to the present. If, instead of decreasing to a DM of 4.0×10^{22} A m^2, the field switches to its 5 Ma average of 8.67×10^{22} A m^2, the calculated activities are much lower than the coral activities in the Late Pleistocene (Fig. 3).

Thus, the fluctuation calculations show that the high activities suggested by the Barbados coral data can be explained by a low DM in the Late Pleistocene, using a reasonable ^{14}C reservoir model that includes a sizeable sedimentary sink. The long-term trend of the Holocene record can also be explained by geomagnetic modulation. Mazaud *et al.* (1991a) draw the same conclusion.[1] A lower production function, such as that of O'Brien (1979), would require a higher DC gain to generate the required activities, yet this would be inconsistent with the tendency of the sedimentary sink to lower DC gain.

[1]*Note added in proof*: The paper by Mazaud *et al.* (1991b) was published after original submission of this manuscript. Utilizing relative paleointensity data from Tric *et al.* (in press), they reach virtually identical conclusions that the ^{14}C fluctuations shown in the coral record can be explained by a generally low DM in the Late Pleistocene.

LASCHAMP FLUCTUATIONS

A Laschamp-type event would have a negligible effect on the present inventory, because the best estimate for its timing is about seven ^{14}C half-lives ago. This would not be true necessarily for ^{14}C activity measured soon after the time of Laschamp itself. Grey (1971) first examined this problem, but, at that time, Laschamp was believed to have occurred about 20 ka BP. Grey (1971) also assumed that the DM had been oscillating sinusoidally for several cycles to determine initial conditions. To simplify modeling, Grey (1971) used steady-state equations for the mixed-layer and deep-sea reservoirs.

We have run a number of Laschamp models to examine the effect on the atmospheric activity record. The Laschamp event was superimposed upon a steady-state DM of 4.0×10^{22} A m^2; the initial conditions were also generated from this steady-state DM. Our standard Laschamp event is centered at 45 ka BP, lasting for 10 ka, decreasing to a minimum DM with a triangular shape (Fig. 4). Other cases changed the timing, duration or minimum DM. We used a different DM shape only for the 20 ka duration event – the DM decreased linearly for 5 ka to the minimum, remained constant for 10 ka, then increased linearly for 5 ka to the baseline value.

Figure 4 shows the results of the standard Laschamp event on atmospheric $\Delta^{14}C$. Table 2, which summarizes results for other models of the Laschamp event, shows the peak value of $\Delta^{14}C$ generated, as well as the values at 20 and 10 ka BP. None of these models is absolutely precluded by

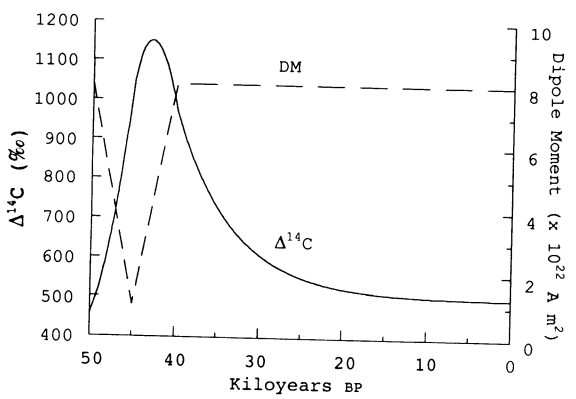

Fig. 4. The standard DM model for the Laschamp event and the corresponding atmospheric ^{14}C activity

TABLE 2. Effects of Laschamp-Type Events on ^{14}C Activity

Case	Age* (ka)	Length* (ka)	DM* (10^{22} A m^2)	Peak** (‰)	Time** (ka)	20 ka† (‰)	10 ka† (‰)
1	45	10	1.0	666	43.1	24	6
2	45	10	0.5	1219	43.1	46	10
3	45	10	2.0	275	43.1	10	2
4	45	5	1.0	444	44.1	12	3
5	45	20	1.0	1289	40.0	89	20
6	50	10	1.0	666	48.1	12	1
7	30	10	1.0	666	28.1	231	52

*Age, length and DM specify the midpoint in years BP, duration and minimum DM for Laschamp events.
**Peak indicates the resulting maximum in atmospheric ^{14}C above the steady-state value at the adjacent time in years BP.
†Resulting increases of ^{14}C above the steady-state value for 20 and 10 ka BP.

the ^{14}C calibration data. Higher amounts of Laschamp-generated ^{14}C at 20 and 10 ka BP, such as for Cases 5 and 7 in Table 2, are permitted, if other causes generate a ^{14}C deficiency, such as for some DM/initial conditions (*e.g.*, Beer *et al.* 1988: Fig. 3; Stuiver *et al.* 1991: Figs. 6, 8). However, as Figure 3 shows, this extra ^{14}C from a deep event is not required.

If the ^{14}C time scale could be calibrated back to 30 ka BP, the effects of a Laschamp pulse would become evident for most of these cases. The large pulse generated by longer or "deeper" events might also generate dating anomalies or inversions.

We wish to note, without undue speculation, the existence of a spike in the ^{10}Be record from two Antarctic ice cores at about 35 ka BP, lasting 1–2 ka (Raisbeck *et al.* 1987).

CONCLUSIONS

Our three major conclusions are:

1. The ^{14}C inventory, including sedimentary sink, implies both a low Late Pleistocene DM strength and a relatively high ^{14}C production function.
2. The ^{14}C activity record also requires a low DM, and is consistent with a low DC gain due to the sedimentary sink and a correspondingly high production function.
3. A global Laschamp event at 40–50 ka BP, with a significantly decreased DM, is not ruled out by the extant ^{14}C record; pushing this record back to 30 ka BP could constrain models for Laschamp.

Important research that would shed additional light on the problems discussed here include:

1. More research on tree rings, varves and corals to extend the calibration of the ^{14}C time scale for ambient reservoirs into the Pleistocene.
2. A search for the effects of a Laschamp event in older ^{14}C dates, *e.g.*, young dates and dating inversions.
3. More absolute and relative paleointensity data for the Late Pleistocene.
4. More research on the geographic extent, timing and magnetic recording of the Laschamp event.

ACKNOWLEDGMENTS

This work was supported by NSF grants ATM-9143542 and EAR-8721466, and Franklin and Marshall College. Computer assistance to R. S. Sternberg was provided by R. Folk. An anonymous reviewer pointed out several useful references.

REFERENCES

Barbetti, M. 1980 Geomagnetic strength over the last 50,000 years and changes in atmospheric ^{14}C concentration: Emerging trends. *In* Stuiver, M. and Kra, R. S., eds., Proceedings of the 10th International ^{14}C Conference. *Radiocarbon* 22(2): 192–199.

Barbetti, M. and Flude, K. 1979 Geomagnetic variation during the late Pleistocene period and changes in the radiocarbon time scale. *Nature* 279: 202–205.

Bard, E., Hamelin, B., Arnold, M. and Buigues, D. 1991 $^{230}Th/^{234}U$ and ^{14}C ages obtained by mass spectrometry on corals from Mururoa Atoll, French Polynesia. Abstract. *Radiocarbon* 33(2): 173.

Bard, E., Hamelin, B., Fairbanks, R. G. and Zindler, A. 1990a Calibration of the ^{14}C timescale over the past 30,000 years using mass spectrometric U-Th ages from Barbados corals. *Nature* 345: 405–410.

Bard, E., Hamelin, B., Fairbanks, R. G., Zindler, A., Mathieu, G. and Arnold, M. 1990b U/Th and ^{14}C ages of corals from Barbados and their use for calibrating the ^{14}C time scale beyond 9000 years B.P. *In* Yiou, F. and Raisbeck, G. M., eds., Proceedings of the 5th International Conference on Accelerator Mass Spectrometry. *Nuclear Instruments and Methods* B52: 461–468.

Beer, J., Siegenthaler, U., Bonani, G., Finkel, R. C., Oeschger, H., Suter, M. and Wölfli, W. 1988 Information on past solar activity and geomagnetism from ^{10}Be in the Camp Century ice core. *Nature* 331: 675–679.

Blinov, A. 1988 The dependence of cosmogenic isotope production rate on solar activity and geomagnetic field variations. *In* Stephenson, F. R. and Wolfendale, A. W., eds., *Secular Solar and Geomagnetic Variations in the Last 10,000 Years*. Dordrecht, The Netherlands, Kluwer Publishing Co.: 329–340.

Bonhommet, N. and Babkine, J. 1967 Sur la présence d'aimantations inversées dans la Chaîne de Puys. *Comptes Rendus de l'Academie des Sciences* B264: 92–94.

Castagnoli, G. and Lal, D. 1980 Solar modulation effects in terrestrial production of carbon-14. *In* Stuiver, M. and Kra, R. S., eds., Proceedings of the 10th International ^{14}C Conference. *Radiocarbon* 22 (2): 133–158.

Champion, D. E. 1980 Holocene geomagnetic secular variation in the western United States: Implications for the global geomagnetic field. *US Geological Survey Open-File Report* 80-824. Denver, Colorado: 314 p.

Coe, R. S., Grommé, S. and Mankinen, E. A. 1978 Geomagnetic paleointensities from radiocarbon-dated lava flows on Hawaii and the question of the Pacific nondipole low. *Journal of Geophysical Research* 83: 1740–1756.

Damon, P. E. 1970 Climatic versus magnetic perturbation of the atmospheric C14 reservoir. *In* Olsson, I. U., ed., *Radiocarbon Variations and Absolute Chronology*. Proceedings of the 12th Nobel Symposium. Stockholm, Almqvist & Wiksell: 571–593.

_____1988 Production and decay of radiocarbon and its modulation by geomagnetic field-solar activity changes with possible implications for global environment. *In* Stephenson, F. R. and Wolfendale, A. W., eds., *Secular Solar and Geomagnetic Variations in the Last 10,000 Years*. Dordrecht, The Netherlands, Kluwer Publishing Co.: 267–283.

Damon, P. E., Cheng, S. and Linick, T. W. 1989 Fine and hyperfine structure in the spectrum of secular variations of atmospheric ^{14}C. *In* Long, A. and Kra, R. S., eds., Proceedings of the 13th International ^{14}C Conference. *Radiocarbon* 31(3): 704–718.

Damon, P. E., Lerman, J. C. and Long, A. 1978 Temporal fluctuations of atmospheric ^{14}C: Causal factors and implications. *Annual Reviews of Earth and Planetary Sciences* 6: 457–494.

Damon, P. E. and Sonett, C. P. 1991 Solar and terrestrial components of the atmospheric ^{14}C variation spectrum. *In* Sonett, C. P., Giampapa, M. S. and Mathews, M. S., eds., *The Sun in Time*. Tucson, The University of Arizona Press: 360–388.

Damon, P. E. and Sternberg, R. S. 1989 Global production and decay of radiocarbon. *In* Long, A. and Kra, R. S., eds., Proceedings of the 13th International ^{14}C Conference. *Radiocarbon* 31(3): 697–703.

Damon, P. E., Sternberg, R. S. and Radnell, C. J. 1983 Modeling of atmospheric radiocarbon fluctuations for the past three centuries. *In* Stuiver, M. and Kra, R. S., eds., Proceedings of the 11th International ^{14}C Conference. *Radiocarbon* 25(2): 249–258.

Elsasser, W., Ney, E. P. and Winckler, J. R. 1956 Cosmic-ray intensity and geomagnetism. *Nature* 178: 1226–1227.

Grey, D. C. 1971 ^{14}C data and the Laschamp reversed event. *Journal of Geomagnetism and Geoelectricity* 23(1): 123–127.

Heller, F. and Petersen, N. 1982 The Laschamp excursion. *Philosophical Transactions of the Royal Society of London* A306(1492): 169–177.

Houtermans, J. 1966 On the quantitative relationships between geophysical parameters and the natural C^{14} inventory. *Zeitschrift für Physik* 193: 1–12.

Karlén, I., Olsson, I. U., Kållberg, P. and Kilicci, S. 1964 Absolute determination of the activity of two C^{14} dating standards. *Arkiv för Geofysik* 4(22): 465–471.

Lal, D. 1988 Theoretically expected variations in the terrestrial cosmic-ray production rates of isotopes. *In* Castagnoli, G. C., ed., *Solar-Terrestrial Relationships and the Earth Environment in the Last Millennia*. Amsterdam, Elsevier: 216–233.

Lazear, G., Damon, P. E. and Sternberg, R. 1980 The concept of DC gain in modeling secular variations in atmospheric ^{14}C. *In* Stuiver, M. and Kra, R. S., eds., Proceedings of the 10th International ^{14}C Conference. *Radiocarbon* 22(2): 318–327.

Levi, S., Audunnson, H., Duncan, R. A., Kristjánnson, L., Gillot, P.-Y. and Jakobsson, S. P. 1990 Late Pleistocene geomagnetic excursion in Icelandic lavas: Confirmation of the Laschamp excursion. *Earth and Planetary Science Letters* 96: 443–457.

Libby, W. F. 1967 Radiocarbon and paleomagnetism. *In* Hindmarsh, W. R., Lowes, F. J., Roberts, P. H. and Runcorn, S. K., eds., *Magnetism and the Cosmos*. New York, American Elsevier: 60–65.

Lingenfelter, R. E. and Ramaty, R. 1970 Astrophysical and geophysical variations in C14 production. *In* Olsson, I. U., ed., *Radiocarbon Variations and Absolute Chronology*. Proceedings of the 12th Nobel Symposium. Stockholm, Almqvist & Wiksell: 513–535.

Marshall, M., Chauvin, A. and Bonhommet, N. 1988 Preliminary paleointensity measurements and detailed magnetic analyses of basalts from the Skalamaelifell excursion, southwest Iceland. *Journal of Geophysical Research* 93(B10): 11,681–11,698.

Mazaud, A., Laj, C., Bard, E., Arnold, M. and Tric, E. 1991a Geomagnetic field control of ^{14}C production over the last 80 Ky: Implications for the radiocarbon time-scale. Abstract. *EOS, Transactions, American Geophysical Union* 72(44): 71–72.

_____1991b Geomagnetic field control of ^{14}C production over the last 80 Ky: Implications for the radiocarbon time-scale. *Geophysical Research Letters* 18(10): 1885–1888.

McElhinny, M. W. and Senanayake, W. E. 1982 Variations in the geomagnetic dipole 1: The past 50,000 years. *Journal of Geomagnetism and Geoelectricity* 34: 39–51.

McFadden, P. L. and McElhinny, M. W. 1982 Variations in the geomagnetic dipole, 2. Statistical analysis of VDMs for the past 5 million years. *Journal of Geomagnetism and Geoelectricity* 34: 163–189.

O'Brien, K. J. 1979 Secular variation in the production of cosmogenic isotopes. *Journal of Geophysical Research* 84(A2): 423–431.

Olsson, I. U., ed. 1970 *Radiocarbon Variations and Absolute Chronology*. Proceedings of the 12th Nobel Symposium. Stockholm, Almqvist & Wiksell: 652 p.

Phillips, F. W., Sharma, P. and Wigand, P. E. 1991 Deciphering variations in cosmic radiation using cosmogenic ^{36}Cl in ancient rat urine. Abstract. *EOS, Transactions, American Geophysical Union* 72(44): 72.

Raisbeck, G. M., Yiou, F., Bourles, D., Lorius, C., Jouzel, J. and Barkov, N. I. 1987 Evidence for two intervals of enhanced ^{10}Be deposition in Antarctic ice during the last glacial period. *Nature* 326: 273–277.

Ramaty, R. 1967 The influence of geomagnetic shielding on C14 production and content. *In* Hindmarsh, W. R., Lowes, F. J., Roberts, P. H. and Runcorn, S. K., eds., *Magnetism and the Cosmos*. New York, American Elsevier: 66–78.

Richmond, B., Peterson, S. and Vescuso P. 1987 *An Academic User's Guide to STELLA*. Lyme, New Hampshire, High Performance Systems: 392 p.

Roperch, P., Bonhommet, N. and Levi, S. 1988 Paleointensity of the earth's magnetic field during the Laschamp excursion and its geomagnetic implications. *Earth and Planetary Science Letters* 88: 209–219.

Salis, J.-S., Bonhommet, N. and Levi, S. 1989 Paleointensity of the geomagnetic field from dated lavas of the Chaîne des Puys, France. 1. 7–12 thousand years before present. *Journal of Geophysical Research* 94(B11): 15,771–15,784.

Schweitzer, C. and Soffel, H. C. 1980 Paleointensity measurements on postglacial lavas from Iceland. *Journal of Geophysics* 47: 57–60.

Sternberg, R. S. 1992 Radiocarbon fluctuations and the geomagnetic field. *In* Taylor, R. E., Long, A. and Kra, R. S., eds., *Radiocarbon After Four Decades: An Interdisciplinary Perspective*. New York, Springer-Verlag: 93–116.

Sternberg, R. S. and Damon, P. E. 1979 Sensitivity of radiocarbon fluctuations and inventory to geomagnetic and reservoir parameters. *In* Berger, R. and Suess, H. E., eds., *Radiocarbon Dating*. Proceedings of the 9th International ^{14}C Conference. Berkeley, University of California Press: 691–717.

Stuiver, M., Braziunas, T. F., Becker, B. and Kromer, B. 1991 Climatic, solar, oceanic, and geomagnetic influences on Late-Glacial and Holocene atmospheric $^{14}C/^{12}C$ change. *Quaternary Research* 35: 1–24.

Stuiver, M. and Kra, R. S., eds. 1986 Calibration Issue. Proceedings of the 12th International ^{14}C Conference. *Radiocarbon* 28(2B): 805–1030.

Tanaka, H. 1990 Paleointensity high at 9000 years from volcanic rocks in Japan. *Journal of Geophysical Research* 95(B11): 17,517–17,531.

Tauxe, L. and Valet, J.-P. 1989 Relative paleointensity of the earth's magnetic field from marine sedimentary rocks: A global perspective. *Physics of the Earth and Planetary Interiors* 13: 241–244.

Thouveny, N. and Creer, K. M. 1991 Laschamp: An ephemeral geomagnetic anomaly. Paper presented at XX General Assembly of IUGG, Vienna, August 11–24.

Thouveny, N., Creer, K. M. and Blunk, I. 1990 Extension of the Lac du Bouchet paleomagnetic record over the last 120,000 years. *Earth and Planetary Science Letters* 97: 140–161.

Tric, E., Valet, J.-P., Tucholka, P., Paterne, M., Labeyrie, L., Guichard, F., Tauxe, L. and Fontugne, M., in press, Paleointensity of the geomagnetic field during the last eighty thousand years. *Journal of Geophysical Research*.

Wada, M. and Inoue, A. 1966 Relation between the carbon 14 production rate and the geomagnetic moment. *Journal of Geomagnetism and Geoelectricity* 18(4): 485–488.

[RADIOCARBON, VOL. 34, No. 2, 1992, P. 199–205]

THE SUN AS A LOW-FREQUENCY HARMONIC OSCILLATOR

P. E. DAMON and J. L. JIRIKOWIC

Laboratory of Isotope Geochemistry and The NSF-Arizona Accelerator Facility for Radioisotope Analysis, Department of Geosciences, The University of Arizona, Tucson, Arizona 85721 USA

ABSTRACT. Solar activity, as expressed by interplanetary solar wind magnetic field fluctuations, modulates the atmospheric production of ^{14}C. Variations of atmospheric ^{14}C can be precisely established from the cellulose within annual tree rings, an independently dated conservative archive of atmospheric carbon isotopes. $\Delta^{14}C$ time series interpretation shows that solar activity has varied with a recurrence period of 2115 ± 15 (95% confidence) yr (Hallstattzeit) (Damon & Sonett 1991) over the past 7160 yr. From a non-stationary oscillation solar activity hypothesis, 52 possible spectral harmonics may result from this period. Damon and Sonett (1991) identify powerful harmonics such as the 211.5-yr (Suess) and the 88.1-yr (Gleissberg) cycles as independent fundamental periods. These stronger harmonics appear to modulate the 11-yr (Schwabe) sunspot cycle. Variations in the solar magnetic field, thus, may respond to longer period variations of the solar diameter envelope (Ribes *et al.* 1989). Such variations would affect solar radiative energy output and, consequently, change total solar irradiance (Sofia 1984).

HARMONIC ANALYSIS OF THE ^{14}C SPECTRUM

Spectral analysis of the available high-precision $\Delta^{14}C$ data by Stuiver and Braziunas (1989), using the maximum entropy method (MEM), led them to postulate a fundamental 420-yr oscillation related to changes in the solar convective zone. After increasing the model autoregressive order (AR, equivalent to the length of the prediction error filter, for the purposes of this paper), Stuiver and Braziunas observed that additional periods became important. They note that the 420-yr period splits into periods of 504, 355 and 299 yr. We have observed that this apparent splitting of the 420-yr peak results from the limited frequency resolution, and to oversmoothing by the MEM spectral method when too small an AR order is chosen. Our experience suggests that frequency resolution for MEM (AR = 160) spectral analysis lies between $1/\tau$ and $1/1.25\tau$, where τ is the length of the time series. Although the analysis above seems to suggest subjectivity, MEM analyses provide excellent frequency resolution when comparing between many AR orders and with the results of alternative spectral estimate methods (such as the discrete Fourier transform (DFT), multi-taper estimates, maximum-likelihood-Bayesian methods and singularity spectral-analysis estimates). By varying the number of sampled points and AR order, it becomes apparent that the 420-yr peak does not split, but each of these peaks is always present with relative peak heights varying with chosen AR order.

However, these low-frequency variations remain poorly resolved, whatever the spectral method employed, until either the data time series lengthens, or a hypothesis develops relating the poorly resolved low-frequency variations to better-resolved higher-frequency variations (see Damon & Jirikowic 1992, for details). We have used the simplest non-stationary model, a harmonic oscillator, as our working hypothesis. The well-resolved higher-frequency variations represent a set of harmonic and combination overtones of lower-frequency variations. For example, concerning the ~504-yr period, its 2nd–13th apparent overtones observed in spectral analyses of the last 7160 yr of the high-precision bidecadal $\Delta^{14}C$ calibration time series (Stuiver & Kra 1986) establish the period more precisely as 526 yr. Similarly, the 9 apparent overtones of the 420-yr peak define it as 424 yr; the 8 apparent overtones of the 355-yr period establish it as 356 yr, and analysis of the 299-yr period with 6 apparent overtones established it more precisely at 300 yr. Further, each of these longer periods appears to modulate shorter periods producing peak triplets, quintets and higher. Further analyses show these spectral peak frequencies may be related as elements of the

harmonic series T/n, T/2n, T/3n, . . ., where n is any positive integer, 1, 2, 3, . . . Assuming n = 1, and finding an approximate least-common multiple to obtain the shortest possible estimated period of the fundamental, T, we obtained (keeping 4 significant figures to reduce truncation errors):

$$526 \times 4 = 2104$$
$$424 \times 5 = 2120$$
$$356 \times 6 = 2136$$
$$300 \times 7 = 2100$$
$$T = 2115 \pm 9 \text{ yr } (\bar{\sigma})$$

Thus, the supposed fundamentals may be harmonic overtones of a ~2115-yr Hallstattzeit period (Damon & Sonett 1991). By hypothesis that the Hallstattzeit period may have 52 harmonic overtones present in the spectral analyses (limited only by the 40-yr Nyquist period of the bidecadal $\Delta^{14}C$ time series), the fundamental period may be established from the observed peak power frequencies with a precision of 0.1 ± 3.1 yr (95% confidence level). The agreement of the Hallstattzeit overtones with reference to both the DFT and MEM (AR = 160) spectra (Fig. 1) strongly suggests that the causal phenomenon is independent of the spectral method. Thus, modulation side-lobe "leakage" due to spectral window truncation does not seem to influence greatly our results.

PROBABILISTIC VALIDATION OF THE HALLSTATTZEIT OVERTONES

The probabilistic[1] significance of this agreement may be investigated in several ways. For example, of the 20 DFT frequencies with spectral power > 95% χ^2-confidence, 7 have frequencies matching the hypothesized Hallstattzeit harmonic overtone frequencies within the frequency resolution.[2] From the discrete, multinomial distribution of these sets of frequencies, the probability of equaling the performance of the Hallstattzeit harmonic hypothesis with 52 randomly chosen frequencies is 0.12%. The likelihood of the harmonic hypothesis reaches a maximum near a fundamental period of 2115 yr, and remains above 95% from 2120 to 2105 yr. From Bayesian analysis, we are able to infer from the null hypothesis *a priori* probability distribution of random matching that the *a posteriori* probability of random matching remains zero within 95% confidence for hypothetical fundamental periods between 2130 and 2100 yr. The final test employed the second order norm between the observed spectral peak frequencies and the hypothesized overtone frequencies. A Hallstattzeit fundamental period of 2116-yr minimized the second order norm with a 2σ (~95%) range from 2128 to 2104 yr. Thus, the solar harmonic oscillator hypothesis with a fundamental Hallstattzeit period between 2130 and 2100 yr provides a compelling explanation of much of the observed $\Delta^{14}C$ time series spectrum.

MODULATION OF THE SOLAR SCHWABE CYCLE BY THE SUESS AND GLEISSBERG HARMONICS

A harmonic oscillator would be a particular solution to the general differential equation

$$\ddot{D}(t) + f[\dot{D}(t)] + g[D(t)] = F(t) \qquad (1)$$

[1]Because the hypothesized 2115-yr Hallstattzeit variation recurs only three times in the ^{14}C calibration time series, and the harmonic overtones may not have independent statistical distributions, non-parametric probability analyses may be more reliable and informative than traditional parametric statistics.

[2]At any given frequency, the MEM absolute power depends upon the chosen AR order. Thus, conventional confidence-level calculation analysis of MEM spectral peaks is inappropriate without independent *a priori* determination of the AR order.

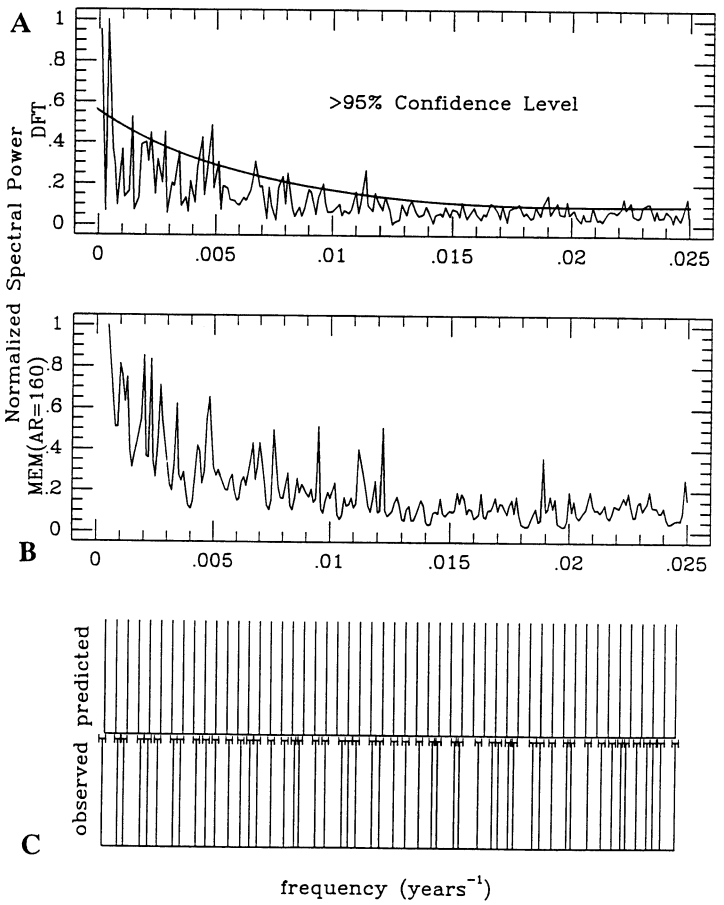

Fig. 1. A. DFT power spectrum of the high-precision $\Delta^{14}C$ data. Vertical lines represent the Hallstattzeit fundamental and 52 harmonic overtones. The heavy curve estimates the lower 95% χ^2-confidence limit and the "red-noise continuum" likely due to non-stationarity and time persistence. B. MEM (AR = 160) spectrum. Note that although much of the spectrum trends as a red-noise continuum, 20 spectral peaks extend above the 95% χ^2-confidence limit, suggesting substantial periodicity. C. compares the observed and predicted spectral peaks. The error bars on the top of the observed lines represent the frequency resolution.

where D(t) represents solar activity, f, a damping function, g, a restoring function and F(t), an external forcing. The harmonic oscillator particular solution of Equation (1) may take the form of a Fourier sum of harmonics

$$D(t) = A_0 + \sum_{i=1}^{n} [A_i\cos(\omega_i t-\phi_i)-B_i\sin(\omega_i t-\phi_i)] \qquad (2)$$

where ω_i are harmonic frequencies, A_i and B_i are amplitude coefficients and ϕ_i are phase coefficients. Note that A_i, B_i and ϕ_i may be complex functions of both the harmonic frequencies and time.

Certain harmonics of the Hallstattzeit with observed power greater than expected for a simple system of harmonics act as apparent fundamentals (*i.e.*, 211.5-yr Suess and 88.1-yr Gleissberg variations). These periods appear in the DFT and MEM (AR = 160) spectra of the annual Wolf sunspot indices as harmonic overtones and modulating periods (Fig. 2). For example, the first two

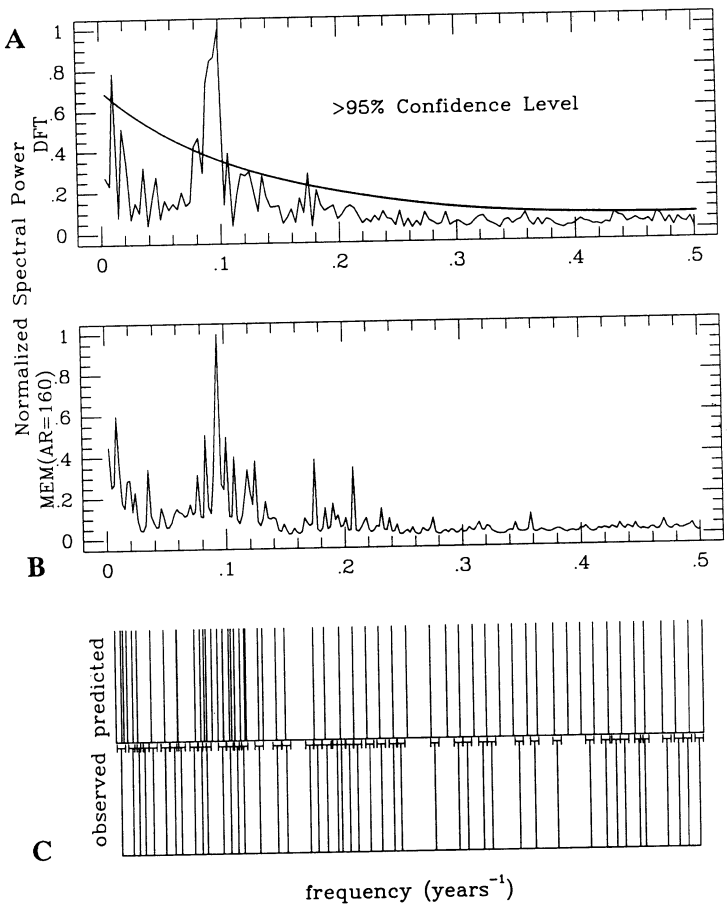

Fig. 2. A. DFT power spectrum of the annual Wolf sunspot index. Vertical lines represent the 211.5, 88.3 and 11.1-yr periods, their overtones and sidebands produced by amplitude modulation of the 11.1-yr carrier period (after Sonett 1982). The heavy curve estimates the lower 95% χ^2-confidence level and the red-noise continuum. B. MEM (AR = 160) spectrum. Vertical lines represent observed peaks. Modulation sidebands appear in the annual Wolf sunspot index spectra, features not seen in the $\Delta^{14}C$ spectra in Figure 1. C. compares the observed spectral peaks with those predicted from the amplitude modulation model of the 11-yr cycle. The error bars on the top of observed lines represent the frequency resolution.

harmonic overtones of the 211.5-yr Suess period cannot be resolved from the 88.1-yr Gleissberg period, and not all side bands of the 11.1-yr Schwabe cycle carrier modulated by these longer periods and their overtones can be resolved from one another (Fig. 2). Higher-frequency overtones appear, including four overtones of the 11.1-yr carrier (5.55, 3.70, 2.78 and 2.22-yr, see Fig. 2). The 211.5-yr period and its 2nd (105.8-yr) and 4th (52.9-yr) overtones, combined with the Gleissberg period (88.1-yr), appear to modulate strongly the 11.1-yr carrier. A reasonable fit to the observed annual Wolf sunspot indices can be obtained, using a squared amplitude modulation model (after Sonett 1982) by allowing these periods (211.5, 105.8, 52.9 and 88.1-yr) to amplitude modulate the 11.1-yr carrier signal (see Fig. 3, Table 1)

$$R_z = \sum_{i=1}^{4} \alpha_i \cos^2(\omega_i t + \phi_i)\alpha_c \cos^2(\omega_c t + \phi_c) \quad . \tag{3}$$

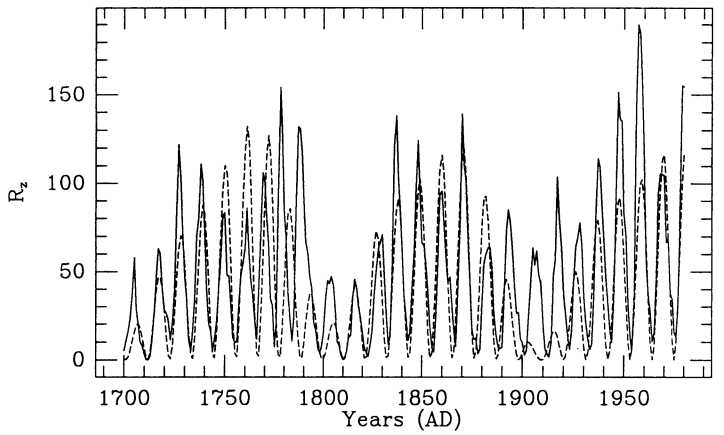

Fig. 3. (– – –) simulation of the (——) annual Wolf sunspot indices by modulation of the 11.1-yr carrier by the 211.5, 105.75, 88.125 and 52.875-yr periods with the amplitudes and phases shown in Table 1. Note that the 211.5-yr periodicity has a low modulation coefficient. Also note that the model underestimates sunspot indices during the late 19th century solar activity minimum. Because the Hallstattzeit gate strongly affects the 211.5-yr harmonic and this millennium's Hallstattzeit-gating epoch ends before the late 19th century, the weak 211.5-yr and the weak late 19th century solar minimum would support the Hallstattzeit non-stationarity hypothesis (see text for details).

TABLE 1. Model Parameters for Modulation of the 11.1-Year Schwabe Carrier

Index	Period	α	ϕ
1	52.875	0.66	0.62
2	88.125	0.43	-1.82
3	105.75	1.31	1.10
4	212.5	0.01	1.33
c	11.1	65.4	1.46

Note that the cosine series modulation function expressed in Equation 3 is a member of the family of harmonic oscillator solutions given in Equation 2. Notably, the model fits the late 19th century minimum poorly. Mean sunspot indices do not fall to the very low levels predicted by our model. Also note that the modulation coefficient, alpha, for the 211.5-yr period is quite small. Both events may be explained by the non-stationarity present in the Wolf sunspot index data set. The Hallstattzeit epoch encompassing the Wolf, Spörer, Maunder and Dalton solar activity minima wanes in the first half of the sunspot index data. Thus, the stationary model assumption has been compromised. The Hallstattzeit variation also appears to modulate strongly the 211.5-yr period (Damon & Sonett, 1991). A more sophisticated model would include the Hallstattzeit gating.

HALLSTATTZEIT GATING: PHYSICAL MANIFESTATION AND PALEOCLIMATIC CONSEQUENCES?

The Hallstattzeit variation appears to act as a gate (Damon 1988) allowing more intense century-scale oscillation during the high $\Delta^{14}C$ phase of the cycle (*e.g.*, the Maunder and Hallstattzeit low solar activity epochs; Schmidt & Gruhle 1988). If we assume the wave form for the Hallstattzeit period, shown in Figure 4, with the high $\Delta^{14}C$ phases appearing as the square-wave gate portions, the square wave generates the harmonic overtones and strongly modulates the 211.5, 88.1-yr periods. Figure 4 presents the $\Delta^{14}C$ variations after the removal of a very long-term trend ascribed to changes in the Earth's magnetic dipole moment (see Damon & Sonett 1991 for review). The

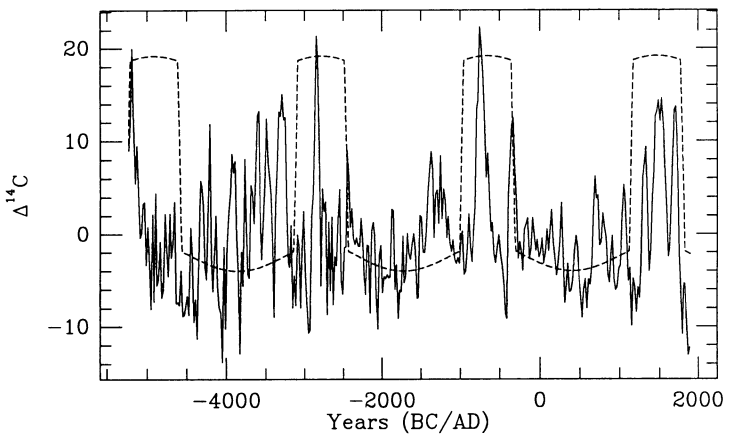

Fig. 4. (– – –) wave-form model generating the Hallstattzeit harmonics and amplitude gating of the (——) century-scale $\Delta^{14}C$ variations compared to the detrended high-precision $\Delta^{14}C$ time series. Note that the weaker century-scale oscillations appear modulated by variations of the Earth's magnetic field as described in the text, yet the stronger gated variations appear comparatively unmodulated.

trend can be closely fit by a sine curve with a 10,780-yr period for the last eight millennia, but deviates markedly during the early Holocene (Damon, Cheng & Linick 1989). The Earth's magnetic dipole moment is weak during the negative portion of this cycle before 2600 BC and stronger during the positive part of the cycle between 2600 BC and AD 1650. The effect of this geomagnetic field variation can be seen by relative suppression or enhancement of the century-scale $\Delta^{14}C$ variations. This amplitude modulation of $\Delta^{14}C$ variations by the geomagnetic field appears weak during the high $\Delta^{14}C$ gating portion of the Hallstattzeit cycle. The Hallstattzeit variation may have also affected paleoclimate by changing solar output and the Suess and Gleissberg cycles may have contributed in part to the global warming trend evidence since the last decade of the 19th century (Damon 1989; Damon & Jirikowic 1992; see Damon & Sonett 1991 for review).

The physical manifestation of the Hallstattzeit solar variation has yet to be conclusively determined. Ribes (1990: 96), reviewing the evidence for periodicities in the solar diameter, concludes that, "the Sun's apparent radius was larger in the deep of the Maunder Minimum (late in the Little Ice Age, when practically no sunspots were seen) than it was at the end when solar activity has resumed (from 1705 onwards). An expansion of solar envelope of about 3 arc seconds on the diameter would be consistent with cooling of the envelope and with a slowing down of surface rotation." With relation to Ribes' (1990) interpretation, the Hallstattzeit wave form in Figure 4 suggests that the Sun slowly expands, lingers at maximum diameter and then contracts. This structural modulation partitions potential energy and radiant energy (Sofia 1984) between two intransitive states.

Concluding remarks

The harmonic overtone periods may represent a dynamic-system response and other non-stationary phenomena or a mathematical manifestation of the non-sinusoidal Hallstattzeit variation. The observation of variations, such as the ~88-yr Gleissberg cycle, strongly suggests that several variations also have a physical reality beyond being harmonic overtones of the fundamental Hallstattzeit variation. Such secular solar variations would have obvious implications as possible factors in global climate change. Associating these Hallstattzeit solar variations with climate variations may require a time-variant climate model. Further, the apparent non-stationarity of the

solar variations prohibits extrapolating linear regression models calibrated over a single 11-yr cycle between solar activity and solar radiant output beyond a Hallstattzeit variation. Predictions based solely upon the cyclicity of $\Delta^{14}C$ variations, without consideration of these Hallstattzeit non-stationarities, may be more misleading than informative. Understanding both the modeling and geophysical implications of the Hallstattzeit variation would advance our ability to predict solar activity and understand the Sun as a harmonic oscillator.

ACKNOWLEDGMENTS

This work was supported by NSF Grants ATM-8919535 and EAR-8822292 and the State of Arizona. Prof. C. P. Sonett contributed the MEM, DFT and Bayesian-Maximum Likelihood algorithms and Henry Diaz and Roger Pulwarty, the Singularity Spectral Analysis algorithm. Only the painstaking efforts of the workers producing the high-precision $\Delta^{14}C$ data make precision in establishing the fundamental Hallstattzeit period possible. Special thanks to Aran Armstrong for his assistance in checking the calculations and the manuscript.

REFERENCES

Damon, P. E. 1988 Production and decay of radiocarbon and its modulation by geomagnetic field-solar activity changes with possible implications for the global environment. *In* Stephenson, F. R. and Wolfendale, A. W., eds., *Secular Solar and Geomagnetic Variations in the Last 10,000 Years*. Dordrecht, The Netherlands, Kluwer Academic Publishers: 267–286.

_____1989 Radiocarbon, solar activity and climate. *In* Avery, S. K. and Tinsley, B. A., eds., *Proceedings from the Workshop on Mechanisms for Tropospheric Effects of Solar Variability and the Quasi-Biennial Oscillation*: 198–208.

Damon, P. E., Cheng, S. and Linick, T. W. 1989 Fine and hyperfine structure in the spectrum of secular variations of atmospheric ^{14}C. *In* Long, A. and Kra, R. S., eds., Proceedings of the 13th International ^{14}C Conference. *Radiocarbon* 31(3): 704-718.

Damon, P. E. and Jirikowic, J. L. 1992 Radiocarbon evidence for low frequency solar oscillations. *In* Povinec, P., ed., *Rare Nuclear Processes, Proceedings of the 14th Europhysics Conference on Nuclear Physics*. Singapore, World Scientific Publishing Co.: 177–202.

Damon, P. E. and Sonett, C. P. 1991 Solar and terrestrial components of the atmospheric ^{14}C variance spectra. *In* Sonett, C. P., Giampapa, M. S. and Matthews, M. S., eds., *The Sun in Time*. Tucson, The University of Arizona Press: 360–388.

Ribes, E. 1990 Astronomical determinations of the solar variability. *Philosophical Transactions of the Royal Society of London* A 330: 487–497.

Ribes, E., Merlin, P., Ribes, J. C. and Barthalot, R. 1989 Absolute periodicities of the solar diameter, derived from historical and modern time-series. *Annals Geofisica* 1: 321–329.

Schmidt, B. and Gruhle, W. 1988 Radiokohlenstoffgehalt und dendrochronologie. *Naturwissenschaftliche Rundschau* 5: 177–182.

Sofia, S. 1984 Solar variation as a source of climate change. *In* Hansen, J. E. and Takahashi, T., eds., *Climate Processes and Climate Sensitivity*. Washington, American Geophysical Union: 202–206.

Sonett, C. P. 1982 Sunspot time series: Spectrum from square law modulation of the Hale Cycle. *Geophysical Research Letters* 9: 1313–1316.

Stuiver, M. and Braziunas, T. F. 1989 Atmospheric ^{14}C and century-scale solar oscillations. *Nature 338*: 405–408.

Stuiver, M. and Kra, R. S., eds. 1986 Calibration Issue. Proceedings of the 12th International ^{14}C Conference. *Radiocarbon* 28(2B): 805–1030.

[RADIOCARBON, VOL. 34, NO. 2, 1992, P. 207–212]

REFLECTION OF SOLAR ACTIVITY DYNAMICS IN RADIONUCLIDE DATA

A. V. BLINOV and M. N. KREMLIOVSKIJ

St. Petersburg Technical University, Polytechnicheskaya 29, St. Petersburg 195251 Russia

ABSTRACT. Variability of solar magnetic activity manifested within sunspot cycles demonstrates features of chaotic behavior. We have analyzed cosmogenic nuclide proxy records for the presence of the solar activity signals. We have applied numerical methods of nonlinear dynamics to the data showing the contribution of the chaotic component. We have also formulated what kind of cosmogenic nuclide data sets are needed for investigations on solar activity.

INTRODUCTION

Recent advances in nonlinear dynamics make it possible to distinguish stochastic and chaotic behavior of physical systems from long-term observations. Several researchers (Weiss 1988; Morfill *et al.* 1991) have considered the solar magnetic dynamo as a dissipative system demonstrating temporal variability. The only direct data set long enough for solar activity evolution studies is the sunspot (Wolf index) record covering the period from about AD 1700 until the present. The so-called Packard-Takens procedure transforms this one-dimensional record into the topological equivalent of the phase portrait of the initial dynamic system, thus providing a key for solar magnetic dynamo understanding. Unfortunately, direct solar observations did not continuously cover such an important period of its evolution as the Maunder Minimum. The transition from solar "normal" cycling to the depressed magnetic stage and back would give important information on the nature of and the distinction between chaos and order in solar variability. The only opportunity to prolong the time scale is to use the indirect solar signal reflected in cosmogenic nuclide data. The prospects in the field accounting for the advantages of accelerator mass spectrometry (AMS) in these investigations were discussed earlier (Newkirk 1984). In this paper, we attempt to analyze the representative nuclide series in light of the chaotic nature of solar activity.

CHAOS IN THE SOLAR MAGNETIC CYCLE

In a sequence of observations, we have used monthly mean data on sunspot numbers (Zürich, 1749–1985, designated below as {W}). First, we will discuss the assumptions that are made in applying the methods of nonlinear dynamics. We consider the evolution of solar magnetic activity as a temporal chaotic process in a dissipative system. Thus, we assume that its behavior is deterministic, and can be described by combined nonlinear differential equations. The number of equations coincide with the number of system degrees of freedom. A set of scenarios of either chaos or routes to chaos is known (Schuster 1984; Berge, Pomeau & Vidal 1988). Thus, we can generally predict the shapes of the signal and its spectrum and Poincare map of the phase trajectory for model systems. In this sense, it is possible to compare the observed dynamics with canonical scenarios. Based upon the minimal information, we are able to learn the type of nonlinear equations describing processes occurring in the natural system. We have reconstructed the topology of the phase trajectory of the solar activity from {W} following the Packard-Takens procedure (Packard *et al.* 1980; Takens 1981), which corresponds to each element of the primary one-dimensional sequence {W} an n-dimensional vector $\mathbf{W}_i$, in accordance with the rule

$$\mathbf{W}_i \Rightarrow (W_i, W_{i+\tau}, W_{i+2\tau}, \ldots, W_{i+(n-1)\tau}) \quad (1)$$

where τ is a time-delay parameter. The parameter, τ, should be chosen close to the first zero of

the autocorrelation function for the initial quasi-periodical one-dimensional sequence (we have chosen it equal to 35 months). By the phase space for the dissipative system, we mean the basis formed by several mutually independent physical values.

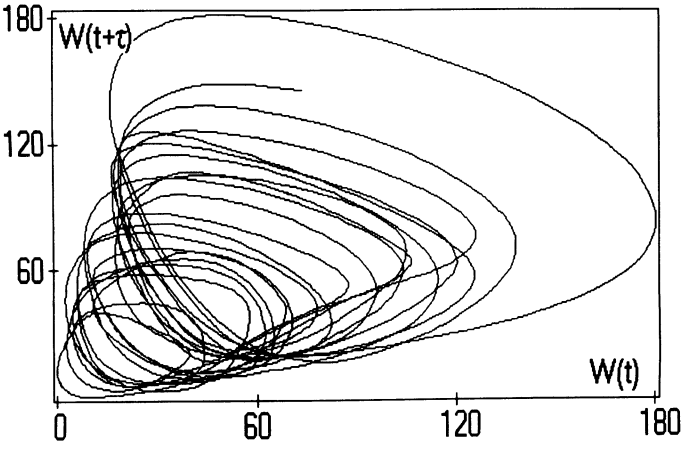

Fig. 1. The two-dimensional projection of the {W} trajectory reconstructed in three-dimensional space

Our calculations show that when τ varies from 30 to 40 months, the basis of the phase space is almost orthogonal. This is the minimal correlation between the neighboring points of the trajectory. The dimension of the embedding space for the phase trajectory may be determined with the help of the Grassberger-Procaccia (1983) algorithm. The analysis of the W_i sequence reveals (Kurtz & Herzel 1987; Kremliovskij, Blinov & Tcherviakov 1992) that the dimension of the solar attractor is <3. Thus, n = 3 may be used in the following calculations. Figure 1 shows the trajectory of the solar activity attractor. The high-frequency ($T < \tau$) noise was subtracted from the primary {W} data before the trajectory reconstruction. The trajectory develops as a broadening coil, one turn corresponding to an 11-yr cycle. The cycles with small maxima lie on the base of the coil. The interval between the trajectory failure at the top to the bottom of the coil corresponds to the 90-yr Gleissberg cycle. The Poincare map (map of the first return) of the trajectory (Fig. 2), which was produced by its crossing by the plane parallel to the coil symmetry axis, contains only 20 points subdividing into 2 groups. The points formed by the first 13 cycles (years before 1900) can be

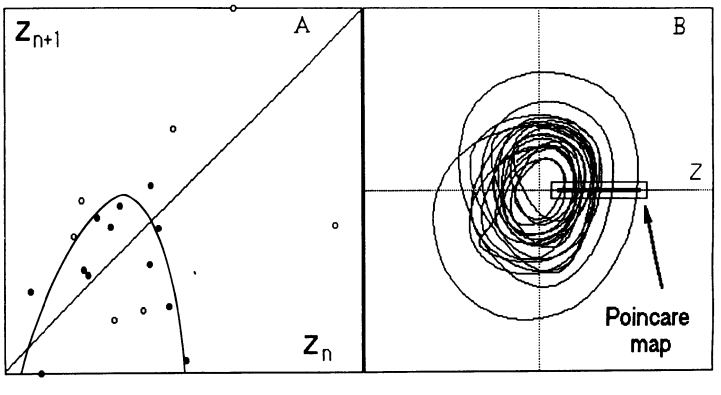

Fig. 2. A. The Poincare map of the phase trajectory: • = 1749–1900 yr; ○ = 1900–1985 yr. B. The {W} phase trajectory turned with its symmetry axis perpendicular to the picture plane; the cross-section plane is shown by the arrow.

approximated by the quadratic-type curve shown on the graph. It provides evidence for the presence of chaotic dynamics during this stage of solar activity history. The next cycles (14–17) show a different distribution on the map. The causes for this discrepancy do not have a single meaning, but the whole picture supports the presence of chaos in solar activity dynamics. See Kremliovskij, Blinov and Tcherviakov (1992) for further elaboration.

COSMOGENIC NUCLIDE DATA ANALYSIS

All the reasoning on the chaos in solar activity was obtained from the {W} data. Although the qualitative relationship between the solar magnetic field density reflected in the sunspot index and the production of cosmogenic nuclides in the Earth's atmosphere was experimentally established for ^{14}C and ^{10}Be (Kocharov *et al.* 1985; Beer *et al.* 1990), the quantitative model describing their relation has not been developed yet. Transport of the magnetic field from the solar surface to the heliosphere is a complicated process, but one would expect that it is nearly random on the monthly time scale. On the other hand, a simple empirical relationship between {W} and the nuclide mean global production rate can be obtained formally as Blinov (1988) did for the yearly series. Thus, the inevitable problem is the choice of proper time scale, which is closely related to another question, "What are the signal and noise in radionuclide records?" To illustrate this, Figures 3 and 4 show the analysis of the ^{10}Be record in the Dye-3 Greenland ice core (Beer *et al.* 1990). The

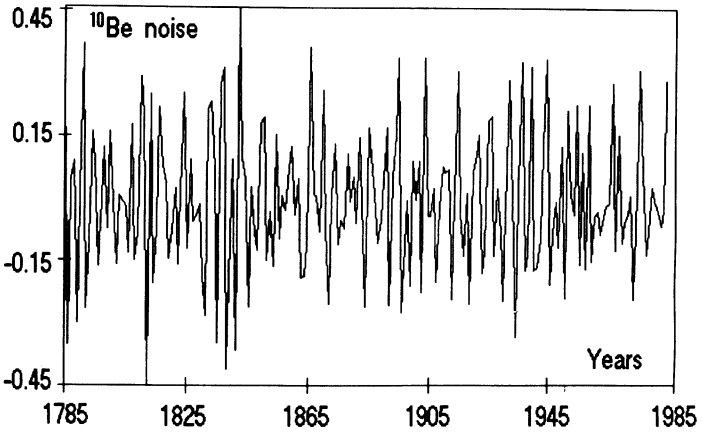

Fig. 3. Noise component of the ^{10}Be Dye-3 (Beer *et al.* 1990) ice-core record

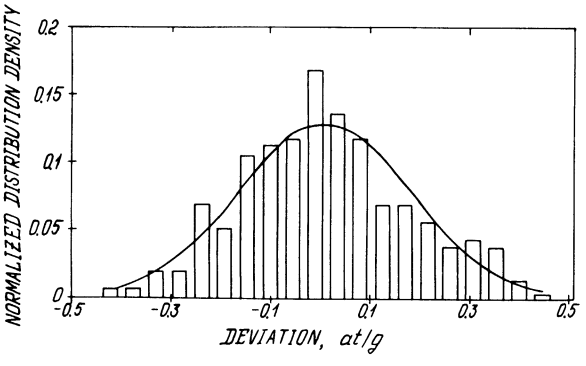

Fig. 4. Histogram of the noise component of ^{10}Be in ice compared with normalized normal distribution

noise component (Fig. 3) has been extracted from the record by subtracting the smoothed data by a 3-yr moving average. It is clear from Figure 4 that the noise component appears to be consistent with normal distribution, based on the noise mean and dispersion.

The increase of the filter length causes an increase in the discrepancy between the noise and the normal distribution. We interpret this to be a lack of a pronounced physical signal in the record on a time scale of <3–4 yr. We found that the noise component of the ^{14}C 400-yr record (Kocharov *et al.* 1985) fits a normal distribution even better than in Figure 4. This can be explained by natural averaging of ^{14}C yearly concentrations by the natural mixing in the environmental exchange reservoirs. Only additional information would allow us to extract the high-frequency (T <3–4 yr) component from these data.

Our attempts to reconstruct the phase trajectories of the records mentioned above have not yielded such simple phase portraits as for {W}. The dimensions of the embedding phase spaces are much larger than those in Figure 1. We understand this to be the complex influence of nuclide production and transport processes upon the archives, which obviously have their own additional dynamics. Thus, extraction of a pure fine structure of the solar signal from these radionuclide records is not possible with the current level of knowledge of such processes.

The next data set we used is the ^{14}C 4 ka tree-ring record (Stuiver & Becker 1986), consisting of decadal measurements. The map $\delta^{14}C\ (t+\tau) = F\ [\delta^{14}C\ (t)]$ with $\tau = 1$ (close to one 11-yr interval) in Figure 5 demonstrates the total lack of memory in the ^{14}C reflection of the Schwabe cycle. Figure 5 should be compared with Figure 2A, which shows a deterministic relation among the successive 11-yr cycles. On the contrary, Figure 5 is more consistent with the map of purely noisy time series, which would show an irregular distribution of the points on the $\{x(t), x(t+\tau)\}$ two-dimensional plane. Thus, we conclude that the information on a solar attractor is obscured in this record and cannot complement the sunspot results.

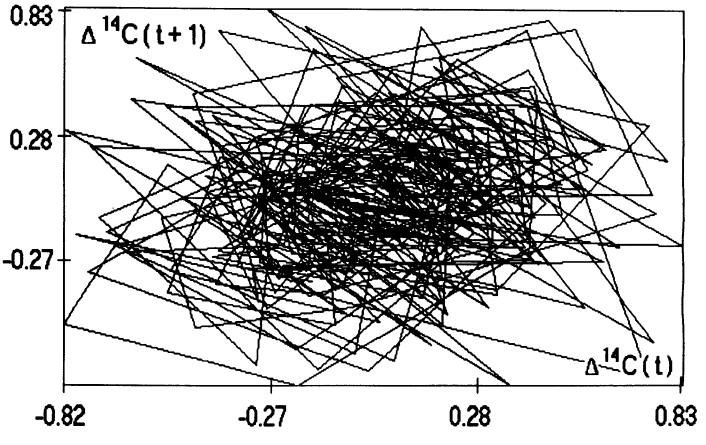

Fig. 5. Two-dimensional map of the ^{14}C record (Stuiver & Becker 1986) cleared of the minima periods and Gleissberg cycle. The time-delay parameter, τ, is taken to equal 1 (10 yr).

Finally, we have examined the distribution of solar minima durations in the ^{14}C 9.7 ka record (Stuiver & Braziunas 1988). Although the perfect determination of the minima beginnings and endings is arguable, Figure 6 compares this distribution with the predictions of the chaotic system following the type-1 intermittence route to chaos. The alternation of laminary and chaotic phases

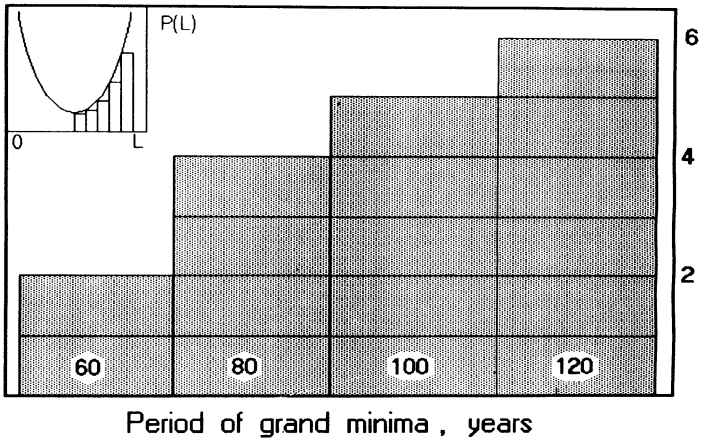

Fig. 6. The distribution of solar minima durations in the ^{14}C tree-ring record (Stuiver & Braziunas 1988). Shown in the upper left corner is the distribution of the durations of laminary stages for the type-1 intermittency route to chaos.

is normally understood under the intermittency in temporal series. Intermittency types are classified according to their Poincare maps, duration of stages, *etc.* (Berge, Pomeau & Vidal 1988). Our proposal of type-1 intermittency agrees with variations in the ^{10}Be concentration in ice during the Maunder Minimum reported by Beer *et al.* (1991). If solar minima are regular (laminary) periods of magnetic activity evolution, they should preserve the Schwabe-like cyclicity, even though its amplitude may be decreased. Evidence for this view of solar activity will yield new radionuclide data on the periods of quiet Sun.

Conclusion

The results of our work show that cosmogenic nuclides are presently the only source of information on the character of the chaotic behavior of solar activity. The ^{14}C and ^{10}Be proxy records support the view of solar activity evolution as a sequence of chaotic and regular stages, similar to the type-1 intermittency route to chaos. The most promising directions for future studies are the Schwabe-type variations during solar minima and more accurate determination of solar minima durations and transitional behavior.

Acknowledgments

We wish to express our gratitude to Dr. N. G. Makarenko for stimulating discussions and interest in our work, and to J. Jirikowic for his careful review of the manuscript and valuable comments.

REFERENCES

Beer, J., Blinov, A. V., Bonani, G., Finkel, R. C., Hofmann, H. J., Lehmann, B., Oeschger, H., Sigg, A., Schwander, J., Staffelbach, T., Stauffer, B., Suter, M. and Wölfli, W. 1990 Use of ^{10}Be in polar ice to trace the 11-year cycle of solar activity. *Nature* 347: 164–166.

Beer, J., Bonani, G., Dietrich, B., Finkel, R. C., Hofmann, H. J., Lehmann, B. E., Oeschger, H., Stauffer, B., Suter, M. and Wölfli, W. (ms.) 1991 A high resolution ^{10}Be record in polar ice. Paper presented at the 14th International ^{14}C Conference, Tucson, Arizona, May 20–24, 1991.

Berge, P., Pomeau, Y. and Vidal, C. 1988 *L'Order Dans le Chaos*. Paris, Editeurs des Science et Arts: 312 p. (in French).

Blinov, A. V. 1988 The dependence of cosmogenic nuclide production rate on solar activity and geomagnetic field variations. *In* Stephenson, F. R. and Wolfendale, A. W., eds., *Secular Solar and Geomagnetic Variations in the Last 10,000 Years*. Dordrecht, The Netherlands, Kluwer Academic Publishers: 329–340.

Grassberger, P. and Procaccia, I. 1983 Characterization of strange attractors. *Physical Review Letters* 50: 346–348.

Kocharov, G. E., Bitvinskas, T. T., Vasilijv, V. A., Dergachev, V. A., Konstantinov, A. N., Metskhvarishvily, R. J., Ostryakov, V. M. and Stupneva, A. V. 1985 Cosmogenic isotopes and astrophysical phenomena. In *Astrophysical Phenomena and Radiocarbon*. Leningrad: 9–142 (in Russian).

Kremliovskij, M. N., Blinov, A. V. and Tcherviakov, T. B. 1992 On the chaotic dynamics of solar activity. *Soviet Astronomy*, in press (in Russian).

Kurtz, J. and Herzel, H. 1987 An attractor in solar time series. *Physica D* 25: 165–172.

Morfill, G. E. Scheingraber, H., Voges, W. and Sonett, C. P. 1991 Sunspot number variations: stochastic or chaotic. *In* Sonett, C., Giampapa, M. and Matthews, M. S., eds., *The Sun in Time*. Tucson, The University of Arizona Press: 30–58.

Newkirk, G., Jr. 1984 What accelerator mass spectrometry can do for solar physics. *In* Wölfli, W., Polach, H. A. and Anderson, H. H., eds., Proceedings of the 3rd International Symposium on Accelerator Mass Spectrometry. *Nuclear Instruments and Methods* B5: 404–410.

Packard, N., Crutchfield, J. P., Farmer, J. D. and Show, R. S. 1980 Geometry from a time series. *Physical Review Letters* 51: 712–731.

Schuster, H. G. 1984 *Deterministic Chaos*. Weinheim, Germany, Physics Verlag: 220 p.

Stuiver, M. and Becker, B. 1986 High-precision decadal calibration of the radiocarbon time scale, AD 1950–2500 BC. *In* Stuiver, M. and Kra, R. S., eds., Proceedings of the 12th International ^{14}C Conference. *Radiocarbon* 28(2B): 836–910.

Stuiver, M. and Braziunas, T. F. 1988 The solar component of the atmospheric radiocarbon record. *In* Stephenson, F. R. and Wolfendale, A. W., eds., *Secular Solar and Geomagnetic Variations in the Last 10,000 Years*. Dordrecht, The Netherlands, Kluwer Academic Publishers: 245–266.

Takens, F. 1981 Detecting strange attractors in turbulence. *In* Dynamical Systems and Turbulence. *Lectural Notes in Mathematics* 898: 336–266.

Weiss, N. O. 1988 Is the solar cycle an example of deterministic chaos? *In* Stephenson, F. R. and Wolfendale, A. W., eds., *Secular Solar and Geomagnetic Variations in the Last 10,000 Years*. Dordrecht, The Netherlands, Kluwer Academic Publishers: 69–78.

[RADIOCARBON, VOL. 34, NO. 2, 1992, P. 213–217]

VARIATION OF RADIOCARBON CONTENT IN TREE RINGS DURING THE MAUNDER MINIMUM OF SOLAR ACTIVITY

G. E. KOCHAROV, A. N. PERISTYKH

A. F. Ioffe Physical-Technical Institute, St. Petersburg 194021 Russia

P. G. KERESELIDZE, Z. N. LOMTATIDZE, R. YA. METSKHVARISHVILI, Z. A. TAGAURI S. L. TSERETELI and I. V. ZHORZHOLIANI

Tbilisi State University, Tbilisi 380028 Georgia

ABSTRACT. We present here annual data on ^{14}C abundance in tree rings during the Maunder minimum of solar activity (AD 1645–1715). We show that the solar modulation persisted during the minimum. We also compare these data with measurements of ^{10}Be concentration in dated polar ice cores and with records of aurorae recurrence during this time interval.

INTRODUCTION

The use of cosmogenic isotopes provides a unique opportunity to study past solar activity in terms of proxy indices. Available data on the cosmogenic isotopes, ^{14}C and ^{10}Be, in dated natural archives allow reliable determination of the level of solar activity over several hundred years (Kocharov *et al.* 1985). A particular goal of the study of short-term variations of solar activity is to obtain precise radiocarbon data, which is of special importance in the problem of the Maunder minimum of solar activity (AD 1645–1715).

During the last 20 years in the USSR, two cycles of high-precision measurements of ^{14}C abundance in tree rings were performed. Vasiliev and Kocharov (1983) reported initial data for even years in the interval, AD 1600–1730. In this effort, pine tree-ring samples were dated using liquid scintillation counting (LSC); the new and unpredicted result concerned the existence of ^{14}C variations during the Maunder minimum. Considering the significance of the problem, we measured a different set of samples from fir tree rings taken from another locality (Zhorzholiani *et al.* 1988; Kocharov *et al.* 1990).

METHODOLOGY

The time series presented in this report depicts annual values of $\Delta^{14}C$ in dated rings of dead (archaeological) and living fir-tree wood collected in the western Ukraine (Zhorzholiani *et al.* 1988). Samples for the interval, AD 1600–1650, were taken from an old house in Lvov (50°N, 24°E). For AD 1665–1699, samples were collected from a church in Busk (50°N, 25°E) (Bitvinskas *et al.* 1988). Tree-ring samples (since AD 1701) were taken from living trees in the Karpaty Mountains near the Goverla peak (48°N, 24°E). Unfortunately, due to existing uncertainties in dating dead wood, tree-ring measurements revealed a gap of 14 years, from AD 1651 to 1664.

We dated our samples using LSC, and followed the protocol for the pretreatment of wood samples according to Arslanov (1970). Acetylene was synthesized from lithium carbide in a hand-made chemical unit. Benzene synthesis was performed by cyclotrimerization of acetylene on an aluminosilicate catalyst activated by Cr_2O_3; benzene yield was 90–98%.

Each LSC unit was designed as a two-channel system (Kocharov & Metskhvarishvili 1986). The detectors are surrounded by mercury-iron shielding. Spherical vials for benzene samples are made of potassium-free glass. Measurement precision is 0.2–0.3%.

Corrections for isotopic fractionation were based on $\delta^{13}C$ values of benzene. Small benzene samples were completely converted to CO_2 by oxygen combustion in a calorimetric bomb designed by Burchuladze *et al.* (1970). Samples were analyzed by the two-beam bridge method to a precision of 0.03% in a commercial MI-1305 mass spectrometer.

Discussion

Figure 1 shows the raw $\Delta^{14}C$ data for the period, AD 1600–1760. Here we also plotted a curve of the data smoothed by a 3-point moving average procedure, along with a long-term variation curve derived by smoothing a 29-point moving average. We see the ^{14}C increase from *ca.* AD 1650 to 1720, as well as short-term variations during the Maunder minimum.

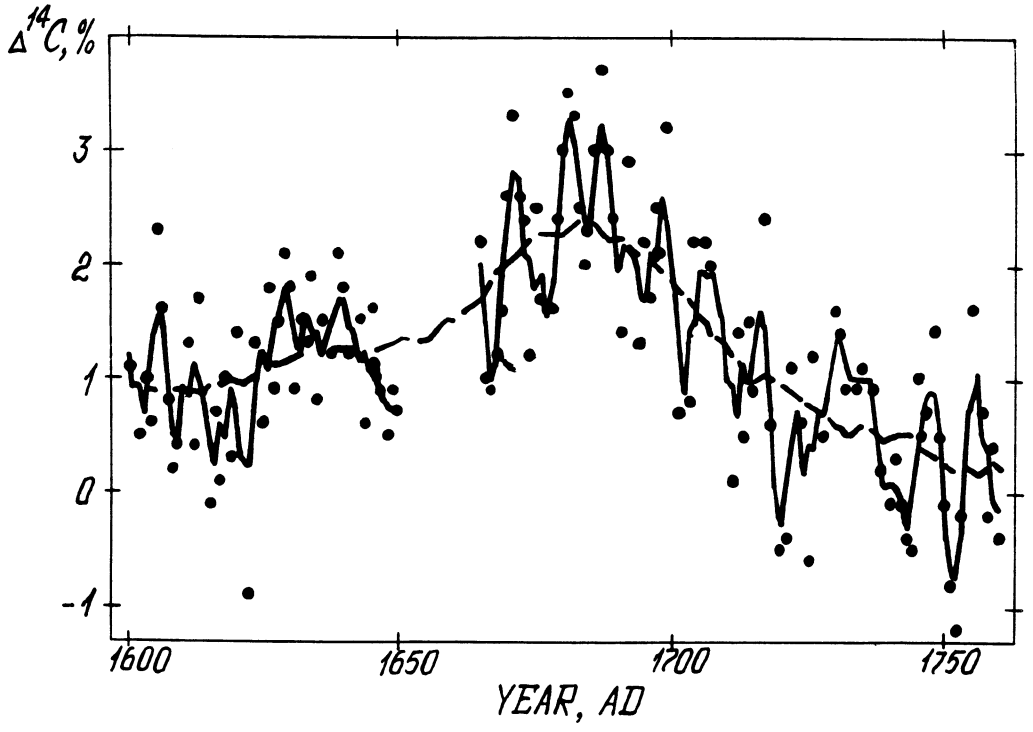

Fig. 1. Variations of $\Delta^{14}C$ in the annual rings of a fir tree from the western Ukraine, AD 1600–1940: the raw data (•) and the data smoothed by the 3-point (—) and by the 29-point moving average (– –).

In order to match the short-term variations in both ^{14}C records, we suppressed the long-term trends by first-order difference filtering (Jenkins & Watts 1968). Before that, in order to obtain the annual record, both sets of data were padded by a linear interpolation procedure. The resultant series for AD 1660–1730, smoothed by a 5-point moving average, is depicted in Figure 2. It is obvious that increases and decreases of both curves fall generally in the same time intervals. Thus, we can note that they are in sufficient agreement; our data confirm the conclusion made by Vasiliev and Kocharov (1983) on the modulation of galactic cosmic radiation by the Sun during the Maunder minimum.

It is important to compare the behavior of short-term variations in our ^{14}C data with that of ^{10}Be data obtained from Greenland ice cores. The data were padded by linear interpolation to obtain the annual record. Here, the long-term trend, derived by smoothing a 29-point moving average, was

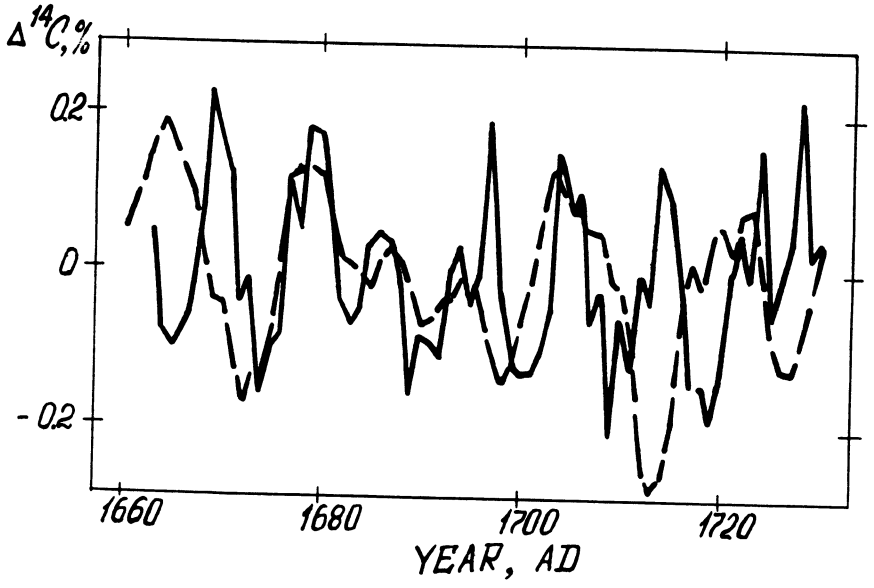

Fig. 2. Short-term variations of $\Delta^{14}C$ in the annual rings of a fir tree from the western Ukraine, AD 1665–1730 (—) and pine from the southern Ural, AD 1660–1730 (– –) derived by the first-order difference, and then by the 5-point moving average filtering.

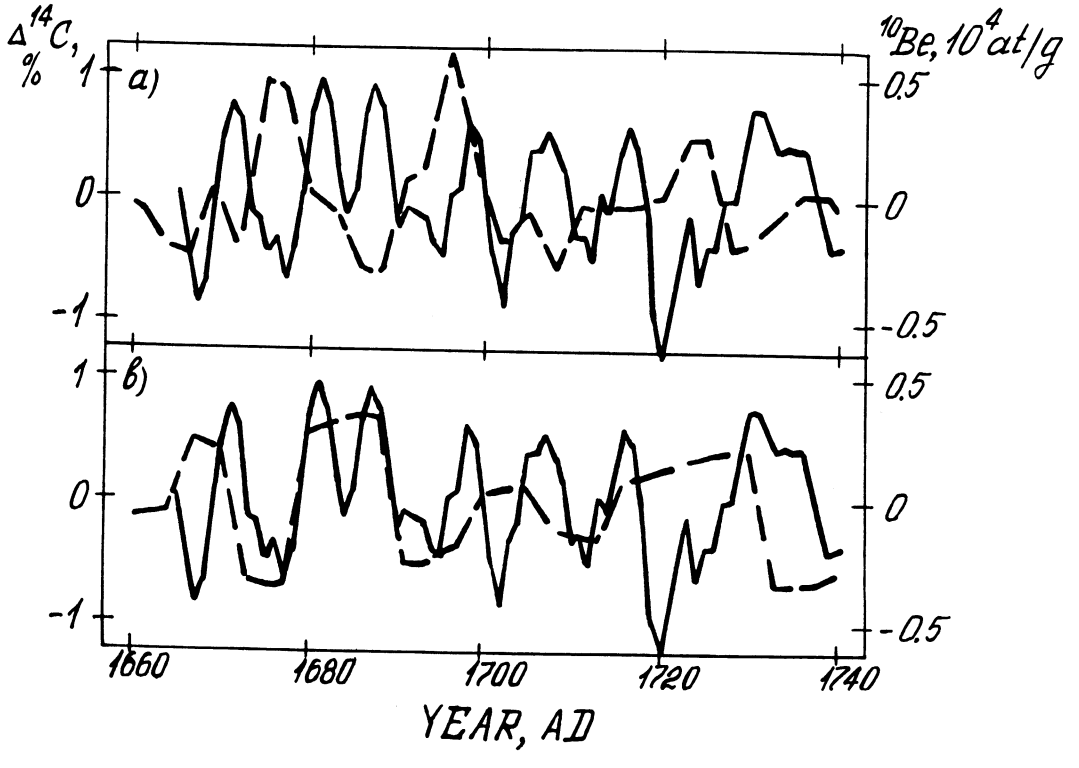

Fig. 3. Short-term variations of $\Delta^{14}C$ in the annual rings of a fir tree from the western Ukraine, AD 1665–1730 (—) and in the ^{10}Be concentration in Greenland ice cores, AD 1660–1740 (– –) from Milcent site (A) and Dye 3 station (B). Data were processed by the subtraction of trends derived by the 29-point moving average, and then by the 3-point moving average smoothing.

subtracted from all the series under consideration. We chose this method of high-pass filtering, taking into account the noisiness of these signals. Resultant series were smoothed by a 3-point moving average. Figure 3A shows comparison of our data with data for the Milcent core (Beer *et al.* 1983). Figure 3B displays data for the Camp Century core (Beer *et al.* 1984) for AD 1660–1760, which shows better agreement with the data in Figure 3A. Note, however, that the two ^{10}Be series are not in phase with each other, possibly due to the paleorainfall effect.

We also compared smoothed curves derived by first-order difference filtering, and then by a 3-point moving average to observe short-term variations in our ^{14}C series, and in the record of annual recurrence of aurorae borealis over AD 1645–1706 (Schroeder 1988) (Fig. 4). Clearly, the maxima and minima of both curves fall generally in the same time intervals, and their behaviors are in good agreement.

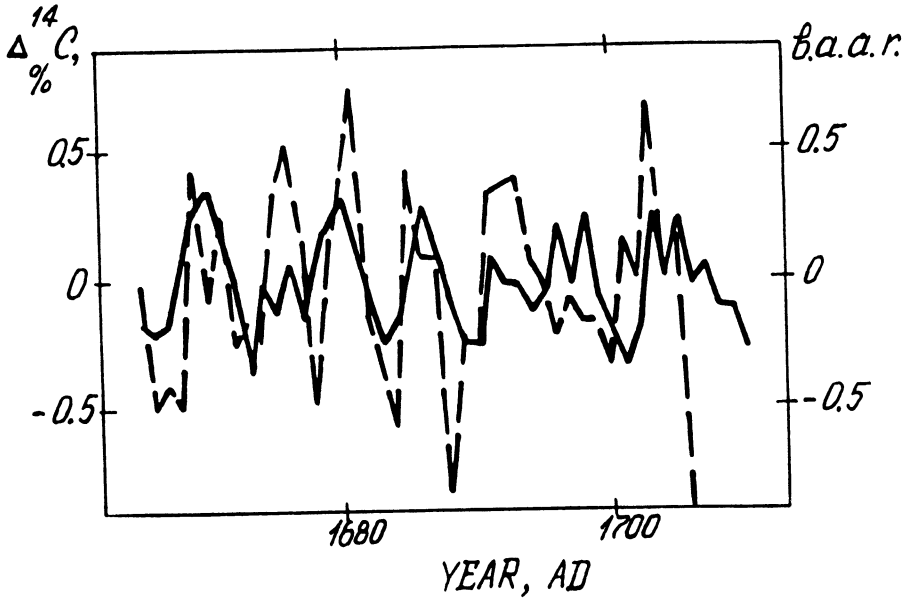

Fig. 4. Short-term variations of Δ^{14}C in the annual rings of a fir tree from the western Ukraine, AD 1665–1710 (—) and in the aurorae borealis annual recurrence, AD 1665-1706 (– –). The first-order difference and the 3-point moving average filtering were used.

CONCLUSIONS

During the Maunder minimum, radiocarbon abundance in annual tree rings changed over time; this result agrees with data on aurorae borealis recurrence and ^{10}Be variation in polar ice cores. This indicates that the intensity of galactic cosmic radiation is modulated by the Sun, even during conditions of minimal sunspot activity.

REFERENCES

Arslanov, Kh. A. 1970 Chemical preparation of tree ring samples for determination of radiocarbon abundance. *In* Kocharov, G. E., Dergachev, V. A. and Mirianashvili, G. M., eds., *Proceedings of the All-Union Consult on the Problem, Astrophysical Phenomena and Radiocarbon.* Tbilisi, Tbilisi University Publication Office: 37–40 (in Russian).

Beer, J., Andrée, M., Oeschger, H., Siegenthaler, U., Bonani, G., Hofmann, H., Morenzoni, E., Nessi, M., Suter, M., Wölfli, W., Finkel, R. C. and Langway, C. C., Jr. 1984 The Camp Century ^{10}Be record: Implications for long-term variations of the geomagnetic dipole moment. *In* Wölfli, W., Polach, H. A. and Anderson, H. H., eds., Proceedings of the 3rd International Symposium on Accelerator Mass Spectrometry. *Nuclear Instruments and Methods* B5: 380–384.

Beer, J., Siegenthaler, U., Oeschger, H., Andrée, M., Bonani, G., Suter, M., Wölfli, W., Finkel, R. C. and Langway, C. C., Jr. 1983 Temporal ^{10}Be variations. *Proceedings of the 18th International Cosmic Ray Conference* 9: 317–320.

Bitvinskas, T. T., Dergachev, V. A., Kolyshchuk, V. G., Kocharov, G. E. and Chesnokov, V. I. 1988 Tree ring analysis in astrophysical and geophysical investigations. *In* Kocharov, G. E., ed., *Experimental Methods in Research of Astrophysical and Geophysical Phenomena.* Leningrad, PhTI Publication Office: 9–55 (in Russian).

Burchuladze, A. A., Togonidze, G. I., Oganezov, P. S. and Pagava, S. V. 1970 The new type unit for the burning of samples for radiocarbon measurements. *In* Kocharov, G. E., Dergachev, V. A. and Mirianashvili, G. M., eds., *Proceedings of the All-Union Consult on the Problem, Astrophysical Phenomena and Radiocarbon.* Tbilisi, Tbilisi University Publication Office: 51–53 (in Russian).

Jenkins, J. M. and Watts, D. G. 1968 *Spectral Analysis and its Applications.* San Francisco, California, Holden-Day: 525 p.

Kocharov, G. E., Bitvinskas, T. T., Vasiliev, V. A., Dergachev, V. A., Konstantinov, A. N., Metskhvarishvili, R. Ya., Ostryakov, V. M. and Stupneva, A. V. 1985 Cosmogenic isotopes and astrophysical phenomena. *In* Kocharov, G. E., ed., *Astrophysical Phenomena and Radiocarbon.* Leningrad, PhTI Publication Office: 9–142 (in Russian).

Kocharov, G. E. and Metskhvarishvili, R. Ya. 1986 Complex of high sensitivity scintillation β-spectrometers for measurements of radiocarbon abundance in the Earth's atmosphere. *Preprint No. 1003 of A. F. Ioffe Physical-Technical Institute.* Leningrad, PhTI Publication Office, 24 p. (in Russian).

Kocharov, G. E., Zhorzholiani, I. V., Lomtatidze, Z. V., Peristykh, A. N., Tsereteli, S. S. L. and Chesnokov, V. I. 1990 On the solar activity characteristics during the past 400 years. *Pis'ma v Astronomicheskii Zhurnal* 16(8): 723–728 (in Russian).

Schroeder, W. 1988 Aurorae during the Maunder minimum. *Meteorology and Atmospheric Physics* 38: 246–251.

Vasiliev, V. A. and Kocharov, G. E. 1983 On the solar activity dynamics during the Maunder minimum. *In* Kocharov, G. E., ed., *Proceedings of the 13th International Seminar on Cosmophysics.* Leningrad, PhTI Publication Office: 75–100 (in Russian).

Zhorzholiani, I. V., Kereselidze, P. G., Kocharov, G. E., Lomtatidze, Z. V., Marchilashvili, N. M., Metskhvarishvili, R. Ya., Tagauri, Z. A., Tsereteli, S. L. and Chesnokov, V. I. 1988 Measurement of radiocarbon content in tree rings for the period 1600–1940 with corrections for isotopic fractionation. *In* Kocharov, G. E., ed., *Experimental Methods in Research of Astrophysical and Geophysical Phenomena.* Leningrad, PhTI Publication Office: 92–113 (in Russian).

[RADIOCARBON, VOL. 34, NO. 2, 1992, P. 219–225]

SUBTLE ^{14}C SIGNALS: THE INFLUENCE OF ATMOSPHERIC MIXING, GROWING SEASON AND IN-SITU PRODUCTION

PIETER M. GROOTES

Quaternary Isotope Laboratory AK-60, University of Washington, Seattle, Washington 98195 USA

ABSTRACT. Atmospheric ^{14}C concentrations vary with time and latitude. These variations, measured directly on atmospheric samples, or in independently-dated organic material such as tree rings, supply data essential for the calibration of dynamic models of the global carbon cycle. Short variations in the production rate of atmospheric ^{14}C are strongly attenuated in the relatively large atmospheric CO_2 reservoir. *In-situ* production of ^{14}C should be negligible for ages up to 80 ka BP. Background problems in AMS dating are more likely attributable to contamination of very small samples.

INTRODUCTION

A major factor in the success of radiocarbon as a dating tool is that its atmospheric residence time is long enough for atmospheric mixing to produce nearly uniform ^{14}C concentrations throughout the troposphere. Deviations from this uniformity, which can be measured directly on atmospheric samples or on organic materials, are small. These subtle deviations are, however, of considerable interest because they provide details of the cycling of carbon within a reservoir and between reservoirs, as well as of the spatial and temporal variability of the production of cosmogenic isotopes and their injection into the troposphere. Because all processes act simultaneously and semi-independently on ^{14}C concentrations, a dynamic model of the interacting atmosphere-ocean-biosphere system is needed to fully interpret observed ^{14}C concentration changes.

SPATIAL AND TEMPORAL VARIABILITY

Spatial and temporal variability in atmospheric ^{14}C concentrations have been made quite "visible" by the nuclear bomb tests of the early 1960s. The familiar increase in atmospheric $^{14}CO_2$ in the northern hemisphere shows a clear latitude dependence (Fig. 1). The maximum $\Delta^{14}C$ value obtained decreases with latitude and is delayed by one year for a lower latitude station, such as Trapani (38°02′N). The $\Delta^{14}C$ values for Nordkapp (71°06′N) and Vermunt (46°55′N) show a cross-over, with values at Vermunt being higher than those at Nordkapp in spring (20‰ May 1962, 70‰ in June 1963), but lower in fall (−50‰ in September 1962, −110‰ in October-November 1963). This dynamic behavior cannot be obtained from atmospheric box models. However, several features have already been reproduced in runs of a three-dimensional global tracer transport model (Braziunas, personal communication 1991). Detailed time series of atmospheric $^{14}CO_2$ concentrations at different locations are needed to fine-tune the model.

During the early 1960s, only a few stations collected atmospheric CO_2 samples. Consequently, we have relied on tree rings and other dated organic materials for additional information on the atmospheric response to the bomb ^{14}C input (Fig. 2). A proper interpretation of such proxy data for this period of rapidly changing $^{14}CO_2$ concentrations obviously requires that the time period when the carbon was taken up by the plant is known (see *e.g.*, the ^{14}C concentration profile of the 1963 ring of a Sitka spruce in Grootes *et al.* (1989), Fig. 1). A one-month delay in the start of the growing season, related, for example, to high elevation or latitude, increased in 1963 the average ring $\Delta^{14}C$ value by ~35‰. Samples containing carbon photo-assimilated over several months show an average $\Delta^{14}C$ value that was highest in 1964. I plotted the $\Delta^{14}C$ values for July 1, the midpoint of the growing season. The growth-weighted average time may be slightly different.

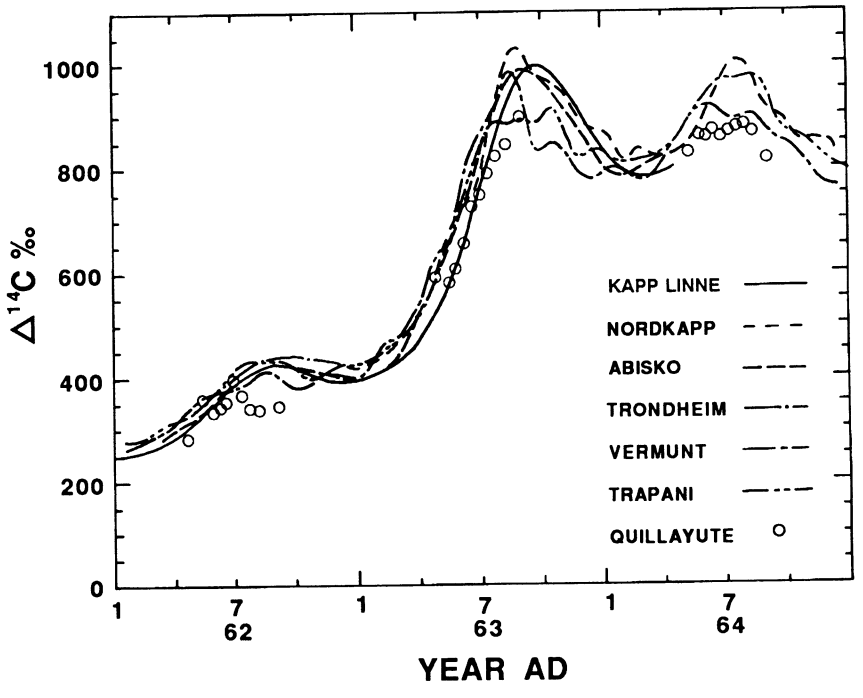

Fig. 1. ^{14}C concentrations of atmospheric CO_2 following the 1961/1962 nuclear bomb tests: Kapp Linne (78°04′N, 13°38′E) (Olsson & Karlén 1965); Nordkapp (71°06′N, 23°59′E) (Nydal & Lövseth 1983); Abisko (68°20′N, 18°49′E) (Olsson & Karlén 1965); Trondheim (63°N, 10°E) (Nydal & Lövseth 1983); Vermunt (46°55′N, 10°03′E) (Levin *et al.* 1985); Trapani (38°02′N, 12°31′E) (Münnich & Roether 1967); Quillayute Sitka spruce (47°57′N, 124°33′W) (Grootes *et al.* 1989).

The ^{14}C concentration of tree rings and other organic materials generally matches the tropospheric ^{14}C concentration quite well. Higher-latitude materials contain higher $\Delta^{14}C$, just as in the atmosphere. The Mingyin spruce (27°13′N, 100°20′E) samples the air of the 0–30° N tropical Hadley circulation cell, and, consequently, shows considerably lower $\Delta^{14}C$ values in 1963 and 1964. The Mackenzie delta white spruce shows high $\Delta^{14}C$ values for 1962 and 1963. The results from this tree have been used to argue that slow meridional mixing in the troposphere can result in significant latitudinal concentration gradients in the northern hemisphere troposphere (Dai & Fan 1986). This conclusion then supported the large (10‰) amplitude $\Delta^{14}C$ signal attributed to the 11-year sunspot cycle deduced from ring measurements on this tree (Fan *et al.* 1983, 1986). Comparison with atmospheric $\Delta^{14}C$ values at high northern-latitude stations (Trondheim, 63°N, Abisko, 68°20′N, Nordkapp, 71°06′N, and Kapp Linne, 78°04′N) shows that the ^{14}C value of 606‰ of the Mackenzie spruce (68°N) is ~150‰ higher than values observed in the atmosphere in 1962. This indicates that the sample dated as the 1962 ring included lignin and/or oils and resins of 1963 or later. Similarly, some 1964 material may contribute to the high 1963 $\Delta^{14}C$ value. Although direct atmospheric CO_2 measurements show that latitudinal $\Delta^{14}C$ gradients exist, they are significantly smaller and more variable than indicated by Dai and Fan (1986).

We may conclude that tree rings and short-lived organic materials closely monitor atmospheric $^{14}CO_2$ concentrations. The pattern of spatial and temporal variability in $\Delta^{14}C$ observed for the bomb ^{14}C in the northern hemisphere also applies to the injection into the troposphere of natural, *i.e.*, cosmogenic stratospheric ^{14}C. Provided the exact period of uptake of the measured carbon is known, and the measuring precision is adequate, tree rings can be used to determine natural latitudinal and short-term temporal variations of ^{14}C in the atmosphere.

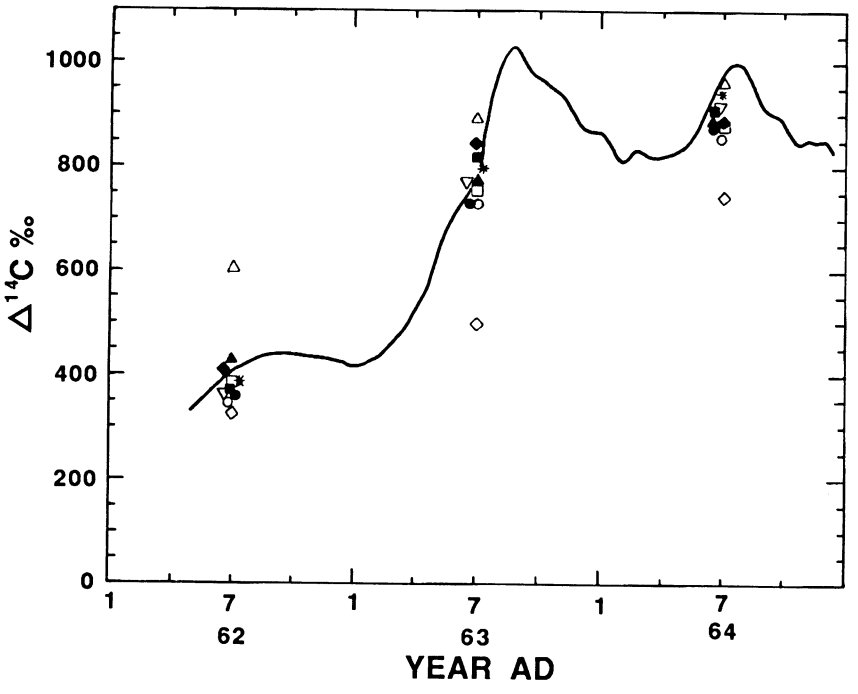

Fig. 2. Atmospheric $^{14}CO_2$ concentrations as measured at Nordkapp (71°06'N, 23°59'E) and Trondheim (63°N, 10°E) (Nydal & Lövseth 1983) and ^{14}C concentration in organic samples from various latitudes. ▵ = Mackenzie delta (68°N, 130°W) (Dai & Fan 1986); □ = Lowland USSR (60°N, 31°E) (Kolesnikov, Gorshkova & Biryulin 1970); ◇ = Mingyin, China (27°N, 100°E) (Dai & Fan 1986); ▲ = Treeless Height, USSR (Kolesnikov, Gorshkova & Biryulin 1970); ✳ = Copenhagen, Denmark (56°N, 13°E) (Tauber 1967); ♦ = Kiel, Germany (54°N, 10°E) (Willkomm & Erlenkeuser 1968); ○ = Quillayute, USA (48°N, 125°W) (Grootes *et al.* 1989); ▽ = Dailing, China (48°N, 129°E) (Dai & Fan 1986); • = New York, USA (41°N, 74°W) (Cain & Suess 1976); ■ = Georgia, USSR (38°N, 45°E) (Burchuladze *et al.* 1989).

Temporal variations of ^{14}C concentration in the atmosphere have been known since the 1950s. The advent of high-precision ^{14}C dating has led to a detailed calibration of atmospheric ^{14}C variability against tree-ring chronology throughout the Holocene. This record of ^{14}C variability has been used not only to calibrate ^{14}C dates, but also to derive the periodicity of factors influencing the ^{14}C production rate. Stuiver & Quay (1980) established two different modes by which the sun modulates cosmogenic isotope production on a century time scale. Several papers devoted to the shorter Schwabe or "sunspot" cycle, have, however, yielded conflicting conclusions about its magnitude (Baxter & Farmer 1973; Damon, Long & Wallick 1973; Burchuladze *et al.* 1980; Fan *et al.* 1986; Stuiver & Quay 1981). Using a three-dimensional global tracer transport model, Braziunas (personal communication 1991) obtains peak-to-peak values of 2–4‰ for the 11-year sunspot cycle (dependent on the strength of the solar forcing). This agrees with results of earlier box-model calculations (Damon, Long & Wallick 1973) and high-precision tree-ring measurements (Stuiver & Quay 1981). Because of its small size, the sunspot cycle in $\Delta^{14}C$ is very hard to detect, even with high-precision (≤2‰) counters. For ^{10}Be, which does not have a significant atmospheric reservoir, concentration variations corresponding to the 11-year sunspot cycle have been observed in the Dye-3 Greenland ice core (Beer *et al.* 1988).

When the tracer-transport model is used with a seasonally varying injection of stratospheric ^{14}C into the troposphere, as well as a wind-dependent ocean-atmosphere exchange, it produces a small seasonal ^{14}C concentration cycle and a latitudinal ^{14}C concentration gradient (Braziunas, personal

communication 1991). Levin *et al.* (1989) estimate 3–5‰ for the seasonal $\Delta^{14}C$ cycle in Europe. A question is whether the seasonal cycle can amplify the 11-year sunspot cycle at high latitudes. The nuclear bomb-test ^{14}C has shown little delay between the production of stratospheric ^{14}C and its injection into the troposphere. Increased ^{14}C production related to lower solar activity will be followed by increased injection of stratospheric ^{14}C into the troposphere the next year. The maximum/minimum seasonal $\Delta^{14}C$ cycles will be found when the 11-year ^{14}C concentration cycle passes through its average value. At the extremes of the ^{14}C sunspot cycle, the seasonal $\Delta^{14}C$ cycle will be of average amplitude. Thus, the seasonal $\Delta^{14}C$ cycle does not contribute to the amplitude of the 11-year sunspot cycle, and we expect an effect of the order of 2–4‰. Fan *et al.* (1983, 1986) reported larger values for a white spruce in the Mackenzie delta (10‰ peak-to-peak) as did Burchuladze *et al.* (1980) for Georgian wines (4.3 ± 1.1‰ amplitude). The highest correlation between $\Delta^{14}C$ of the white spruce and sunspot number, obtained when $\Delta^{14}C$ values were delayed by 4 yr, was −0.38 (−0.48 when the AD 1823–1833 cycle was excluded) (Fan *et al.* 1986). This correlation explains only 15% (23% with exclusion) of the observed variance, and the observed variance in the Mackenzie delta spruce is not incompatible with a much smaller true sunspot $\Delta^{14}C$ cycle in tropospheric CO_2 (See Damon *et al.* 1992).

IN-SITU ^{14}C PRODUCTION AND ^{14}C BACKGROUND

Production of ^{14}C occurs not only in the atmosphere, but also at the Earth's surface and inside the Earth by cosmic radiation and radiation from natural radioactive elements. This so-called "*in-situ*" production is the basis of exposure age dating and measurements of accumulation and erosion/ablation rates. ^{14}C production *in situ* in a sample that is to be dated or used as a background material is, however, a continuing worry for ^{14}C dating. As part of a ^{14}C enrichment and dating project, I checked the likely *in-situ* production of ^{14}C for a buried peat sample and for the anthracite used as background standard in the Groningen ^{14}C laboratory (Table 1). For these materials, the most important reaction for *in-situ* production is $^{14}N(n, p)^{14}C$ induced by low-energy (<1000 eV) neutrons. The contribution of fast neutrons to this reaction and that of reactions of the type $^{13}C(n, \gamma)^{14}C$ is small (~10%, Sawelski 1968). The neutron flux through a sample buried underground is produced by cosmic radiation (at greater depth almost exclusively muons) and by spontaneous fission reactions of uranium in the soil. We can calculate the activity of the sample due to the *in-situ* production of ^{14}C from

$$A_{is} = P(1-e^{-\lambda T}) \text{ (dpm g}^{-1} \text{ carbon)} \tag{1}$$

where P is the production rate of ^{14}C

$$P = \frac{60\phi\sigma_N N f_N}{f_C M} \text{ (^{14}C atoms min}^{-1} \text{ g}^{-1} \text{ carbon)} \tag{2}$$

λ is the ^{14}C decay constant, T is the time of exposure to neutron irradiation, 60ϕ is the neutron flux in neutrons per minute per cm^2, σ_N is the effective cross section of nitrogen for thermal neutrons, N is Avogadro's number, f_N and f_C are the relative nitrogen and carbon content of the sample expressed as weight fraction, and M is the atomic weight. If not only the reaction $^{14}N(n,p)^{14}C$ is considered, but also the combined production rate of all possible reactions, P has to be multiplied by a factor, R~1.1. The neutron flux at the position of the sample was calculated as the sum of the cosmic neutron flux and that due to uranium fission. Table 2 lists parameters used in the calculation. For the calculation of the neutron flux from ^{238}U fission, I assumed that the attenuation length of fission neutrons underground is comparable to that for cosmic-ray neutrons in water. Because the neutron capture cross-section for hydrogen is of the same order as for several of the

TABLE 1 . Description of Samples and Estimated *In-situ* Production of ^{14}C

Sample	Anthracite	Amersfoort III
Depth below surface		8.40 m
Thickness of layer		0.35 m
Sample composition		
Total dry organic material*	97%	86.5%
Carbon content	88.5%	54.2%
Hydrogen content	3.8%	5.6%
Nitrogen content	0.83%	1.1%
Uranium concentration, ash**	26 ± 5 ppm	18 ± 5 ppm
Neutron flux ϕ ($ncm^{-2}\ s^{-1}$)		
In thick sample layer†	1.9×10^{-5}	1.6×10^{-5}
In embedded layer‡	6.3×10^{-4}	4.43×10^{-4}
Due to cosmic rays		6.6×10^{-5}
Produced activity (dpm g^{-1} C)		
Thick layer	8.3×10^{-7}	7.8×10^{-6}
Embedded layer	2.8×10^{-5}	4.7×10^{-5}
Apparent age (yr BP)§		
Thick layer	1.34×10^{5}	1.15×10^{5}
Embedded layer	1.05×10^{5}	1.01×10^{5}

*Analyses carried out by J. Ebels of the Analytical Department, Chemical Laboratory, University of Groningen; C, H, and N content based on total sample. The water content of the samples can be estimated based on the fact that moist peat contains about three times more water than dry organic matter.

**X-ray fluorescence spectrometry analysis by E. A. Th. Verdurmen of Zuiver Wetenschappelijk Onderzoek Laboratory for Isotope Geology, Amsterdam.

†"Thick" means several attenuation lengths (170 g cm^{-2}) *i.e.*, several meters; the neutron production over one attenuation length is assumed to contribute to the flux.

‡Composition of the surrounding layers assumed to be equal to that of the ash

§Calculated using a recent activity of 13.56 dpm g^{-1} C (Karlén *et al.* 1964).

TABLE 2. Neutron flux parameters

		Reference*
Neutron flux ϕ at air-land interface 0.05–2.0 MeV**	2.3×10^{-3} $ncm^{-2}\ s^{-1}$	1
Relative μ meson contribution to ϕ	4%	2
Decay constant for spontaneous fission of ^{238}U, λ_{sf}^{238}	$2.7 \times 10^{-24}\ s^{-1}$	3
Decay constant for spontaneous fission of ^{235}U, λ_{sf}^{235}	$(1.1 \pm 0.7) \times 10^{-25}\ s^{-1}$	3
Average number of neutrons from ^{238}U fission	2.2 ± 0.3	3
Attenuation length of neutrons in air	~120 g cm^{-2}	4
Attenuation length of neutrons in water	169 +19/−16 g cm^{-2}	5
Attenuation length of nucleons in water	~160 g cm^{-2}	2
Attenuation length of μ mesons in water	~4000 g cm^{-2}	2
Non-cosmic neutron flux in rock	$(0.14–1.44) \times 10^{-3}$ $ncm^{-2}\ s^{-1}$	6
Thermal neutron capture cross section σ_H	$(332 \pm 2) \times 10^{-27}$ cm^2	7
σ_N	$(1.8 \pm 0.1) \times 10^{-24}$ cm^2	7

*1. Gold (1968); 2. Cocconi & Cocconi Tongiorgi (1951) and estimate; 3. Segré (1952); 4. Harkness & Burleigh (1974); 5. Bagge & Skorka (1958); 6. Sawelski (1968); 7. Goldman *et al.* (1972).

**Measured at 200 m altitude at 42°N, 88°W; geomagnetic latitude 53°N.

more important rock elements, this assumption seems reasonable. For muons and nucleons, I also assumed that the attenuation length underground is approximately equal to that in water.

I calculated the *in-situ* production (T~infinite) for two cases, one in which the sample came from a thick layer of the same composition, and the other in which the sample was embedded as a thin layer in sediments with a composition equal to that of the sample ash. The assumption that the uranium content of the overlying and underlying inorganic layers is equal to that of the ash of the organic material provides an upper limit for the fission-produced flux, since uranium tends to be enriched in organic material relative to its inorganic surroundings (Felber & Hernegger 1971). The neutron fluxes calculated for thin sample layers agree well with measured neutron fluxes in boreholes (Sawelski 1968). The apparent ages in Table 1 clearly show that *in-situ* ^{14}C production in these materials has a negligible influence for samples up to 80 ka. This is even more so because probably a fraction of the ^{14}C produced is removed during sample pretreatment (*c.f.*, Harkness & Burleigh 1974). Thus, it seems likely that the general difficulty that accelerator mass spectrometry (AMS) laboratories have with obtaining background samples without ^{14}C results from contamination of the very small samples used with ^{14}C during sample preparation, rather than from *in-situ* production of ^{14}C. Improved sample preparation should hold the key to lower backgrounds and a higher AMS ^{14}C age range.

CONCLUSIONS

Subtle variations in ^{14}C concentrations related to latitude, season and solar modulation may be revealed by high-precision measurements, and can provide important information on atmospheric mixing and the dynamics of the global carbon cycle when interpreted with dynamic 3-D atmospheric models. The magnitude of these cycles is of the order of 3–5‰. *In-situ* production of ^{14}C in carbon-rich samples is still below the current detection limit, and background problems encountered in AMS measurements must be attributed to contamination.

REFERENCES

Bagge, E. and Skorka, S. 1958. Der Übergangseffekt der Ultrastrahlungsneutronen an der Grenzfläche Luft-Wasser. *Zeitschrift Physik* 152: 34–40.

Baxter, M. S. and Farmer, J. G. 1973 Radiocarbon: Short term variations. *Earth and Planetary Science Letters* 20: 295–299.

Beer, J., Siegenthaler, U., Bonani, G., Finkel, R. C., Oeschger, H., Suter, M. and Wölfli, W. 1988 Information on past solar activity and geomagnetism from ^{10}Be in the Camp Century ice core. *Nature* 331: 675–679.

Burchuladze, A. A., Chudy, M., Eristavi, I. V., Pagava, S. V., Povinec, P., Sivo, A. and Togonidze, G. I. 1989 Anthropogenic ^{14}C variations in atmospheric CO_2 and wines. *In* Long, A. and Kra, R. S., eds., Proceedings of the 13th International ^{14}C Conference. *Radiocarbon* 31(3): 771–776.

Burchuladze, A. A., Pagava, S. V., Povinec, P., Togonidze, G. I. and Usacev, S. 1980 Radiocarbon variations with the 11-year solar cycle during the last century. *Nature* 287: 320–322.

Cain, W. F. and Suess, H. E. 1976 Carbon 14 in tree rings. *Journal of Geophysical Research* 81: 3688–3694.

Cocconi, G. and Cocconi Tongiorgi, V. 1951 Nuclear disintegrations induced by μ-mesons. *Physics Reviews* 84: 29–32.

Dai, K. M. and Fan, C. Y. 1986 Bomb produced ^{14}C content in tree rings grown in different latitudes. *In* Stuiver, M. and Kra, R. S., eds., Proceedings of the 12th International Radiocarbon Conference. *Radiocarbon* 28(2A): 346–349.

Damon, P. E., Burr, G., Cain, W. J. and Donahue, D. J. 1992 Anomalous 11-year $\delta^{14}C$ cycle at high latitudes. *In* Damon, P. E., Long, A. and Kra., R. S., eds., Proceedings of the Paleoastrophysics Workshop. *Radiocarbon*, this issue.

Damon, P. E., Long, A. and Wallick, E. I. 1973 On the magnitude of the 11-year radiocarbon cycle. *Earth and Planetary Science Letters* 20: 300–306.

Fan, C. Y., Chen, T. M., Yun, S. X. and Dai, K. M. 1983 Radiocarbon activity variation in dated tree rings grown in Mackenzie delta. *In* Stuiver, M. and Kra, R. S., eds., Proceedings of the 11th International ^{14}C Conference. *Radiocarbon* 25(2): 205–212.

_____1986 Radiocarbon activity variation in dated tree rings grown in Mackenzie delta. *In* Stuiver, M. and Kra, R. S., eds., Proceedings of the 12th International

^{14}C Conference. *Radiocarbon* 28(2A): 300–305.

Felber, H. and Hernegger, G. 1971 Über die Anreicherung von Uran in den Fossilfunden aus dem Bänderton von Baumkirchen (Inntal, Tirol). *Zeitschrift für Gletscherkunde und Glazialgeologie* BD VII: 31–40.

Gold, R. 1968 Cosmic ray neutrons near sea level. *Physics Review* 165: 1411–1422.

Goldman, D. T., Aline, P., Sher, R. and Stehn, J. R. 1972 Twenty-two hundred meter per second neutron absorption cross sections. *In Handbook of Chemistry and Physics*. CRC Press: B245.

Grootes, P. M., Farwell, G. W., Schmidt, F. H., Leach, D. D. and Stuiver, M. 1989 Rapid response of tree cellulose radiocarbon content to changes in atmospheric $^{14}CO_2$ concentration. *Tellus* 41B: 134–148.

Harkness, D. D. and Burleigh, R. 1974 Possible carbon-14 enrichment in high altitude wood. *Archaeometry* 16(2) 121–127.

Karlén, I., Olsson, I. U., Kållberg, P. and Kilicci, S. 1964 Absolute determination of the activity of two ^{14}C dating standards. *Arkiv för Geofysik* 4: 465–477.

Kolesnikov, N. V., Gorshkova, I. A. and Biryulin, Y. F. 1970 Variation of the radiocarbon concentration in the atmosphere during the period 1957–1968 (according to dendrological data). *Atmospheric and Oceanic Physics* 6(6): 647–649.

Levin, I., Kromer, B., Schoch-Fischer, H., Bruns, M., Münnich, M., Berdau, D., Vogel, J. C. and Münnich, K. O. 1985 25 years of tropospheric ^{14}C observations in central Europe. *Radiocarbon* 27(1): 1–19.

Levin, I., Schuchard, J. Kromer, B. and Münnich, K. O. 1989 The continental European Suess effect. *In* Long, A. and Kra, R. S., eds., Proceedings of the 13th International ^{14}C Conference. *Radiocarbon* 31(3): 431–440.

Münnich, K. O. and Roether, W. 1967 Transfer of radiocarbon and tritium from the atmosphere to the ocean. Internal mixing of the ocean on the basis of tritium and ^{14}C profiles. *In* Radioactive dating and methods of low-level counting. Proceedings of IAEA/ICSU Symposium, Monaco. Vienna, IAEA: 93–104.

Nydal, R. and Lövseth, K. 1983 Tracing bomb ^{14}C in the atmosphere 1962–1980. *Journal of Geophysical Research* 88: 3621–3642.

Olsson, I. U. and Karlén, I. 1965 Uppsala radiocarbon measurements VI. *Radiocarbon* 7: 331–335.

Sawelski, F. S. 1968 A further refinement of the radiocarbon dating method. *Proceedings of the Academy of Sciences USSR, Geological Series* B 180: 1189–1197.

Segré, E. 1952 Spontaneous fission. *Physics Reviews* 86: 21–26.

Stuiver, M. and Quay, P. D. 1980 Changes in atmospheric carbon-14 attributed to a variable sun. *Science* 207: 11–19.

_____1981 Atmospheric ^{14}C changes resulting from fossil fuel CO_2 release and cosmic flux variability. *Earth and Planetary Science Letters* 53: 349–362.

Tauber, M. 1967 Copenhagen radiocarbon measurements VIII. Geographic variations in atmospheric ^{14}C activity. *Radiocarbon* 9: 246–256.

Willkomm, H. and Erlenkeuser, H. 1968 University of Kiel radiocarbon measurements III. *Radiocarbon* 10(2): 328–332.

[RADIOCARBON, VOL. 34, NO. 2, 1992, P. 227–233]

COSMOGENIC NUCLIDES IN ICE SHEETS

DEVENDRA LAL

Scripps Institution of Oceanography, Geological Research Division, La Jolla, California 92093-0220 USA

and

A. J. T. JULL

NSF-Arizona Accelerator Facility for Radioisotope Analysis, The University of Arizona, Tucson Arizona 85721 USA

ABSTRACT. We discuss the nature of the twofold record of cosmogenic nuclides in ice sheets, of nuclei produced in the atmosphere, and of nuclei produced *in situ* due to interactions of cosmic-ray particles with oxygen nuclei in ice. We show that a wealth of geophysical information, in principle, can be derived from a suitable combination of nuclides in ice deposited at different latitudes. Such knowledge includes temporal changes in the cosmic-ray flux, in the geomagnetic field and in climate. The rate of deposition of cosmogenic atmospheric nuclei in ice depends on the global cosmic-ray flux and a host of climatic factors. The global cosmic-ray flux, in turn, depends on the level of solar activity, and of the geomagnetic dipole field. Thus, the task of deconvolution of the record of cosmogenic nuclides is difficult, but can be facilitated by considering the recently discovered record of *in-situ*-produced cosmogenic ^{14}C, whose production rate at high latitudes is independent of the geomagnetic dipole field (Lal 1992b). We also present a brief review of work done to date and new prospects for deciphering geophysical records using ice sheets.

INTRODUCTION

Seven long-lived cosmogenic nuclides with half-lives exceeding ten years, ^{3}H, ^{32}Si, ^{14}C, ^{36}Cl, ^{26}Al, ^{10}Be and ^{81}Kr, have been studied in polar ice (Coachman, Enns & Scholander 1958; Lal & Peters 1967; Aegerter *et al.* 1969; Fireman & Norris 1982; Elmore *et al.* 1987; Beer *et al.* 1983; Nijampurkar, Bhandari & Puri 1984; Oeschger 1985; Stauffer 1989; Craig *et al.* 1990). These investigations have focused on changes in historic/prehistoric cosmic-ray flux and terrestrial climate, and on ages of ice deposits. In this paper, we discuss applications of these nuclides for the study of prehistoric changes in cosmic-ray flux, due either to variations in the Earth's geomagnetic field or to a nearby supernova event. Thus, for this study, we do not consider the relatively short-lived nuclides, ^{3}H and ^{32}Si. We also exclude ^{36}Cl; the relation of its concentration to meteorological factors makes it difficult to correlate the record with changes in cosmic-ray flux (Elmore *et al.* 1987).

The remaining nuclides, ^{10}Be, ^{14}C, ^{26}Al and ^{81}Kr, with different half-lives, chemistry and production mechanisms, promise to be helpful in unravelling the nature of changes in the prehistoric cosmic-ray flux. Several cosmic-ray events, with rapid and slow changes have been identified in the ^{14}C record in tree rings, and in the ^{10}Be record in polar ice (Suess 1970; Kocharov 1990; Stuiver *et al.* 1991; Raisbeck *et al.* 1981, 1990, 1992; Raisbeck & Yiou 1988; Beer *et al.* 1983, 1984, 1988). However, because similar time scales are involved in climatic changes, and because these climatic changes produce significant modulations in cosmogenic records (Lal 1985, 1987), it is not always possible to assert what fraction of the amplitude modulation in the record is due to change in the cosmic-ray flux.

Two prominent records are seen in the records mentioned above:

1. The 200-year periodicity and a slow variation on time scales of 5–10 ka in $^{14}C/^{12}C$ ratios in tree rings
2. Spikes in ^{10}Be concentrations in polar ice, particularly at ~35 and 60 ka BP.

In this paper, we discuss causative mechanisms for variations in cosmogenic nuclide abundances. No consensus exists at present for causes of the prominent changes; extreme views are often presented. For example, in the case of ^{14}C variations, one group advocates that these fluctuations are due entirely to changes in the cosmic-ray flux, primarily because of changes in solar activity and in the geomagnetic field (Stuiver *et al.* 1991; Damon & Sonett 1991). Another view attributes the fluctuations to a major climatic component (Lal 1985). In the case of the ^{10}Be record in ice sheets, concentration enhancements have been attributed to an increased cosmic-ray flux due to interstellar shock waves (Sonett, Morfill & Jokipii 1987) and to nearby supernova explosions (Kocharov & Konstantinov 1983; Kocharov 1990). Lal (1987) and Lal and Lingenfelter (1991) discuss recent controversies.

INTERPRETATION OF THE COSMOGENIC RECORD

The cosmic-ray-flux incident on the Earth is more variable in time than that in interstellar space. First, the solar plasma modulates the incoming cosmic-ray flux in an energy-dependent fashion (Garcia-Munoz, Mason & Simpson 1977; Castagnoli & Lal 1980). The magnitude of production depends on solar activity, which displays a range of characteristic periods, *e.g., ca.* 11, 80, 200 and 2000 yr (Damon & Sonett 1991). The geomagnetic field of the Earth, principally the dipole field, determines the cosmic-ray flux at different geomagnetic latitudes. The field (dipole?) appears to have undergone dramatic changes in the past 80 ka (*cf.* Mazaud *et al.* 1991). The production rates of ^{14}C and ^{10}Be for different levels of solar activity and geomagnetic field intensities can be calculated fairly accurately (Lal 1988, 1992a, b).

Prior to the availability of the record of long-lived cosmogenic radionuclides in ice sheets, the most useful accessible long time series of a cosmogenic radionuclide was that of ^{14}C in tree rings. A time series now exists to ~10^5 BP for ^{10}Be (Raisbeck *et al.* 1990). Beer *et al.* (1988) compared the ^{14}C time series in tree rings with the ^{10}Be time series in ice. They concluded that both series show similar short-term trends; the 200-yr cycle in the ^{14}C record is also clearly seen in the ^{10}Be record, but the geomagnetic dipole field variation seen prominently in the ^{14}C record is not apparent in the ^{10}Be sequence. In a recent high-resolution study of ^{10}Be concentration in a south Greenland ice core from Dye 3, Beer *et al.* (1990) found a fairly large amplitude variation with a period of 11 yr.

Pre-Holocene ^{10}Be concentrations in polar ice are higher than those during the Holocene. The principal cause of this variation is believed to be lower precipitation rates during cooler periods, evidenced by the good inverse correlation between ^{10}Be concentration and $\delta^{18}O$ values of ice (Raisbeck & Yiou 1988). In the pre-Holocene ^{10}Be time series in Vostok ice, two prominent peaks are present at ~35 and 60 ka BP, which are not correlated with $\delta^{18}O$ (see Sonett 1992).

Explanations have been offered for observed oscillations and excursions in the time series of ^{14}C in tree rings and of ^{10}Be in ice sheets. Bard *et al.* (1990) extended the $^{14}C/^{12}C$ time series back to 30 ka BP, and observed larger amplitude variability than in the Holocene period. For ^{14}C, whose principal reservoir is the ocean, it may be that climatic changes, along with corresponding changes in ocean chemistry and in parameters governing atmosphere-ocean ^{14}C exchange, would strongly modulate atmospheric $^{14}C/^{12}C$ ratios. Theoretical considerations for the Holocene (Lal 1985) seem to support this. However, as mentioned above, there appears to be a general consensus that variations in $^{14}C/^{12}C$ ratios are related primarily to changes in cosmic-ray flux, due either to variation in the geomagnetic dipole field (*cf.* Damon & Sonett 1991; Stuiver *et al.* 1991; Bard *et al.* 1990), or in solar activity (*cf.* Damon & Sonett 1991; Stuiver *et al.* 1991).

A question exists regarding the cause of enhanced $^{14}C/^{12}C$ events observed in corals, and the high ^{10}Be concentration in ice samples in the (10–150) × 10^3 BP epoch. Raisbeck *et al.* (1992) recently

considered this question in detail, and concluded that the only likely reason is that ^{14}C and ^{10}Be were produced in ratios much higher than those due to the galactic cosmic-ray flux. The mechanism of this production is not yet clear; solar flare particles, supernova shock waves or γ-rays are suspected (Raisbeck *et al.* 1992; see also Sonett 1992).

Direct production of the radionuclides, ^{3}H, ^{14}C, ^{10}Be, in ice is expected from nuclear spallation of oxygen in ice. Lal, Nishiizumi and Arnold (1987) estimated their production rates; they showed that *in-situ* ^{14}C could be detected easily, but the expected concentration of *in-situ* ^{10}Be is much lower than that added to ice from the removal of atmospheric ^{10}Be, by one order of magnitude.

Thus, the application of *in-situ* ^{10}Be to ice sheets should be considered only in special cases. For example, if the rate of ice accumulation decreases rapidly, a higher *in-situ* production rate of ^{10}Be would result. In theory, then, changes in ice accumulation rates can possibly be delineated using *in-situ* ^{10}Be.

In-situ production rates of ^{14}C in surface polar ice are estimated to be 15, 38, 84, 164 and 480 ^{14}C atoms $(g\ ice \cdot yr)^{-1}$, at altitudes of 0 (sea level), 1, 2, 3 and 5 km, respectively (Lal *et al.* 1990). Recent data have shown that ^{14}C accumulated during ablation agrees well with these expectations, yielding model ablation ages for Allan Hills and Cul-de-Sac ablation ice consistent with those measured using the stake method (Lal *et al.* 1990). Measurements in progress also establish high retention of *in-situ* ^{14}C in accumulation ice (Jull & Lal, ms. in preparation).

Lal, Nishiizumi and Arnold (1987) and Lal and Jull (1990) have discussed expected concentrations of ^{14}C in accumulation and ablation ice. For a constant accumulation rate, the peak ^{14}C concentration in the ice, C_m is

$$C_m = 0.176 \frac{P_o}{s}$$

where s is the accumulation rate, and P_o is the production rate of ^{14}C in ice at the surface. Thus, the resulting concentration of ^{14}C produced *in situ* is inversely proportional to the ice accumulation rate, s, and proportional to the ^{14}C surface production rate, P_o. A similar effect is mimicked by atmospheric ^{10}Be deposited in ice by wet precipitation.

Any changes in the dipole moment of the Earth's geomagnetic field would not change the *in-situ* production rate of ^{14}C or ^{10}Be in ice in the polar regions. But the concentrations of atmospheric ^{14}C and ^{10}Be would respond to changes in the Earth's dipole field.

In light of the foregoing, we recognize three principal records (time series) of long-lived cosmogenic nuclides in ice, which contain clues to temporal variations in geophysical parameters:

1. Atmospheric cosmogenic nuclides present in air trapped during firn-ice transition, namely ^{3}He, ^{14}C and ^{81}Kr
2. Atmospheric cosmogenic nuclides deposited by wet precipitation, namely ^{3}H, ^{10}Be, ^{26}Al and ^{36}Cl
3. *In-situ* cosmogenic nuclides produced by nuclear spallation of oxygen in ice, namely ^{3}H, ^{10}Be and ^{14}C.

Nuclides in Category (1)

Temporal changes in the relative proportions of ^{3}He : ^{4}He : N_2 in trapped air in ice are expected due to changes in: 1) temperature at the base of the exosphere; 2) solar wind accretion of ^{3}He; 3) changes in the cosmic-ray production rates of ^{3}H and ^{3}He in the atmosphere. In principle, then, much useful information can be obtained from such studies. During strong polar blackout events

caused by large solar flares, or during brief periods of low or zero geomagnetic field intensity, appreciable amounts of solar ^{3}He (with $^{3}He/^{4}He$ ratios ~200 times the atmospheric value), may be accreted.

The nuclides, ^{14}C and ^{81}Kr, can provide a record of atmospheric $^{14}C/^{12}C$ and $^{81}Kr/Kr$ ratios, which depend on several parameters. The relatively shorter-lived ^{14}C provides information regarding average cosmic-ray flux over a period of *ca.* 10^{4} years prior to ice formation. This record will reflect changes in the geomagnetic field and any changes in the cosmic-ray flux due to a nearby supernova; cosmic-ray-flux modulations due to solar activity variations will largely be averaged out. On the other hand, the nuclide, ^{81}Kr (produced in thermal neutron capture by ^{80}Kr), will average out changes in solar activity and presumably the geomagnetic field, judging from variations in the geomagnetic field intensity during the past 80 ka (Mazaud *et al.* 1991). Any temporal deviations in $^{81}Kr/Kr$ ratios would then be due primarily to a nearby supernova event or other event that changes the cosmic-ray flux in the vicinity of the solar system (Sonett, Morfill & Jokipii 1987; Kocharov & Konstantinov 1983; Kocharov 1990; see also Sonett 1992).

Nuclides in Categories (2) and (3)

We have briefly outlined the observed records of ^{36}Cl and ^{10}Be in ice; concentrations derive primarily from their removal from atmospheric inventories by wet precipitation. The nuclides, ^{36}Cl (and ^{26}Al), cannot be produced significantly *in situ* in ice.

In Table 1, we show the response of different nuclides to changes in geophysical and astrophysical parameters for nuclides in categories (2) and (3). Among the nuclides considered, ^{26}Al is the only one whose concentration in ice would be sensitive to temporal changes in the flux of cosmic dust.

TABLE 1. Comments on the response of the record of cosmic-ray nuclides in ice sheets in polar/temperate latitudes to changes in cosmic-ray flux arising from three different mechanisms

Cause of change	*In-situ* production in ice sheets				Depositional flux			
	Polar regions		Temperate latitudes		Polar regions		Temperate latitudes	
	^{14}C	^{10}Be	^{14}C	^{10}Be	^{10}Be	^{26}Al	^{10}Be	^{26}Al
Geomagnetic dipole field	×	×	√	√	√ (w)	√ (w)	√ (w)	√ (w)
Solar activity	√	√	×	×	√ (w)	√ (w)	×	×
Nearby supernova	√	√	√ (w)	√ (w)	√	√	√ (w)	√ (w)

√ = a good signal is expected
(w) = a weak or a weaker signal
× = no signal is expected

It is important to note that some cosmogenic records are of *integral* type, whereas others are of *differential* type. Records of trapped ^{14}C and ^{81}Kr are integral records, whereas the record of *in-situ*-produced ^{14}C is a differential record; the depositional flux of ^{10}Be also yields a differential record. Integral records are low-pass records; higher frequencies are attenuated more severely. For example, assume that the observed excursions in ^{10}Be concentrations at 35 and 60 ka BP are due to nearby supernova explosions. If these events led to cosmic-ray-intensity increases lasting for effective average periods of ~1 ka, the average $^{81}Kr/Kr$ ratios in 0–30 ka ice may only show a small increase of ~0.7% for a 100% increase in cosmic-ray flux. The attenuation would be much less in the case of atmospheric trapped ^{14}C.

CONCLUSIONS

We have discussed three principal records of cosmogenic nuclides in ice sheets: atmospheric nuclides trapped with air occluded in ice, atmospheric nuclides deposited by wet precipitation, and nuclides produced *in situ* in ice by spallation of oxygen in ice. Records of long-lived nuclides are available in each case. Deconvolution of the records to delineate temporal changes in the following geophysical parameters: 1) cosmic-ray intensity in the heliosphere; 2) geomagnetic dipole field intensity; and 3) solar activity is complex, however. Climatic changes produce appreciable perturbations in these records. We have shown that a careful study of the three records can delineate the cause of temporal variation in each.

A case in point concerns the observed sharp changes in the concentrations of ^{10}Be in Vostok ice at ~35 and 60 ka BP. Do these constitute a record of nearby supernova explosions? If there was an appreciable change in the cosmic-ray flux in the heliosphere due to a nearby supernova, one would expect an increase in the *in-situ* ^{14}C production rate also, as well as in the ratio of ^{14}C/^{12}C in the trapped air. However, resultant changes in ^{10}Be concentration would be much larger, because the latter is an integral record.

Therefore, we hope that the current debate regarding causes for the observed oscillations and excursions in the time series of cosmogenic nuclides can be addressed from a combined study of cosmogenic records in ice and in tree rings. Studies in ice sheets in temperate latitudes would be of particular significance in describing temporal changes in the geomagnetic dipole field. It would be useful to include studies of cosmogenic ^{32}Si in ice deposited during 50–300 BP in investigating climatic effects during its removal from the atmosphere, expected to be similar to that for ^{10}Be. However, in the case of ^{10}Be, appreciable amounts can be redeposited by recirculation of atmospheric dust; this is not expected to be important in the case of ^{32}Si.

ACKNOWLEDGEMENTS

We are grateful to Drs. D. J. Donahue, G. Raisbeck and F. Yiou for discussions. This work was supported in part by NSF Grant DPP-9017827, to D. Lal.

REFERENCES

Aegerter, S., Oeschger, H., Renaud, A. and Schumacher, E. 1969 Studies based on the tritium content of the samples. *In* Renaud, A., ed., *Etudes Physiques et Chimiques sur la Glace de l'Indlandis du Groenland 1959* EGIG 1957–1960 5(3). Copenhagen, Bianco Lunos Bogtrykker A/S: 76–88.

Bard, E., Hamelin, B., Fairbanks, R. G. and Zindler, A. 1990 Calibration of the ^{14}C timescale over the past 30,000 years using mass spectrometric U-Th ages from Barbados corals. *Nature* 345: 405–410.

Beer, J., Andrée, M., Oeschger, H., Siegenthaler, U., Bonani, G., Hofmann, H., Morenzoni, E., Nesi, M., Suter, M., Wölfli, W., Finkel, R. and Langway, C. C., Jr. 1984 The Camp Century ^{10}Be record: Implications for long-term variations of the geomagnetic dipole moment. *In* Wölfli, W., Polach, H. A. and Anderson, H. H., eds., Proceedings of the 3rd International Symposium on Accelerator Mass Spectrometry. *Nuclear Instruments and Methods* B5: 380–384.

Beer, J., Andrée, M., Oeschger, H., Stauffer, B., Balzer, R., Bonani, G., Stoller, M., Suter, M., Wölfli, W. and Finkel, R. C. 1983 Temporal ^{10}Be variations in ice. *In* Stuiver, M. and Kra, R. S., eds., Proceedings of the 11th International ^{14}C Conference. *Radiocarbon* 25 (2): 269–278.

Beer, J., Blinov, A., Bonani, G., Finkel, R. C., Hofmann, H. J., Lehmann, B., Oeschger, H., Sigg, A., Schwander, J., Staffenbach, T., Stauffer, B., Suter, M. and Wölfli, W. 1990 Use of ^{10}Be in polar ice to trace the 11-year cycle of solar activity. *Nature* 347: 164–166.

Beer, J., Siegenthaler, U., Bonani, G., Finkel, R. C., Oeschger, H., Suter, M. and Wölfli, W. 1988 Information on past solar activity and geomagnetism from ^{10}Be in the Camp Century ice core. *Nature* 331: 675–679.

Castagnoli, G. and Lal, D. 1980 Solar modulation effects in terrestrial production of carbon-14. *In* Stuiver, M. and Kra, R. S., eds., Proceedings of the 10th International ^{14}C Conference. *Radiocarbon* 22

(2): 133–158.

Coachman, L. K., Enns, T. and Scholander, P. F. 1958 Gas loss from a temperate glacier. *Tellus* 10: 493–495.

Craig, H., Cerling, T. E., Willis, R. D., Davis, W. A., Joyner, C. and Thonnard, N. 1990 Krypton 81 in Antarctic Ice: First measurement of a Krypton age on ancient ice. *EOS* 71: 1825.

Damon, P. E. and Sonett, C. P. 1991 Solar and terrestrial components of the atmospheric ^{14}C variation spectrum. *In* Sonett, C. P., Giampapa, N. S. and Matthews, M. S., eds., *The Sun in Time.* Tucson, The University of Arizona Press: 360–388.

Elmore, D., Conrad, N. J., Kubik, P. W. and Gove, H. E. 1987 ^{36}Cl and ^{10}Be profiles in Greenland ice: dating and production rate variations. *In* Gove, H. E., Litherland, A. E. and Elmore, D., eds., Proceedings of the 4th International Symposium on Accelerator Mass Spectrometry. *Nuclear Instruments and Methods* B29: 207–210.

Fireman, E. L. and Norris, T. 1981 Carbon-14 ages of Allan Hills meteorites and ice. *Proceedings of the Lunar and Planetary Science Conference* 12: 1019–1025.

Garcia-Munoz, M., Mason, M. and Simpson, J. 1977 New aspects of the cosmic-ray modulation in 1974–1975 near-solar minimum. *Astrophysical Journal* 231: 263–268.

Kocharov, G. E. 1990 Investigation of astrophysical and geophysical problems by AMS: Successes achieved and prospects. *In* Yiou, F. and Raisbeck, G. M., eds., Proceedings of the 5th International Conference on Accelerator Mass Spectrometry. *Nuclear Instruments and Methods* B52: 583–587.

Kocharov, G. E. and Konstantinov, A. N. 1983 Cosmogenic nuclide ^{10}Be abundance in the ice cores and the time variation of cosmic rays. In *Conference Papers*, 18th International Cosmic Ray Conference, Bangalore, India. OG 2, OG 7-1: 333–336.

Lal, D. 1985 Carbon cycle variations during the past 50,000 years: Atmospheric $^{14}C/^{12}C$ ratio as an isotopic indicator. *In* Sundquist, E. T. and Broecker, W. S., eds., *American Geophysical Union Monograph* 32: 221–233.

_____1987 ^{10}Be in polar ice: Data reflect changes in cosmic ray flux or polar meteorology? *Geophysical Research Letters.* 14(8): 785–788.

_____1988 Theoretically expected variations in the terrestrial cosmic-ray productions rates of isotopes. *In* Castagnoli, G. C., ed., *Solar Terrestrial Relationships and the Earth Environment in the Last Millennia.* Amsterdam, North Holland: 216–233.

_____1992a Expected secular variations in the global terrestrial production rate of radiocarbon. *In* Bard, E. and Broecker, W. S., eds., *The Last Deglaciation: Absolute and Radiocarbon Chronologies.* NATO ASI Series I-2. Berlin Heidelberg, Springer-Verlag: 113–126.

_____1992b Cosmogenic *in situ* radiocarbon on the Earth. *In* Taylor, R. E., Long, A. and Kra, R. S., eds., *Radiocarbon After Four Decades: An Interdisciplinary Perspective.* New York, Springer-Verlag: 146–162.

Lal, D. and Jull, A. J. T. 1990 On determining ice accumulation rates in the past 40,000 years using *in situ* cosmogenic ^{14}C. *Geophysical Research Letters* 17(9): 1303–1306.

Lal, D., Jull, A. J. T., Donahue, D. J., Burtner, D. and Nishiizumi, K. 1990 Polar ice ablation rates measured *in situ* cosmogenic ^{14}C. *Nature* 346: 350–352.

Lal, D. and Lingenfelter, R. E. 1991 History of the sun during the past 4.5 Gyr as revealed by studies of energetic solar particles recorded in extraterrestrial and terrestrial samples. *In* Sonett, C. P., Giampapa, M. S. and Matthews, M. S., eds., *The Sun in Time.* Tucson, The University of Arizona Press: 221–231.

Lal, D., Nishiizumi, K. and Arnold, J. R. 1987 In situ cosmogenic ^{3}H, ^{14}C and ^{10}Be for determining the net accumulation and ablation rates of ice sheets. *Journal of Geophysical Research* 92: 4947–4952.

Lal, D. and Peters, B. 1967 Cosmic-ray produced radioactivity on the Earth. *In* Sitte, K., ed., *Encyclopedia of Physics* 46/2. Amsterdam, North Holland: 551–612.

Mazaud, A., Laj, C., Bard, E., Arnold, M. and Tric, E. 1991 Geomagnetic field control of ^{14}C production over the last 80 ky: Implications for the radiocarbon time-scale. *Geophysical Research Letters* 18: 1885–1888.

Nijampurkar, N., Bhandari, N. and Puri, V. M. K. 1984 Ice dynamics and accumulation rates on Changme-Khangpu glacier, Sikkim. In *Isotope Hydrology 1983.* Vienna, IAEA: 31–41.

Oeschger, H. 1985 The contribution of ice core studies to the understanding of environmental processes. *In* Langway, C. C., Jr., Oeschger, H. and Dansgaard, W., eds., Greenland Ice Core: Geophysics, Geochemistry and the Environment. *American Geophysical Union Monograph* 33: 9–17.

Raisbeck, G. M. and Yiou, F. 1988 ^{10}Be as a proxy indicator of variations in solar activity and geomagnetic field intensity during the last 10,000 years. *In* Stephenson, F. R. and Wolfendale, A. W., eds., *Secular Solar and Geomagnetic Variations in the Last 10,000 Years.* Dordrecht, The Netherlands, Kluwer Academic Publishers: 287–296.

Raisbeck, G. M., Yiou, F., Fruneau, M., Loiseaux, J. M., Lieuvin, M., Ravel, J. C. and Lorius, C. 1981 Cosmogenic ^{10}Be concentrations in Antarctic ice during the past 30,000 years. *Nature* 292: 825–826.

Raisbeck, G. M., Yiou, F., Jouzel, J. and Petit, J. R. 1990 ^{10}Be and δ^2H in polar ice cores as a probe of the solar variability's influence on climate. *Philosophical Transactions of the Royal Society of London* A330: 463–470.

Raisbeck, G. M., Yiou, F., Jouzel, J., Petit, J. R., Barkov, N. I. and Bard, E. 1992 ^{10}Be deposition at

Vostok, Antarctica during the last 50,000 years and its relationship to possible cosmogenic production variations during this period. *In* Bard, E. and Broecker, W. S., eds., *The Last Deglaciation: Absolute and Radiocarbon Chronologies.* NATO ASI Series I-2. Berlin Heidelberg, Springer-Verlag: 127–139.

Sonett, C. P., Morfill, G. E. and Jokipii, J. R. 1987 Interstellar shock waves and ^{10}Be from ice cores. *Nature* 330: 458–460.

Stauffer, B. R. 1989 Dating of ice by radioactive isotopes. *In* Oeschger, H. and Langway, C.C., Jr., eds., *The Environment Record in Glaciers and Ice Sheets.* New York, John Wiley & Sons: 123–140.

Stuiver, M., Braziunas, T. F., Becker, B. and Kromer, B. 1991 Climatic, solar, oceanic and geomagnetic influences on Late-Glacial and Holocene atmospheric $^{14}C/^{12}C$ change. *Quaternary Research* 35: 1–24.

Suess, H. E. 1970 Bristlecone-pine calibration of the radiocarbon time-scale 5200 BC to the present. *In* Olsson, I. U., ed., *Radiocarbon Variations and Absolute Chronology.* Proceedings of the 12th Nobel Symposium. New York, John Wiley & Sons: 595–612.

[RADIOCARBON, VOL. 34, NO. 2, 1992, P. 235–238]

ANOMALOUS 11-YEAR $\Delta^{14}C$ CYCLE AT HIGH LATITUDES?

P. E. DAMON, GEORGE BURR, W. J. CAIN[1] and D. J. DONAHUE

NSF-Arizona Accelerator Facility for Radioisotope Analysis, The University of Arizona, Tucson Arizona 85721 USA

ABSTRACT. We find no evidence for an anomalously intense 11-yr cycle in $\Delta^{14}C$ at high latitudes during the period, AD 1870–1885, as reported by Fan *et al.* (1983, 1986). However, there does appear to be a regional effect within the MacKenzie River region (67°N, 130°W), with atmospheric ^{14}C depressed by 2.6 ± 0.9 ($\bar{\sigma}$) ‰ relative to the Olympic Peninsula. Such an effect would require only 5% of CO_2 in the air mass to have been derived from 5% ^{14}C-depleted soil gas CO_2. This small but apparently significant regional effect could be caused by accumulation of CO_2 within the frozen earth followed by outgassing during the spring thaw. The short growing season would enhance the effect by allowing insufficient time for global atmospheric equilibration.

INTRODUCTION

Fan *et al.* (1983, 1986) reported $\Delta^{14}C$ measurements on tree rings from the MacKenzie Delta, Canada (68°N, 130°W). In order to obtain enough wood, the authors used samples that included 2 and occasionally 3 years of growth. They conclude that their results "exhibit a 10‰ fluctuation with an 11-year periodicity anticorrelated with the solar activity cycle" (Fan *et al.* 1986: 300). This amplitude is much greater than any of the theoretical models predict for a well-mixed atmosphere (*e.g.*, see Damon, Sternberg & Radnell 1983). However, it is possible that the polar continental air mass does not completely equilibrate with other global air masses during the short growing season at high latitudes where ^{14}C production rates are greater than in lower latitudes. Thus, we decided to check the results of Fan *et al.* (1983, 1986).

METHODOLOGY

Dr. Gordon Jacoby of the Lamont-Doherty Geological Observatory made available dendrochronologically dated white spruce wood from the Grand View site, MacKenzie River area of the Northwest Territory of Canada (67°N, 130°W). Thomas Harlan of the University of Arizona Laboratory of Tree-Ring Research separated individual annual rings for the years, AD 1870–1885. We chose those years because the data of Fan *et al.* (1983, 1986) show the greatest variation during that period.

Wood from the individual years was converted to cellulose by the technique described by Linick *et al.* (1986b). After burning the cellulose to obtain purified CO_2 gas, we converted it to graphite by the catalytic reaction described by Slota *et al.* (1987). The milligram-size graphite sample was then pressed at high pressure into a cup within an aluminum "target" holder and inserted into a ten-position ion source carousel. The carousel typically contains 2 standards (NBS oxalic acid I and II), 1 background sample and 7 sample targets. We then proceeded with tandem accelerator mass spectrometer (AMS) analysis, after mounting the carousel and pumping down to below 10^{-6} torr, as described in detail by Linick *et al.* (1986a).

The analysis provides the measured ratio, $^{14}C/^{13}C$, for the samples and standards. The ratios are appropriately corrected for isotopic fractionation, and the ratio of the standards are calculated to AD 1950 (see Donahue, Linick & Jull 1990 for details). From the corrected ratios, a fraction modern is obtained, defined as

$$F = \frac{(^{14}C/^{13}C)_{sample}}{(^{14}C/^{13}C)_{STD}} \quad . \qquad (1)$$

[1]Department of Chemistry, Loyola-Marymount University, Los Angeles, California 90045 USA

The quantity, F, is then used in Equation 2

$$\Delta^{14}C = [Fe^{\lambda(1950-t_{cal})}-1)\ 1000. \quad (2)$$

Calculations of $\Delta^{14}C$ are based on the 5730-year half-life ($\lambda = \frac{1}{8270}$ yr^{-1}), and time is measured in calendar years.

RESULTS

The results are given in Table 1, and plotted along with the data of Fan *et al.* (1983, 1986) and Stuiver and Quay (1981) in Figure 1. Our result at 1870 is clearly anomalous. Four targets were measured at different times over a period of about 14 months. There is no significant difference in the measurements during that time, and we have no reason to doubt the result (Table 2). We have arranged to obtain more wood to repeat the 1870 measurements and obtain measurements for the previous decade. Our other results, in per mil units, average −7.0 ± 0.7 ($\bar{\sigma}$), with any signal masked by the measurement error. The same is true for the data of Fan *et al.* that average −6.8 ± 2.6 ($\bar{\sigma}$). Except for the one datum from 1876, all of their data overlap at 1σ error with our high latitude data, and there is no significant difference between the means of the two results. However, the mean of the Stuiver and Quay Seattle data, −4.4 ± 0.3 ($\bar{\sigma}$) for the period, 1870–1885, is significantly different from our mean at the 95% confidence level. The difference between these two means is 2.6 ± 0.9 ($\bar{\sigma}$).

The question arises whether or not there is any significant variation in $\Delta^{14}C$ for the high-precision $\Delta^{14}C$ data of Stuiver and Quay. We observe that their data are lower, 3.2 ± 0.6 ($\bar{\sigma}$), during the years, 1870–1879, inclusive, than during the following years 1880–1885, inclusive, 5.2 ± 0.6 ($\bar{\sigma}$).

TABLE 1. Analytical data for cellulose from annual tree rings from the Grand View site, NWT (67°N, 130°W)

Date (AD)	F_m*	Poisson (σ)**	σ(N)†	N	$\Delta^{14}C$‰	$\delta^{13}C$
1870	1.0000	0.0033	0.0022	4	9.7	−22.8
1871	0.9832	0.0030	0.0050	4	−7.4	−22.7‡
1872	0.9865	0.0035	0.0037	3	−4.1	−21.8
1873	0.9824	0.0038	0.0040	3	−8.4	−22.7
1874	0.9823	0.0037	0.0017	3	−8.6	−22.7‡
1875	0.9811	0.0037	0.0023	4	−10.0	−22.7‡
1876	0.9836	0.0033	0.0055	4	−7.6	−23.1
1877	0.9868	0.0037	0.0089	3	−4.4	−22.7‡
1878	0.9836	0.0040	0.0061	4	−7.8	−21.8
1879	0.9840	0.0032	0.0038	4	−7.5	−22.7‡
1880	0.9814	0.0041	0.0023	3	−10.3	−22.7‡
1881	0.9836	0.0054	0.0085	2	−8.2	−23.1
1882	0.9874	0.0032	0.0020	4	−4.4	−22.7‡
1883	0.9810	0.0034	0.0034	3	−11.0	−22.7‡
1884	0.9873	0.0034	0.0038	3	−4.8	−23.3
1885	0.9906	0.0030	0.0012	4	−1.6	−22.7‡
					Avg ^{13}C =	−22.68‰
					1σ =	0.39‰

*Weighted average; **Counting statistics; †Standard deviation for N separate analyses; ‡Average of seven analyses

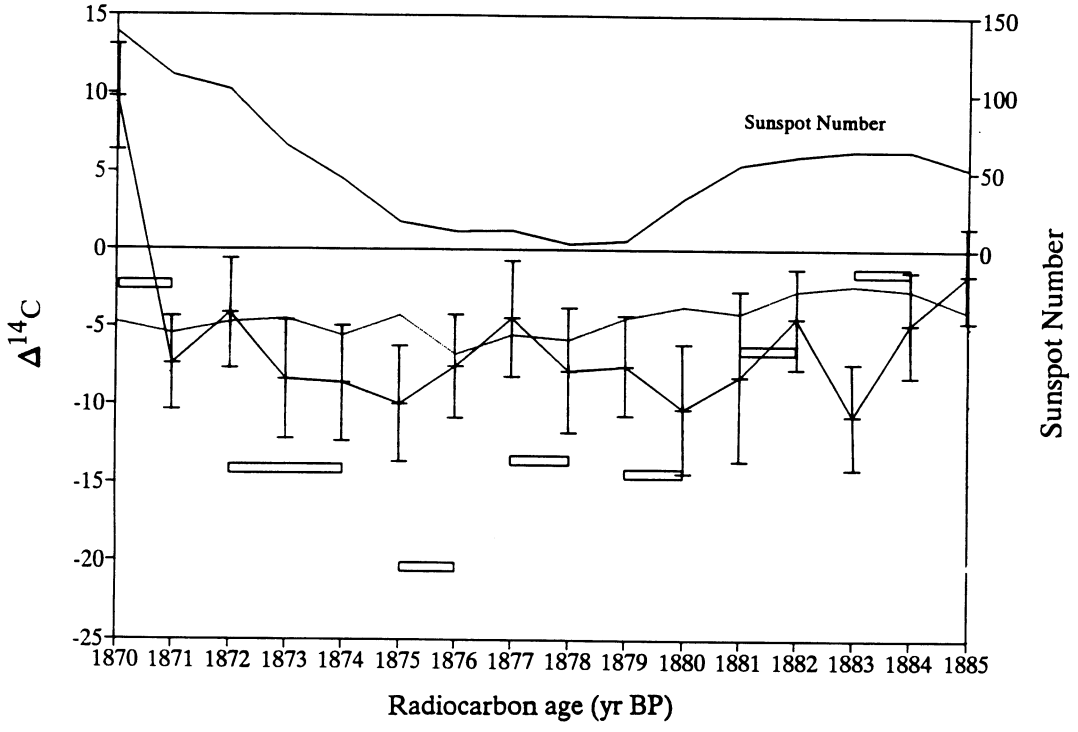

Fig. 1. $\Delta^{14}C$ data for MacKenzie River samples (67–68°N, 130°W) compared with high-precision data from the Olympic Peninsula. ┼ = this work; ▭ = Fan *et al.* (1983, 1986); — = Olympic Peninsula data of Stuiver and Quay (1981). Sunspot number is shown for comparison.

TABLE 2. Fraction modern, F_m, for the anomalous result for AD 1870 cellulose

Date of analysis	Fm	Poisson (σ)
7/27/89	1.0006	0.0068
9/18/90	1.0067	0.0081
10/02/90	0.9974	0.0061
10/03/90	1.0057	0.0058
Weighted average	1.0000	0.0033

The difference, 2.0 ± 0.8 ($\bar{\sigma}$), is significant at the 95% confidence level. This variation is consistent in amplitude, but not in phase with expectation for solar modulation of the galactic cosmic-ray flux, assuming a well-mixed troposphere (Damon, Sternberg & Radnell 1983). Such small variations can be due to various factors, including the tendency for solar and galactic cosmic rays to be anticorrelated (Lingenfelter & Ramaty 1970; Damon, Cheng & Linick 1989).

CONCLUSION AND DISCUSSION

The following conclusions seem to be warranted by the data:

1. There is no evidence for an anomalously intense 11-year cycle at high latitudes in the MacKenzie River area during the time period, AD 1870–1885.
2. There is a difference of 2.6 ± 0.9 ($\bar{\sigma}$) between $\Delta^{14}C$ values from the Olympic peninsula

samples and the high-latitude samples.

3. It is necessary to make more measurements to verify the existence of our anomalously high $\Delta^{14}C$ measurement at 1870.

We suggest that the regional effect may be due to accumulation of ^{14}C-depleted CO_2 within the frozen earth under the snow blanket and release into the atmosphere during the spring thaw. Such an effect has been observed for radon in Ontario, Canada (Jonasson & Dyck 1978). Messerschmidt (1933) attributed high atmospheric concentrations of radon in April and May, to the spring thaw in Germany. Dörr and Münnich (1986) measured seasonal ^{14}C variations in soil CO_2 in a beech/spruce forest in the Rhine Valley, Germany. They found a 10% reduction in $\Delta^{14}C$ values for soil gas collected during the winter, as compared with summertime values. The effect observed for the MacKenzie Delta could be produced if 5% of atmospheric CO_2 had been derived from 5%-depleted soil gas CO_2. The effect would be enhanced by the short growing season at high latitudes and continuing thawing of the frozen tundra during that time.

ACKNOWLEDGMENTS

We thank Dr. Gordon Jacoby for providing the dendrochronologically dated wood from the MacKenzie Valley and Thomas Harlan for preparing the single-year samples. Robert Kalin was responsible for preparing cellulose from the wood samples. We are grateful to him and also Larry Toolin for preparing some targets and overseeing preparation of others. This work was supported by NSF Grants EAR-8822292, ATM-8919535 and the State of Arizona.

REFERENCES

Damon, P. E., Cheng, S. and Linick, T. W. 1989 Fine and hyperfine structure in the spectrum of secular variations of atmospheric ^{14}C. *In* Long, A. and Kra, R. S., eds., Proceedings of the 13th International ^{14}C Conference. *Radiocarbon* 31(3): 704.

Damon, P. E., Sternberg, R. S. and Radnell, C. J. 1983 Modeling of atmospheric radiocarbon fluctuations for the past three centuries. *In* Stuiver, M. and Kra, R. S., eds., Proceedings of the 11th International ^{14}C Conference. *Radiocarbon* 25(2): 249–258.

Donahue, D. J., Linick, T. W. and Jull, A. J. T. 1990 Isotope-ratio and back ground corrections for accelerator mass spectrometry radiocarbon measurements. *Radiocarbon* 32(2): 135–142.

Dörr, H. and Münnich, K. O. 1986 Annual variations of the ^{14}C content of soil and CO_2. *In* Stuiver, M. and Kra, R. S., eds., Proceedings of the 12th International ^{14}C Conference. *Radiocarbon* 28(2A): 338–345.

Fan, C. Y., Chen, T. M., Yun, S. X. and Dai, K. M. 1983 Radiocarbon activity variation in dated tree rings grown in MacKenzie Delta. *In* Stuiver, M. and Kra, R. S., eds., Proceedings of the 11th International ^{14}C Conference. *Radiocarbon* 25(2): 205–212.

_____1986 Radiocarbon activity variation in dated tree rings grown in MacKenzie Delta. *In* Stuiver, M. and Kra, R. S., eds., Proceedings of the 12th International ^{14}C Conference. *Radiocarbon* 28(2A): 300-305.

Jonasson, I. R. and Dyck, W. 1978 Dissolved gases in snow-melt waters. *Chemical Geology* 21: 15–24.

Lingenfelter, R. E. and Ramaty, R. 1970 Astrophysical and geophysical variations in ^{14}C production. *In* Olsson, I. U., ed., *Radiocarbon Variations and Absolute Chronology*. Proceedings of the 12th Nobel Symposium. New York, John Wiley & Sons: 513–537.

Linick, T. W., Jull, A. J. T., Toolin, L. J. and Donahue, D. J. 1986a Operation of the NSF-Arizona accelerator facility for radioisotope analysis and results from selected collaborative research projects. *In* Stuiver, M. and Kra, R. S., eds., Proceedings of the 12th International ^{14}C Conference. *Radiocarbon* 28(2A): 522–533.

Linick, T. W., Long, A., Damon, P. E. and Ferguson, C. W. 1986b High-precision radiocarbon dating of bristlecone pine from 6554 to 5350 BC. *In* Stuiver, M. and Kra, R. S., eds., Proceedings of the 12th International ^{14}C Conference. *Radiocarbon* 28(2B): 943–953.

Messerschmidt, W. 1933 Eine neue Untersuchung der Zusammenhänge mit der Meteorologischen Factoren und des Einflusses den Emanations-gehältes der Atmosphäre auf die Messungen der Ultrastrahlung. *Zeitschrift für Physik* 81: 84–100.

Slota, P. J., Jr., Jull, A. J. T., Linick, T. W. and Toolin, L. J. 1987 Preparation of small samples for ^{14}C accelerator targets by catalytic reduction of CO. *Radiocarbon* 29(2): 303–306.

Stuiver, M. and Quay, P. D. 1981 Atmospheric ^{14}C changes resulting from fossil fuel CO_2 release and cosmic ray variability. *Earth and Planetary Science Letters* 53: 349–362.

[RADIOCARBON, VOL. 34, NO. 2, 1992, P. 239–245]

A SUPERNOVA SHOCK ENSEMBLE MODEL USING VOSTOK ^{10}Be RADIOACTIVITY

C. P. SONETT

Department of Planetary Sciences and Lunar and Planetary Laboratory, The University of Arizona
Tucson, Arizona 85721 USA

ABSTRACT. Analysis of the Vostok ice-core record of ^{10}Be (Raisbeck *et al.* 1987) suggests that the sharply resolved increases in ^{10}Be at 35 ka (kyr) and 60 ka are due to cosmic-ray (CR) increases. As an alternate to long-term solar modulation or strong decreases in the Earth's magnetic field, supernova (SN) forcing is qualitatively consistent with the generation of a forward-reverse shock ensemble from a spherical blast wave of age very approximately at 75 ka. This age agrees with Davelaar, Bleeker and Deerenberg's (1980) identification of 75 ka for the age of a North Polar Spur SN remnant. Confirmation would be the first geochemical detection of supernova forcing of spallogenic and perhaps cosmogenic isotope production in the atmosphere. The three ^{10}Be increases can be satisfied by a modification of the Sonett, Morfill, and Jokipii (1987) model. This consists of 2 or 3 shock waves from a single SN event, which includes the first stage in the expansion, leading to a forward shock, S_{1+}, and a pair of reverse waves, S_{1-} and S_{2-}. One reverse wave arises from the spherical expansion, itself, and the other is a reflected wave from a remnant precursor shell boundary from a more ancient SN. The model requires the solar system to be immersed in the 'bubble' of the earlier post-SN evolution, possibly affecting estimates of heliospheric boundary distance. However more recent analysis of Camp Century ice core data discloses only the 35 ka ^{10}Be peak. This recent result compounds the difficulty of constructing a completely consistent model for the source of the Vostok spikes. This paper is written in the spirit of suggesting only one of possibly several different models, even within the subclass of SN models.

INTRODUCTION

This paper is a qualitative exploration of a model for the origin of the large ^{10}Be increases discovered in the Vostok ice core by Raisbeck and collaborators. Of the several possible explanations of these increases, I confine my discussion to the proposition that the source of the increases is an enhancement of the cosmic-ray (CR) flux at the top of the atmosphere. The seminal aspect is the source of these increases, which are supposedly the result of interstellar shock waves originating in the interaction of an ancient relatively close supernova (SN) with the ambient interstellar medium. Some aspects of the model fit the data qualitatively, whereas others are more speculative, and no claim is made to their certainty.

Radioactive ^{10}Be from the Vostok ice core discloses three peaks in the record, D_2 at 60 ka before present (BP), only 25 ka from a close pair, D_{1a} and D_{1b} in the neighborhood of 35 ka BP[1] (Fig. 1), uncorrelated with accompanying δ^{18}O. (Raisbeck and Yiou (1991) have reported additional uncorrelated ^{2}H.) An upper bound to the separation of D_{1a} and D_{1b} can be estimated as *ca.* 2 ka. An additional core from Dome C is sufficiently long to confirm the presence of the 35 ka peaks, although the two are unresolved (Raisbeck *et al.* 1987).

Detection of SN relics, either direct or secondary, has been a long-sought-after goal; *e.g.*, Lingenfelter (1969) and Higdon and Lingenfelter (1973) proposed the detectibility of enhanced cosmogenic nuclide production from SN cosmic rays. (See also Kocharov *et al.* 1991.) A prompt gamma flash has also been proposed as the source of thermoluminescence (Castagnoli, Bonino & Miono 1982). Such cosmogenic production has generally relied upon either simple streaming or diffusion for transport of SN cosmic rays through interstellar space. The principal long-lived radionuclides produced by CRs in the atmosphere are ^{10}Be and ^{26}Al (Peters 1957). Though of significantly shorter half-life, ^{14}C also may be of interest to the shock model discussed here.

[1]Raisbeck and Yiou (1991) and Raisbeck (personal communication) report the closely spaced increases in the neighborhood in of 35 ka, but Raisbeck *et al.* (1987) did not report these earlier. Figures in this paper reflect the earlier data.

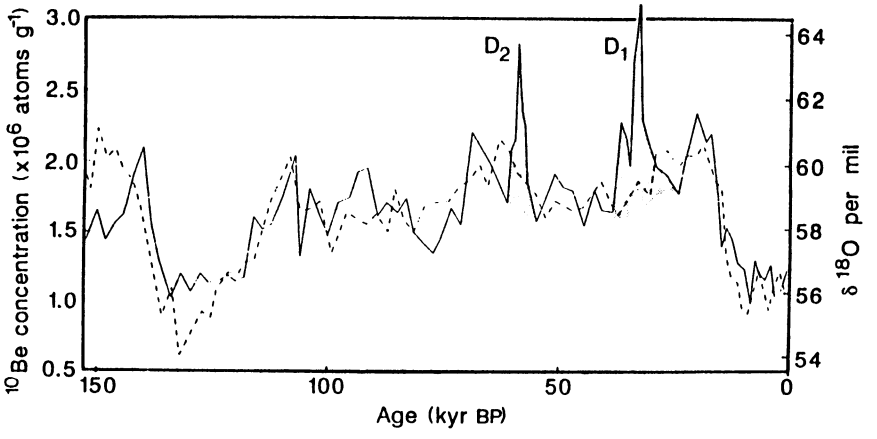

Fig. 1. — = Concentrations of ^{10}Be; - - - - = δ^{18}O from 150 ka to present. Spikes marked by D are putative interstellar shock signatures, D_1 representing the reverse shock, S_-, and D_2, the forward shock, S_+. (Figure adapted from Raisbeck *et al.* 1987).

The model explored here is an extension of that by Sonett, Morfill and Jokipii (1987). It differs in that the CR required for cosmogenic production, though arising from one SN, yields a sequence of shock waves corresponding to the enhancements seen in the ^{10}Be record, but as previously, the cosmogenic and spallogenic production arises from CRs accelerated locally from the interstellar medium (ISM). Thus, its association with SN is with the formation of interstellar shock waves and not necessarily with SN debris.

Qualitative analysis of the mean ages of $D_{1a,b}$ and D_2, based on a Sedov (1959) expansion, yielded an SN age of 45 ka (Sonett, Morfill & Jokipii 1987). The more complete model discussed here accounts for all three increases in the ^{10}Be record, in terms of an SN expansion in a pre-existing remnant bubble from the expansion of a more ancient SN. The age estimate is then determined from the oldest (60 ka) of the three ^{10}Be enhancements. The new shock model age is in reasonable accord with models based primarily upon rocket X-ray, neutral hydrogen and radio data.

Alternate ^{10}Be enhancement mechanisms

Raisbeck *et al.* (1987) discuss four possible sources of the Vostok ^{10}Be enhancements: 1) a decrease in interplanetary CR modulation due to a concomitant decrease in solar activity (perhaps a kind of timewise superMaunder minimum); 2) a decrease in the intensity of the geomagnetic field leading to a corresponding increase in the galactic cosmic-ray (GCR) flux; 3) a change in the atmospheric circulation pattern increasing the transport of cosmogenic Be from the stratosphere to the troposphere; and finally, by way of elimination, 4) a basic increase in the GCR flux. Raisbeck *et al.* (1987) do not favor the possibility of a change in atmospheric circulation, but they do not rule it out completely.

A Maunder-like decrease in solar modulation lasting several thousand years, and so irregular as to correspond jointly to the time separations of $D_{1a,b}$ and D_2 and to the multithousand-year decreases, seems implausible. Unfortunately, the data needed to test this are available only by proxy from the ^{14}C record, which is far too short.

The possibility of geomagnetic reversals underlying the Vostok CR enhancements cannot be fully ruled out, although recent work decreases the likelihood significantly (Tric *et al.* 1992). Anomalous

geomagnetic field values reported from Lake Mungo, Australia (McElhinny & Senanayake 1982) may be due to lightning strikes (McElhinny, personal communication), and Puy de Laschamp (Bonhommet & Babkine 1967) measurements are controversial. Lac du Bouchet shows no evidence for a reversal or excursion of the field in the neighborhood of 30 ka (Creer, personal communication). The Chaîne des Puys discloses two reversals in the Quaternary (Bonhommet & Zahringer 1969), but the ages are in conflict with ^{14}C measurements.

Because the Vostok site is presently almost at the south geomagnetic dip pole, there ought to be no significant local rigidity cutoff (Raisbeck *et al.* 1987). However, the net ^{10}Be flux at the poles is dependent not just on local production, but also upon global production. Note, however, that secular drift of the pole away from the Vostok location would decrease rather than increase cosmogenic production, although sensitivity to reversals would be increased.

The production of ^{10}Be is a strong function of latitude, varying by a factor of 10 to 100 from equator to pole (Lal & Peters 1967); the peak production rate is achieved at 15 km altitude at most latitudes. Although the production rate is maximum at the poles, the solid-angle factor favors the equator; the effect is to reduce the latitude-dependence of production and enhance the equatorial contribution. Raisbeck *et al.* (1981) discussed the possibility of a change in atmospheric circulation possibly increasing the stratosphere/troposphere exchange. Because the stratosphere is estimated to provide 70% of ^{10}Be production and the troposphere 30%, the polar reservoir of Be to some extent depends upon transfer from the global reservoir and also from the stratosphere downward. A change in the atmospheric transfer system would be required to satisfy the Vostok data. Although this cannot be ruled out, the modification would mean a basic change in the thermal structure. There is no evidence to support such a drastic requirement.

SHOCK SYSTEM GEOMETRY

Spherical explosions yield an ensemble of waves (Taylor 1946; Courant & Friedrichs 1948; Kuo 1947; Friedman 1961; Boyer 1960; Brode 1955, 1959; Sedov 1959; Parker 1963). All produce an initial forward wave, S_{1+}, which progresses outward into the ambient interstellar medium (ISM). The wave is followed in order by the shocked ISM, a contact surface or tangential discontinuity, and finally, a system of reverse and reflected waves. The expansion of the driver gas is initially adiabatic and, following ejection of most of the SN mass, if continued into a pileup of ISM, becomes radiatively dominated because of the increased interaction as a result of the enhanced density. Figure 2 shows a schematic from a calculation of Boyer for a laboratory-scale explosion.

Shock expansion, S_{1+}, requires a rearward moving rarefaction, R_1, to establish continuity between the outward-directed post-shocked flow and expanding source gas. Because of the divergence in a cylindrical or spherical expansion, an additional rearward facing shock, S_{1-}, is required to connect the flow behind S_{1+} and that through which R_1 has just passed. S_{1-} progresses towards the origin of the explosion, but is convected outward in the post-shocked flow behind S_{1+}. As witnessed in Eulerian laboratory coordinates, S_{1-} is initially swept out faster than it propagates inward. This is analogous to the forward-reverse shock pair in the solar wind (Sonett & Colburn 1965; Colburn & Sonett 1965; Simon & Axford 1966; Sturrock & Spreiter 1966). Secondary, tertiary and progressive reflections can yield a virtual barrage of subsequent waves, which eventually damp into thermal motions. The model discussed here makes the reasonable assumption that the ^{10}Be spikes are associated with the immediate expansion after the onset prior to any plausible secondary reflections.

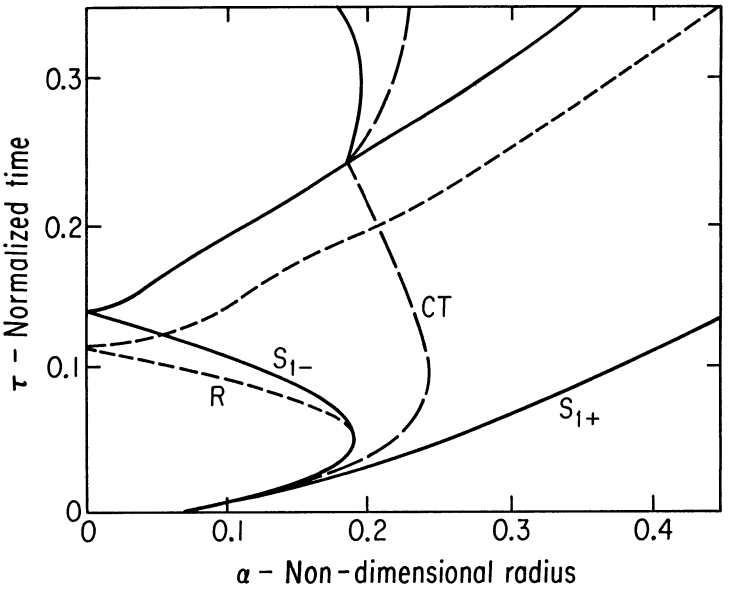

Fig. 2. Example of a shock system arising from the spherical expansion of a blast wave. Waves evolve from the lower part of the figure, expanding to the right. S_{1+} is the forward shock; it progresses to the right followed by a contact discontinuity (CD) (- - -), separating the post-shocked gas behind S_{1+} from the driver gas, reverse shock wave, S_{1-} (—), and rarefaction, (R), which, together with reverse shock, is first swept out, and then, at the end of expansion, reverses (lab coordinates), and progresses to the origin. Subsequent conditions (including reflection at the origin) are indicated qualitatively. The x-axis defines the radius normalized by the quantity, $\alpha = w/P_0$, where w is the total initial system energy, and P_0 the initial pressure; the y-axis is time-normalized by $\tau = \alpha/C_0$, where C_0 is the speed of sound squared (adapted from Brode 1959). This shock configuration is shown to qualitatively indicate the expected expansion regime, though details may differ in the SN case discussed in the paper.

THE PRE-EXISTING SUPERNOVA SCENARIO

An important modification of this scenario results from the case of the SN exploding within a pre-existing remnant bubble formed from a previous SN. In this case, as the boundary of the bubble is a leftover region of enhanced density and temperature, it represents a discontinuity of enhanced sound speed to S_{1+}, resulting in both a transmitted, S_{2+}, and reflected, S_{2-} shock (Courant & Friedrichs 1948). Because S_{2-} moves in the post-shocked flow of S_{1-}, by definition being a shock, it eventually overtakes and merges with S_{1-}.

In the progression of events noted in the Eulerian (laboratory) frame, S_{1+} passes over the observer, O, at time, T_1, a contact surface (or in hydromagnetics, a tangential discontinuity, (TD), at time, T_2, and no other discontinuity is detected so long as the velocity of the reverse shock, S_{1-}, never satisfies $v_{1-} - v_c < 0$, where v_c is the lab velocity (outward) of the post-shocked flow behind S_+. The reverse shock is predicted to eventually leave a second CR record because of a final passage inbound to the supernova when $v_{S1-} - v_c < 0$ is satisfied. The turning point where velocity reversal takes place, $dr/dt = 0$ or $v_{1-} - v_c = 0$ is mentioned for completeness, but its detection would be less probable.

THE FORWARD SHOCK, S_f

In the model explored in this paper, the sequence of hypothesized shock waves yielding the atmospheric spallogenic ^{10}Be is encountered in the remnant bubble. Otherwise, if S_{1+} or S_{2+} were

outside the bubble, S_{1-} and S_{2-} would not display an interaction with the heliosphere. Calculation of the properties of the forward shock, S_{1+}, is easier than for S_{1-} or S_{2-}. Following the earlier Sonett *et al.* calculation, and using the same plasma parameters, the age of the explosion is modified to 72 ka. This value is 75% of that deduced by Cox and Anderson (1982) for a putative SN. The post-shock flow behind S_{1+} is unsteady and varies with time. Passage of the TD over the heliosphere is not accompanied by a change in the CR flux.

THE REVERSE AND REFLECTED SHOCKS, S_{1-} AND S_{2+}

To some extent, the 35 ka Vostok events are complicated by the bifurcated peak recently reported by Raisbeck and coworkers. The theory of point explosions does not account for a dual shock with the small separation indicated in the data. But if the explosion takes place within the confined volume of the bubble of a previous SN (Borken & Iwan 1977), then a shock, additional to the basic reverse wave, is created *via* a reflection, when S_{+1} reaches the bubble boundary (Courant & Friedrichs 1948). As the boundary consists of hotter gas with higher sound speed, the system finally consists of a forward wave, S_{+1}, propagating within the bubble cavity up to the boundary, S_{+2}, propagating into fresh ambient ISM, the reverse wave, S_{1-}, and the reflected wave, S_{2-}. As noted earlier, this model requires that the solar system is immersed within the bubble, so that the cosmo- and/or spallogenic consequences of the panoply of waves can be observed from within the solar system.

CANDIDATE SUPERNOVAE SHOCK SOURCES

Using v_f = 1000 km for the speed of s^{-1}, and an age of 72 ka from the ^{10}Be estimate, I calculate a span of 2×10^{15} km or 60 parsec (pc). Davelaar, Bleeker and Deerenberg (1980) report that a SN remnant associated with the North Polar Spur (NPS) has an age of 75 ka, originating in an explosion within a region of already anomalously low density (10^{-2} cm^{-3}). Berkhuijsen (1973) reports a distance to Loop I center of 130 ± 75 pc.

A major difficulty in reconciling various NPS radio and x-ray parameters is the differing age estimates for the (old) dense H1 region and the (young) x-ray data (Egger 1991). This problem has led to the model of Borken and Iwan (1977) of a SN exploding in the pre-existing relict shell of a more ancient SN event (E = 6×10^{50} ergs, density = 10^{-3} gm/cm^3, and temperature = 2×10^6 K). A second, somewhat less preferred, source is the Cygnus shell (Higdon 1981); identification with the NPS seems preferable, on the basis of age and distance estimates.

20,000–30,000-YEAR-OLD ^{14}C

Using uranium-thorium systematics, Vogel (1983) found a ^{14}C level in a stalactite from the Cango caves, South Africa, elevated to twice nominal at 35 ka ago, followed by a dip to just below normal at 28 ka ago, and finally, 1.5 times nominal (based on U-Th) at 18 ka ago (Fig. 3). Qualitatively, this behavior mimics the ^{10}Be values seen in Figure 1, and strongly implies that the spallogenic production of ^{10}Be at both 35 and 60 ka was accompanied by a corresponding cosmogenic production increase of ^{14}C. The increase of ^{14}C at 18 ka is less certain, for it appears to be accompanied by an increase in ^{18}O.

Dating of Barbados coral (Bard *et al.* 1990), also using U-Th as a standard, shows ^{14}C elevated by a factor of 2 to 4 in the 20–30 ka interval (referred to unit amplitude per Vogel (1983)). Whether part or all of this elevation of the atmospheric inventory of radiocarbon is related to the putative SN is uncertain. But the Bard *et al.* (1990) data errors prevent any disclosure of a putative double maximum, as noted in Vogel's (1983) results. These extraordinary changes in the ^{14}C inventory are

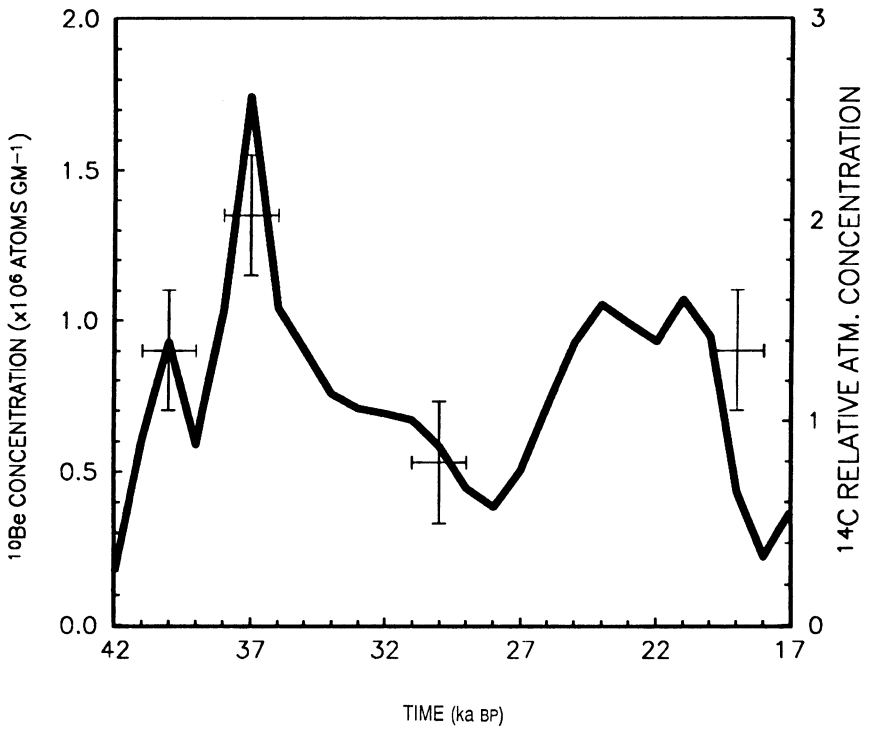

Fig. 3. Vostok ^{10}Be between 17 and 42 ka BP (adapted from Raisbeck *et al.* 1987) with relative ^{14}C from South African stalagmite (Vogel 1983). Error-bar limits for Vogel data are only approximate (visually scaled from Vogel: Fig. 3) and are presumed to be 1 σ limits. The Vogel data is shifted left (to increased age) by 1 ka to match the Rasibeck data. Note that this brings all but the rightmost error bars into close coincidence with the ^{10}Be. This figure should be regarded as only suggestive of a basic relation (cosmic-ray forcing?).

in qualitative accord with the ^{10}Be record for this time interval. Without further research, we cannot be certain that all these results are a consequence of SN CR enhancement. A more complete analysis of the Vostok core data awaits a better partitioning of the covariant and acovariant parts of the ^{10}Be and ^{18}O isotopes and detailed modeling of the blast-wave problem.

ACKNOWLEDGMENTS

I am indebted to my colleagues, J. R. Jokipii and G. E. Morfill for extensive discussions and illumination of the CR and shock dynamics. I am equally indebted (though at the expense of decreased confidence as to the uniqueness of the model discussed herein) to J. Beer for kindly providing a preprint of the analysis by him and coworkers of the isotope record from Camp Century ice. This work was partially supported by a grant from the NSF Atmospheres program.

REFERENCES

Bard, E., Hamelin, B., Fairbanks, R. G. and Zindler, A. 1990 Calibration of the ^{14}C time scale over past 30,000 years using mass spectrometric U-Th ages from Barbados corals. *Nature* 345: 405–410.

Beer, J., Johnsen, S. J., Bonani, G., Finkel, R. C., Langway, C. G., Oeschger, H., Stauffer, B., Suter, M., and Wölfi, W. 1992 ^{10}Be Peaks as time markers in polar ice cores. *In* Bard, E. and Broecker, W. S., eds., *The Last Deglaciation: Absolute and Radiocarbon Chronologies.* NATO ASI Series I-2. Berlin Heidelberg, Springer-Verlag: 141–153.

Berkhuijsen, E. M. 1973 Galactic continuum loops and the diameter-surface brightness relation for supernova remnants. *Astronomy and Astrophysics* 24: 143.

Bonhommet, N. and Babkine, J. 1967 Sur la présence de directions inversées dans la Chaîne du Puys. *Comptes Rendus de l'Academie des Sciences* 264: 92.

Bonhommet, N. and Zahringer, J. 1969 Paleomagnetism and potassium argon age determinations of the Laschamp geomagnetic polarity reversal event. *Earth and Planetary Science Letters* 6: 43–46.

Borken, R. J. and Iwan, D. C. 1977 Spatial structure in the soft x-ray background as observed from OSO-8 and the north polar spur as a reheated supernova remnant. *Astrophysical Journal* 218: 511–520.

Boyer, D. W. 1960 An experimental study of the explosion generated by a pressurized sphere. *Journal of Fluid Mechanics* 9: 401.

Brode, H. L. 1955 Numerical solutions of spherical blast waves. *Journal of Applied Physics* 26: 766.

_____1959 Blast wave from a spherical charge. *Physics of Fluids* 2: 217.

Castagnoli, C. G., Bonino, G. and Miono, S. 1982 Thermoluminescence in sediments and historical supernovae explosions. *Il Nuovo Cimento* 5C: 488–494.

Colburn, D. S. and Sonett, C. P. 1965 Discontinuities in the solar wind. *Space Science Reviews* 5: 439.

Courant, R. and Friedrichs, K. O. 1948 *Supersonic Flow and Shock Waves*. Interscience. Also reprinted 1977 by Springer-Verlag.

Cox, D. P. and Anderson, P. R. 1982 Extended adiabatic blast waves and a model of the soft x-ray background. *Astrophysical Journal* 253: 268–289.

Davelaar, J., Bleeker, A. M. and Deerenberg, A. J. M. 1980 X-ray characteristics of Loop I and the local interstellar medium. *Astronomy and Astrophysics* 92: 231–237.

Egger, R. 1991 The North Polar Spur in the ROSAT/PSPC Survey. *In* Godhalekar, P. M., ed., *Hot Gases in the Galaxy*. RAL-91-082. Chilton Didcot, U. K., Rutherford Appleton Laboratory: 95–105.

Friedman, M. P. 1961 A simplified analysis of spherical and cylindrical blast waves. *Journal of Fluid Mechanics* 11: 1–15.

Higdon, J. C. 1981 The Cygnus "superbubble": A supernova explosion in a tenuous intercloud medium. *Astrophysical Journal* 244: 88–93.

Higdon, J. C. and Lingenfelter, R. E. 1973 Sea sediments, cosmic rays, and pulsars. *Nature* 246: 403–405.

Kocharov, G. E., Konstantinov, A. N., Levchenko, V. A., Amnosov, A. E., Berezko, E. G. and Krymsky, G. F. 1991 Cosmic rays near the Earth from the supernova explosion. Preprint.

Kuo, Y. H. 1947 The propagation of a spherical or a cylindrical wave of finite amplitude and the production of shock waves. *Quarterly of Applied Mathematics* 4: 349–360.

Lal, D. and Peters, B. 1967 Cosmic ray produced radioactivity on the Earth. *In* Flügge, S., ed., *Handbuch der Physik* 46(2): 551.

Lingenfelter, R. E. 1969 Pulsars and local cosmic ray prehistory. *Nature* 224: 1182–1186.

McElhinny, M. W. and Senanayake, W. E. 1982 Variations in the Geomagnetic dipole I: The past 50,000 years. *Journal of Geomagnetism and Geoelectricity* 34: 39–51.

Parker, E. N. 1963 *Interplanetary Dynamical Processes*. New York and London, Wiley Interscience.

Peters, B. 1957 Über die Anwendbarkeit der Be^{10}-Methode zur Messung kosmischer Strahungsintensität und der Abslagerungsgeschwindigkeit von Tiefseesedimenten vor einiger Millionen Jahren. *Zeitschrift für Physik* 148: 93.

Raisbeck, G. M. and Yiou, F. 1991 ^{10}Be profiles as a stratigraphic tool. Abstract. *Radiocarbon* 33(2): 235.

Raisbeck, G. M., Yiou, F., Bourles, D. Lorius, C., Jouzet, J. and Barkov, N. I. 1987 Evidence for two intervals of enhanced ^{10}Be deposition in Antarctic ice during the last glacial period. *Nature* 326: 273–277.

Raisbeck, G. M., Yiou. F., Fruneau, J. M., Loiseaux, M., Lieuvin, J. C., Ravel, J. M. and Lorius, C. 1981 ^{10}Be/^{7}Be as a probe of atmospheric transport processes. *Geophysical Research Letters* 8: 1015–1018.

Sedov, L. I. 1959 *Similarity and Dimensional Methods in Mechanics*. London and New York, Academic Press.

Simon, M. and Axford, W. I. 1966 Shock waves in the interplanetary medium. *Planetary and Space Science* 14: 901–908.

Sonett, C. P. 1991 Long period solar-terrestrial variability. Quadrennial US IUGG report, 1987–1990. *Reviews of Geophysics* 909–914.

Sonett, C. P. and Colburn, D. S. 1965 The SI^{+}-SI^{-} pair and interplanetary forward-reverse shock ensembles. *Planetary and Space Sciences* 13: 675–692.

Sonett, C. P., Morfill, G. E. and Jokipii, J. R. 1987 Interstellar shock waves and ^{10}Be from ice cores. *Nature* 330: 458–460.

Sturrock, P. and Spreiter, J. R. 1965 Shock waves in the solar wind and geomagnetic storms. *Journal of Geophysical Research* 70: 5345–5351.

Taylor, G. I. 1946 The air wave surrounding an expanding sphere. *Proceedings of the Royal Society of London* A 186: 273–292.

Tric, E., Valet, J.-P., Tucholka, P., Labeyrie, L., Guichard, F., Tauxe, L. and Fontugne, M. 1992 Paleointensity of the geomagnetic field during the last 80,000 years. *Journal of Geophysical Research* 97: 9337–9352.

Vogel, J. C. 1983 ^{14}C variations during the upper Pleistocene. *In* Stuiver, M. and Kra, R. S., eds., Proceedings of the 11th International ^{14}C Conference. *Radiocarbon* 25(2): 213–218.

[RADIOCARBON, VOL. 34, NO. 2, 1992, P. 247–253]

THEORETICAL AND EXPERIMENTAL ASPECTS OF SOLAR FLARES MANIFESTATION IN RADIOCARBON ABUNDANCE IN TREE RINGS

A. N. KOSTANTINOV[1], V. A. LEVCHENKO[1], G. E. KOCHAROV[2], I. B. MIKHEEVA[2] STEFANO CECCHINI[3], MENOTTI GALLI[4], TERESA NANNI[5], PAVEL POVINEC[6] LIVIO RUGGIERO[7] and AGOSTINO SALOMONI[8]

ABSTRACT. We describe our method of determining solar cosmic-ray flux and spectrum in the past, based on the comparison of different cosmogenic isotopes. For the period, AD 1781–1950, we have detected several intervals with a high probability of powerful solar flares.

INTRODUCTION

Cosmogenic isotopes can be used as a tool for investigating solar activity in the past. The influence of the Sun on the production of cosmogenic isotopes is two-fold. On the one hand, solar activity modulates the galactic cosmic-ray (GCR) flux, and thus, decreases the cosmogenic isotope production rate. On the other hand, the Sun can generate fluxes of solar cosmic rays (SCR), increasing the cosmogenic isotope production. Until the present, principal interest has been focused on the solar modulation process, as it is the more powerful factor. Nevertheless, the study of solar-flare (SF) activity is, without doubt, of special interest for the investigation of, for example, solar-terrestrial relations and theories of solar and stellar activity.

BACKGROUND

Lingenfelter and Hudson (1980) made one of the first attempts to consider the SF activity in the past, based on cosmogenic isotope data. The authors used a strong assumption of constant mean flux of GCR and established the upper limit of the SF activity in the past. The SCR particle spectrum was presented in the form of

$$dN_s/dR = N_{os} \exp(-R/R_o) \quad (1)$$

where R = particle rigidity, N_s = SCR flux, R_o = characteristic spectrum rigidity, which varies with different flares, and was taken to equal 100 MV.

In our opinion, the most effective way of studying solar activity in the past is to use differences of SCR and GCR spectra. Actually, solar particles have much less mean energy than the galactic particles. However, the SCR flux is much higher than the GCR flux. Thus, one has to compare cosmogenic isotope data with different sensitivities for different parts of the particle spectrum. Fortunately, the well-known isotopes, ^{10}Be and ^{14}C, are suitable for this purpose. These radionuclides are produced in reactions

$$^{14}N(n,p)^{14}C;\ ^{14}N(h,^{5}X)^{10}Be;\ ^{16}O(h,^{7}X)^{10}Be \quad (2)$$

[1]St. Petersburg State Technical University, St. Petersburg 195251 Russia
[2]Ioffe Physico-Technical Institute, St. Petersburg 194021 Russia
[3]Istituto TESRE-CNR, 40126 Bologna, Italy
[4]Dipartimento di Fisica, Universitá di Bologna, 40126 Bologna, Italy
[5]Istituto FISBAT-CNR, 40126 Bologna, Italy
[6]Department of Nuclear Physics, Comenius University, Bratislava, Czecho-Slovakia
[7]Dipartimento di Scienza dei Materiali, Universitá di Lecce, 73100 Lecce, Italy
[8]ENEA-TIB, Universitá degli Studi, 40136 Bologna, Italy

where h = hadrons. The first reaction has practically no energy threshold, so that the ^{14}C and ^{10}Be production rate must have different sensitivities to the galactic and solar particles. Even the production of ^{10}Be, which occurs partly in the troposphere and partly in the stratosphere, has different sensitivities to SCR and GCR. In the troposphere, the production of ^{10}Be is caused by primary particles with higher mean energy than for production in the stratosphere. Thus, it is clear that when strong SCR fluxes arrive on the Earth's atmosphere, the ratios of ^{10}Be and ^{14}C production rates can be drastically different.

Figure 1 shows the relation between ^{14}C and ^{10}Be production rates calculated for GCR flux and SCR fluxes with different R_0. For the GCR, we used the spectrum

$$dN_g/dE = dN_{og} (E+mc^2)^{-2.65} \exp(-k/R) \quad (3)$$

where E = the kinetic energy of the particles, m = the proton mass, k = the solar modulation parameter. For the solar particles, we assumed the spectrum representation (Eq. 1). The calculation model was described earlier (Kostantinov, Kocharov & Levchenko 1987). Figure 1 also shows that a large displacement below the curve for GCR might indicate a contribution from the SCR flux to ^{14}C production.

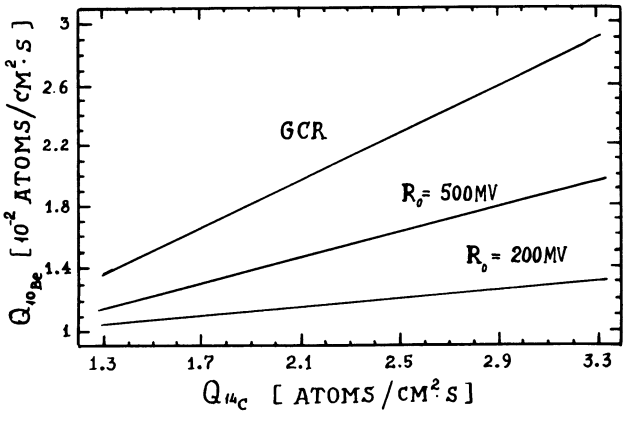

Fig. 1. The relationship between the production rates of ^{14}C (^{14}Q) and ^{10}Be (^{10}Q) for GCR and SCR for different characteristic rigidities (MV)

This method has already been tested (Kostantinov, Levchenko & Mikheeva 1989) on the data of ^{10}Be concentration in an ice core from Greenland, covering the period of the 12th to 17th and 20th centuries AD, and on the corresponding ^{14}C data. Several other periods with possible significant solar flares were also indicated.

In this paper, we present a preliminary attempt to identify solar flares in the past, using recent accurate and detailed data on cosmogenic isotope abundance in terrestrial samples. We used the annual data on ^{10}Be concentration from the Dye 3, Greenland, ice core (Beer *et al.* 1990), and ^{14}C data (Kocharov *et al.* 1987b) covering the period, AD 1781–1950. The general procedure for treating the data is described elsewhere (Kostantinov, Levchenko & Mikheeva 1989). We consider here only the peculiarities of the particular analysis we have carried out.

METHODOLOGY

Figure 2 shows the temporal profile of ^{10}Be and ^{14}C production rates reconstructed from the original data series. The whole period can be divided into two sections. In the first, from 1781 to

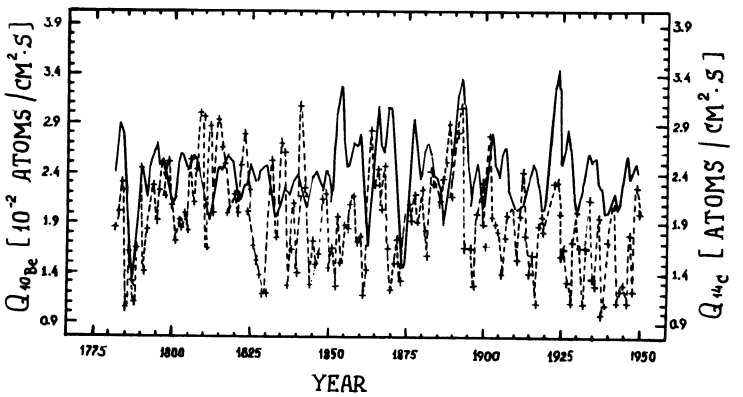

Fig. 2. ^{10}Be and ^{14}C reconstructed production rates: — = ^{14}Q in atoms/cm^2 s; --+-- = ^{10}Q in 10^{-2} atoms/cm^2 s

1900, the ^{10}Be and ^{14}C profiles are more-or-less similar, and in the second, after 1900, ^{10}Be shows a downward trend, with respect to ^{14}C. Thus, we decided to consider these two sections separately.

We constructed the cross-correlation function of ^{10}Be and ^{14}C data on the first time interval, and found some discrepancies between the two profiles. Cross-correlation maximum could be achieved by shifting, by one year, one data sequence with respect to the other. We did this to obtain the best fit of the data. As a matter of fact, the ^{14}C exchange system can introduce some uncertainties in the dating of the ^{14}C production rate, and a one-year discrepancy is a good enough fit. It is important to note that the procedure of shifting can reduce the number of discrepancies only among the time profiles, and thus, the number of possible errors in the search for solar flare manifestations.

Figure 3 presents a plot of the ^{10}Be production rate *vs.* ^{14}C production rate for the period, AD 1781–1900, together with the theoretical expected dependence and one standard deviation ($\pm 1\ \sigma$) strips. The majority of the points is located in this area. According to statistical predictions, one expects about an equal number of points above and below the curve. However, more than twice as many points are below the curve than above. Of course, one can argue that the theoretical expectation is not sufficiently correct, but to that we can reply that our production rate calculations have been tested on experimental data many times before (Kocharov *et al.* 1987a, 1989). In our opinion, the main cause of discrepancy between the theoretical curve and the point distribution is the presence of an additional factor that was not taken into account in the theoretical calculations, namely, the manifestation of SCR contribution in cosmogenic isotope data. Thus, the average asymmetry of the observed distribution from the theoretical predictions can be interpreted as the influence of the SCR on the production rates, and the average SCR flux can be determined from the value of that divergence. For the period, AD 1781–1900, we obtain the value for SCR flux of (70 ± 50) particles/cm^2 s, assuming an average characteristic rigidity of 100 MV. The largest uncertainty is due mainly to the ^{14}C reservoir exchange model used for production rate reconstruction. However, our result still does not contradict the modern, generally accepted values.

We can try to explain some divergent points as the manifestation of particular powerful solar flares. Undoubtedly, some of the points have simple statistical origins, such as those that are located in the upper portion. The fact that more than two thirds of the points are in the lower strip seems to indicate that some carry a flare signal. Further, one can see that they are organized in specific temporal groups. We mean that the divergence occurs in groups of years, 2 or 3 sequential years in a group. We have made more precise investigations of these peculiar time intervals by comparing

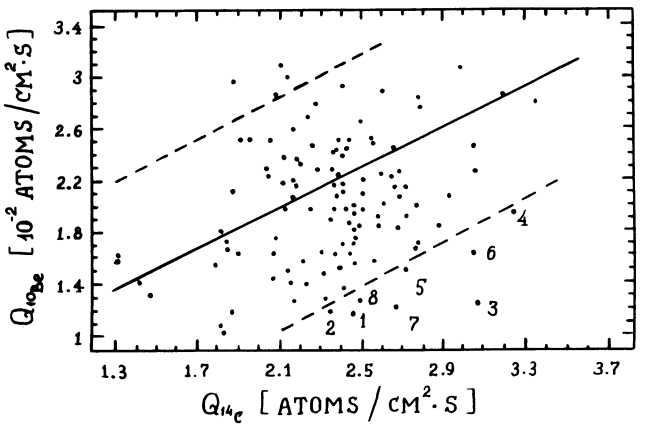

Fig. 3. The observed relationship of reconstructed isotope production rates for the years, AD 1781–1900. — = theoretical correlation for GCR; - - - = regions of ±1 σ uncertainty. Possible flare years: 1–1824; 2–1825; 3–1851; 4–1852; 5–1853; 6–1869; 7–1870; 8–1897

Wolf sunspot numbers. We found that for three of the mentioned groups, namely at 1851–1853, 1869–1870 and 1897, the divergence can be attributed to strong solar-flare contribution. Figure 4 represents the time behavior of the reconstructed isotopic production rates for the period, AD 1848–1864. One can see that the largest contributions are located on the rising and falling branches of the solar cycles, and that the time profile of production rates shows a certain peculiarity. The same is observed in the other two cases. In our opinion, their explanation as signatures of solar-flare contribution is natural.

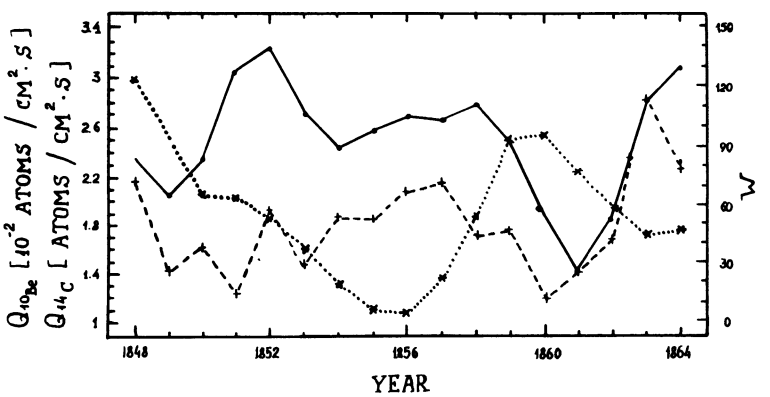

Fig. 4. The comparison of reconstructed isotope production rates (left scale the same as in Fig. 2) and Wolf numbers (right scale) for the years, 1849–1862. — = ^{14}Q; - - - = ^{10}Q; ··· = Wolf numbers

For the 1851–1853 event, we estimated the flux and characteristic rigidity. We have assumed an average level of solar modulation, *i.e.*, the value of the coefficient, k, in (Eq. 3), because we have only 2 records and 3 unknown values. However, our assumption is not far from the truth, as one can infer by looking at the Wolf numbers. We obtained a solar-flare particle flux of 2 10^9 particles/cm^2 s with R_o = 200 MV.

The data of the second part, *i.e.*, the data after AD 1900, were analyzed by the same procedure as described above, with one addition. First, we removed the trend from the ^{10}Be data. We believe this is correct because 1) ^{14}C data were also detrended (Suess effect) beforehand, and 2) such detrending can only diminish the number of divergent points, and thus, the number of our errors. The plot of ^{10}Be production rate *vs.* ^{14}C production rate, together with the sections of uncertainty for the period, AD 1900–1950, is presented in Figure 5. There, also, more points are lying predominantly in the lower portion. As before, we can identify two points, 1923 and 1924, which, with great probability, correspond to enhanced particle fluxes from solar flares. The points corresponding to the mid-1940s lie near the lower boundary of the section, although inside. A strong flare is known to have occurred at that time. Unfortunately, it does not look strong enough to be manifested in our data. Moreover, the year, 1941, is missing from the data sequence.

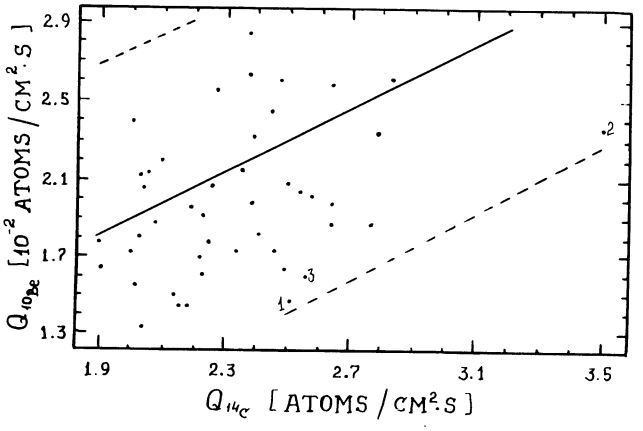

Fig. 5. The comparison of reconstructed isotope production rates for the years, 1900–1950. Legend as in Fig. 3. 1–1925; 2–1924; 3–1946

Shea (1990) made another attempt to find solar-flare particle effects in tree rings ^{14}C abundance for recent flares in September–October 1989.

Because of the non-uniform arrival to the Earth's surface of solar-flare particles due to the anisotropy of the beam, we have looked for local enhancement of ^{14}C production in the northern and southern hemispheres. We measured ^{14}C in samples of wood in which lignin or cellulose supposedly was produced a short time after the flares.

We collected wood samples from a pine tree (*Pinus pinea*) in Ravenna, Italy (46°N Lat) and from a pine tree (*Pinus halepensis*) in Belair National Park near Adelaide, Australia (34°S Lat). From both sites, we measured ^{14}C in early wood and late wood, separately, as late wood was supposedly produced even after the stasis of cell differentiation (Attolini *et al.* 1990), *i.e.*, after September–October in the Ravenna region. A rough correspondence exists between late wood from the northern and early wood from the southern hemispheres.

Results

Results are shown in Figure 6. Corresponding to the second half of 1989, when a solar-flare-particle effect could be expected, a consistent decrease of $\Delta^{14}C$ is apparent, instead of an expected increase of 0.5–0.9%, both at northern and southern latitudes, according to the Lingenfelter model. To check the results obtained with scintillation counters of the Bologna Radiocarbon Laboratory, $\Delta^{14}C$ measurements were also made with proportional counters in Bratislava. The consistency of the measurements is also confirmed in Figure 6.

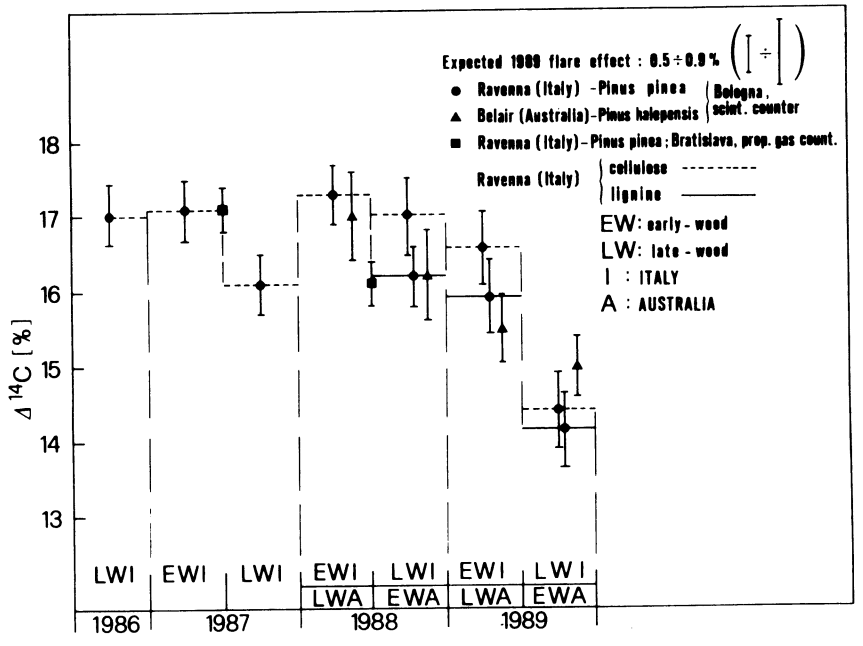

Fig. 6. Results of the search for possible ^{14}C effects in wood caused by solar-flare-particle events of September–October 1989

Thus, we conclude that, as far as the September–October 1989 solar-flare events are concerned, no local anisotropic contribution could be detected.

However, according to our theoretical calculation, a flare effect of the magnitude, 0.5–0.9%, can be expected only in wood of 1990–1991.

Conclusions

The main conclusions of this work are:

1. Our suggested method can be used for investigating powerful solar flares in the past, in order to check the frequency distribution of solar-flare events, and to estimate the upper limit of solar energy.
2. In order to obtain more accurate results, we need a third data record, possibly ^{10}Be from high-latitude stations, such as Vostok or Camp Century.
3. Uncertainties can be eliminated by using two isotope data records, *e.g.*, ^{10}Be and ^{26}Al, in the same samples from stations at different latitudes.
4. Localized ^{14}C production from the September–October 1989 solar-flare-particle events has not been detected. A diffuse, worldwide ^{14}C effect has not yet been detected.

REFERENCES

Attolini, M. R., Calvani, F., Galli, M., Nanni, T., Ruggiero, L., Schaer, E. and Zuanni, F. 1990 The relationship between climatic variable and wood structure in *Pinus Halepensis* Mill. *Theoretical Applications in Climatology* 41: 121–127.

Beer, J., Blinov, A., Bonani, G., Finkel, R. C., Hofman, H. J., Lehmann, B., Oeschger, H., Sigg, A., Schwander, J., Staffelbach, T., Stauffer, B., Suter, M. and Wölfli, W. 1990 Use of ^{10}Be in polar ice to trace the 11-year cycle of solar activity. *Nature* 347: 164–166.

Kocharov, G. E., Blinov, A. V., Kostantinov, A. N. and Levchenko, V. A. 1987a Cosmogenic isotopes: Implications for the cosmic ray spectrum and geomagnetic dipole moment. 20th ICRC, Moscow, *Conference Papers* 4: 311–314 (in Russian).

_____1989 Temporal ^{10}Be and ^{14}C variations: A tool for paleomagnetic research. *Radiocarbon* 31(2): 163–168.

Kocharov, G. E., Kostantinov, A. N., Mikheeva, I. B., Bitvinskas, T. T., Metshvarishvili, R. J., Galli, M., Cini-Castagnoli, G., Attolini, M. R., Cecchini, S. and Nanni, T. 1987b A 400 year radiocarbon record: 11-year and longer cycles. 20th ICRC, Moscow, *Conference Papers* 4: 280–283 (in Russian).

Kostantinov, A. N., Kocharov, G. E. and Levchenko, V. A. 1987 Cosmogenic isotopes ^{10}Be, ^{14}C and ^{36}Cl and astrophysical phenomena. *In* Kocharov, G. E., ed., *Solar Activity and Solar-Terrestrial Relations.* Leningrad, LIYAF Publications: 99–134 (in Russian).

Kostantinov, A. N., Levchenko, V. A. and Mikheeva, I. B. 1989 On the possibility of the reconstruction of solar cosmic ray parameters in the past. *Solnechnye dannye (Solar data)* 1: 107–112 (in Russian).

Lingenfelter, R. E. and Hudson, H. S. 1980 Solar particles fluxes and the ancient Sun. *In* Pepin, R. O., Eddy, J. A. and Merrill, R. B., eds., *The Ancient Sun.* New York, Pergamon Press: 69–75.

Shea, M. A. 1990 Solar cosmic rays 1960–1989. 21st ICRC, Adelaide 1990, *Conference Papers* 12: 196–201.

[RADIOCARBON, VOL. 34, NO. 2, 1992, P. 255–262]

RECENT AND HISTORICAL SOLAR PROTON EVENTS

M. A. SHEA and D. F. SMART

Space Physics Division, Geophysics Directorate/Phillips Laboratory, Hanscom Air Force Base Bedford, Massachusetts 01731-5000 USA

ABSTRACT. A study of the solar proton event data between 1954 and 1986 indicates that the large fluence events at the Earth are usually associated with a sequence of solar activity and related geomagnetic storms. This association appears to be useful to infer the occurrence of major fluence proton events extending back to 1934, albeit in a non-homogeneous manner. We discuss the possibility of identifying major solar proton events prior to 1934, using geomagnetic records as a proxy.

INTRODUCTION

Solar-flare-generated protons impacting the top of the atmosphere account for some of the total radiocarbon inventory. Lingenfelter and Ramaty (1970) have estimated that the solar flare production during the 19th solar cycle was between 6% and 14% of the solar-cycle averaged galactic cosmic-ray production rate. We assume that the source of these protons is associated, in some way, with the occurrence of a solar flare, although a unique acceleration process has not been identified.

Solar-flare accelerated particles travel along the interplanetary magnetic field and impact the Earth's atmosphere principally in the polar regions. Occasionally, the Sun accelerates particles into the GeV energy range; these particles can penetrate the geomagnetic shielding to lower latitudes and, hence, are more effective to ^{14}C production.

Approximately half of the energy of the solar flare is in the interplanetary shock that travels to the Earth's orbit 1 or 2 days after the flare. Under favorable circumstances, particularly during a sequence of solar activity, the shock re-accelerates the ambient solar particle population, thus modifying the observed particle spectrum from what was released into the interplanetary medium during the original flare process.

When the interplanetary shock impacts the Earth's magnetosphere, the structure of the magnetosphere is altered. Often, depending on the direction of the interplanetary magnetic field vectors, a major geomagnetic storm will occur. The current systems involved in the geomagnetic storm can substantially lower the geomagnetic cutoff rigidity (Flückiger, Smart & Shea 1986). The occurrence of mid- and low-latitude aurorae is evidence of a major expansion of the Earth's polar caps, which allows solar particles to penetrate much lower in latitude than during quiescent geomagnetic conditions. Figure 1 represents the major solar-flare emissions and the relative time intervals that these emissions take to travel to the orbit of the Earth.

Using data acquired by both spacecraft and ground-based techniques, we have assembled a list of over 200 significant solar proton events that have reached the Earth between 1954 and 1986. We would like to suggest a method of identifying some of the major proton events over the past century, using a combination of solar flare, solar particle and geomagnetic records.

SOLAR PROTON DATA BASE

Although the first directly measured solar proton event occurred in 1942, it was not until the International Geophysical Year in 1957–1958 that solar proton events could be routinely identified. Even then, the identification of solar proton events was limited to the major events that could be

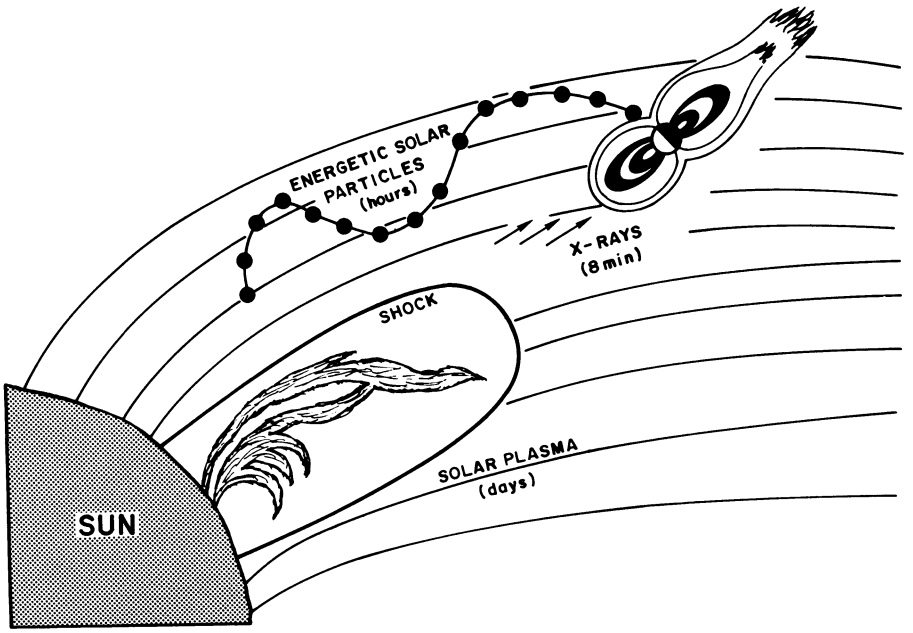

Fig. 1. Pictorial representation of solar emissions from a solar flare. The time intervals that the various emissions take to reach the Earth are also shown.

detected by various ground-based techniques. Routine spacecraft measurements were initiated in 1965; since that time, solar particles have been almost continuously monitored *via* Earth-orbiting or geosynchronous satellites.

The most homogeneous solar proton data base has been obtained from the cosmic radiation records. From 1934, ionization chambers, and, since 1951, neutron monitors, recorded occasional increases in the cosmic-ray intensity that were associated with the release of GeV protons from the Sun. From 1956 until mid-1991, neutron monitor measurements have detected 48 relativistic solar particle events at the Earth. These events include protons with energies above 500 MeV; in some cases, the energy of the solar protons exceed 10 GeV. Figure 2 illustrates the occurrence of these events as a function of time. Although most of the high-energy events occur during periods of enhanced solar activity, as represented by the sunspot number, they can occur even during solar minimum.

Spacecraft observations of solar proton events essentially start near the beginning of the 20th solar cycle. We have examined the relativistic solar proton event data for the 19th solar cycle, and have assembled a data base equivalent to the satellite-sensed data base of the 20th and 21st solar cycles. Thus, our data base is homogeneous for three solar cycles. We identified all events with protons >10 MeV having a peak flux of >10 protons/(cm^2-sec-ster). Shea and Smart (1990a) list these events, together with the peak proton flux and fluence.

We then separated the events by solar cycle, starting with the month of sunspot minimum, to see if there was an identifiable pattern between the cycles. These results are shown in Figure 3, where the 12-month average of the sunspot number is plotted as histograms for each cycle, and the proton events for each 12-month period is shown. Figure 3 also shows a plot of the number of proton events per year *vs.* the yearly average sunspot number. Other than an increase in the number of events during the maximum in solar activity, there does not appear to be a predictable or repeatable pattern between solar proton event occurrence and the solar activity cycle (as measured by the sunspot number).

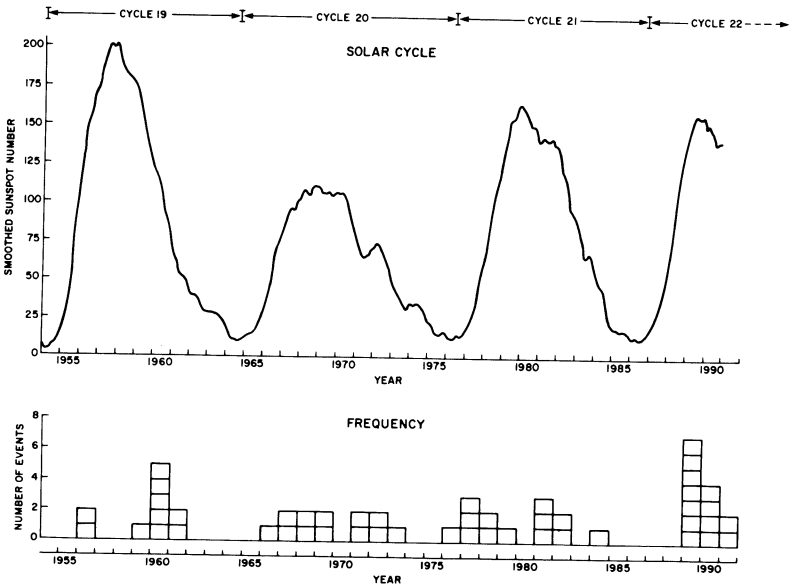

Fig. 2. Relativistic solar proton events observed since 1955. Top – the smoothed sunspot number; Bottom – the number of high energy solar proton events each year.

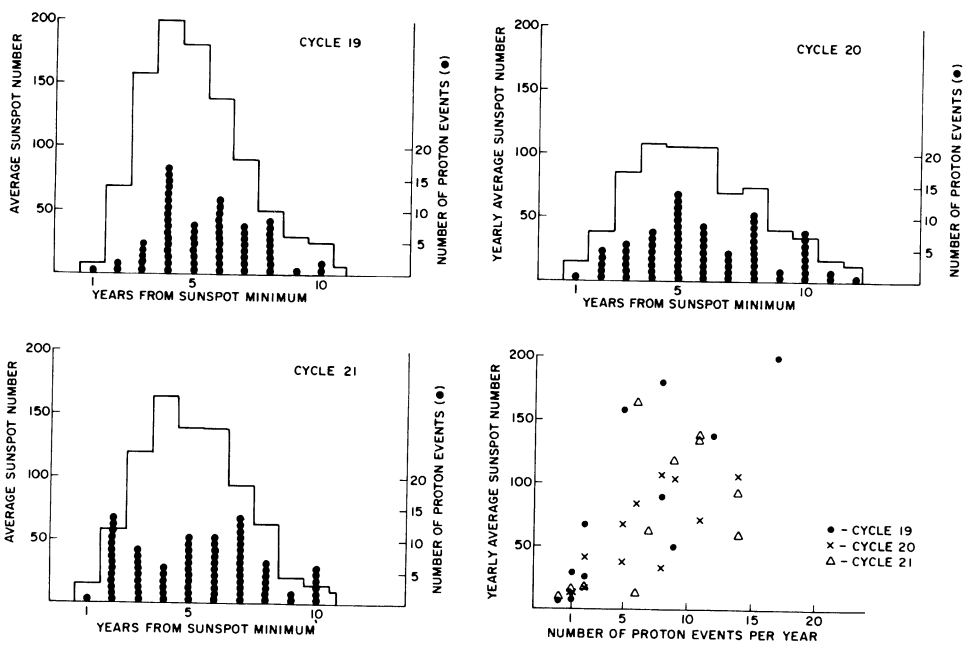

Fig. 3. The number of significant discrete solar proton events for each 12-month period after solar minimum (•) and the 12-month mean sunspot number for the corresponding period (histograms) for solar cycles 19–21. A plot of the number of proton events per year *vs.* the yearly average sunspot number is shown in the lower right hand section.

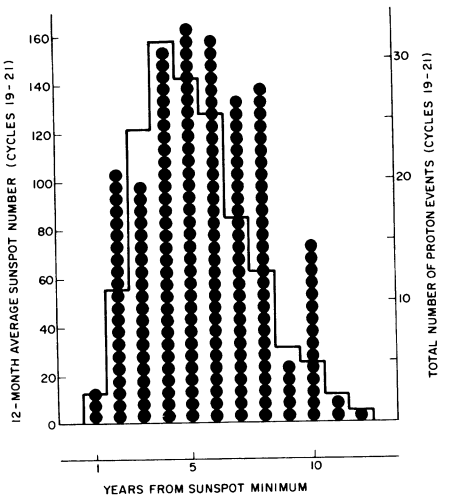

Fig. 4. Summation of significant discrete solar proton events for cycles 19–21 (•) and the corresponding 12-month average sunspot number (histogram). The data are organized in 12-month periods, beginning with the month after sunspot minimum, as defined by the statistically smoothed sunspot number.

In combining these results for the three solar cycles into one figure, we obtain the distribution shown in Figure 4. From this, we conclude that the majority of significant solar proton events occurs from the 2nd through the 10th years of the solar cycle.

SOLAR PROTON FLUENCE

Although most solar particle events are measured in terms of peak proton flux, the fluence is more appropriate for ^{14}C production. Feynman *et al.* (1990) show that the fluence for events in solar cycles 19–21 all fit in one continuous log-normal distribution. Shea and Smart (1990a) indicate that it is not always possible to identify the fluence on an event-by-event basis, because many events occur in episodes of activity. In these cases, the fluence is determined by summing the flux throughout the entire period. An example of a major episode of activity was August 1972, when a series of flares from one solar region, as it traversed the solar disk, produced one-half the proton fluence above 10 MeV for the entire 11-year solar cycle.

EVENTS IN SOLAR CYCLE 22

The present solar cycle, which started in October 1986, has been unexpectedly active, with respect to the generation of major solar proton events in both the energy content, flux and fluence. This reinforces the suggestion that we and other researchers have made that the first two solar cycles of the space era may be atypical cycles rather than normal cycles. This suggestion was first published by Goswami *et al.* (1988), who analyzed the spectral characteristics of solar proton events responsible for the generation of radio nuclei. These authors concluded that the spectral characteristics observed in the 20th and 21st solar cycles were different than observed in the 19th solar cycle. Shea and Smart (1990b) also suggested that the relativistic solar proton events of the 22nd solar cycle were similar to those in the 17–19th cycles with large fluxes and long durations; the relativistic proton events in the 20th and 21st solar cycles were generally smaller events of very short duration. Figure 5 illustrates the difference in duration of two relativistic solar proton events. On 7 May 1978 was the largest event of either the 20th or 21st solar cycle; the high energy solar proton flux, as measured at the Kerguelen Island neutron monitor, lasted for just over two hours. On 29 September 1989 was the largest event of the 22nd solar cycle, to date, and is comparable to the events in November 1960, as well as events measured by ionization chambers prior to 1955.

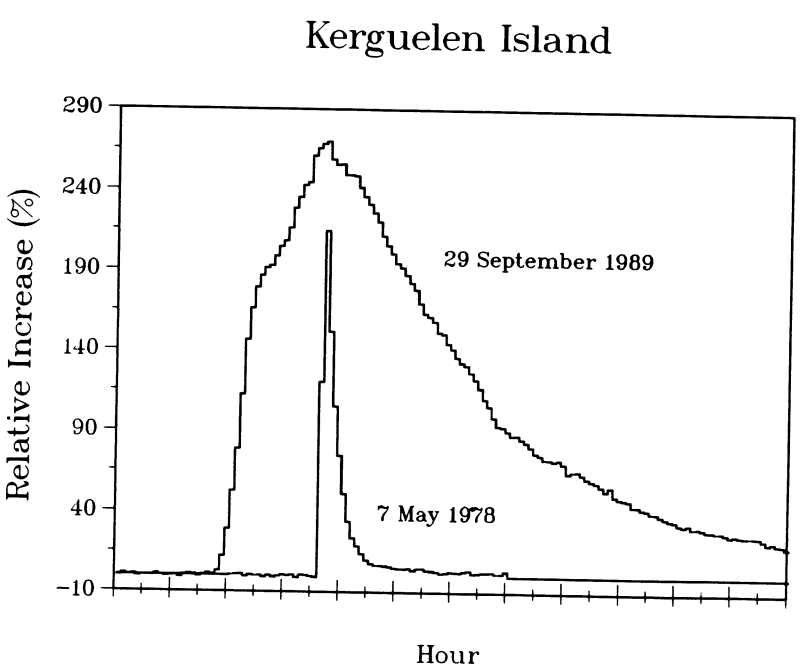

Fig. 5. The duration of the largest relativistic solar proton event of the 22nd solar cycle (29 September 1989) compared with the largest event of the 20th and 21st solar cycles (7 May 1978). The Kerguelen Island neutron monitor is located at 49.35° S, 70.27° E and measures the cosmic radiation above ~500 MeV.

The high-energy solar proton flux was enhanced for about a day. Obviously, the fluence, which is proportional to the area under the respective curves, was considerably greater for the 29 September 1989 event.

One of the conclusions in Shea and Smart (1990a) was that solar proton events occur in episodes of activity. This usually happens when one solar-active region produces a series of major flares with associated proton emission, as the active region rotates with the sun from the east to west limb. When regions such as this are near central meridian, the solar plasma emissions generally intersect the Earth a day or two after major flares, giving rise to major geomagnetic disturbances and often mid-latitude aurorae. At the same time, the traveling interplanetary shock wave associated with the plasma boundary re-accelerates the ambient solar proton flux in such a manner that, when the interplanetary shock arrives at the Earth, the solar particle flux increases as much as an order of magnitude for a few hours. In rare cases, particles up to GeV energies are involved (Levy, Duggal & Pomerantz 1976). The fluences recorded during these episodes of activity can often be the major contribution to the solar proton fluence for a solar cycle.

Episodes of activity have occurred throughout solar cycle 22 with eight major sequences between March 1989 and June 1991. Table 1 presents a summary of the solar proton fluence for the past three solar cycles; fluences for the major events during the 22nd solar cycle are identified at the bottom of the table (Sauer, personal communication 1991, 1992). The solar proton fluence for the 22nd solar cycle has already exceeded the combined solar proton fluence for the 20th and 21st solar cycles, and is approaching the values for the 19th solar cycle.

TABLE 1. Summary of Solar Proton Events for Solar Cycles 19, 20, and 21

Cycle	Start*	End	No. of months in cycle	No. of discrete proton events	No. of discrete proton-producing regions	Solar cycle integrated solar proton fluence** >10 MeV	>30 MeV
19	May 1954	Oct. 1964	126	65	47	7.2×10^{10}	1.8×10^{10}
20	Nov. 1964	June 1976	140	72	56	2.2×10^{10}	6.9×10^{9}
21	July 1976	Sept. 1986	123	81	57	1.8×10^{10}	2.8×10^{9}
22	Mar. 7–25, 1989					0.12×10^{10}	0.03×10^{9}
	Aug. 12–18, 1989					0.76×10^{10}	1.4×10^{9}
	Sept. 29–Oct. 2, 1989					0.38×10^{10}	1.4×10^{9}
	Oct. 19–30, 1989					1.9×10^{10}	4.2×10^{9}
	Dec. 30, 1989–Jan. 2, 1990					0.21×10^{10}	0.13×10^{9}
	May 21–31, 1990					0.035×10^{10}	0.14×10^{9}
	Mar. 22–26, 1991					0.96×10^{10}	1.8×10^{9}
	June 4–21, 1991					0.32×10^{10}	0.79×10^{9}
					Totals:	4.68×10^{10}	9.9×10^{9}

*The start of each solar cycle was selected as the month after the minimum in the smoothed sunspot number (McKinnon 1987).

**Fluence units are protons cm^{-2}.

EVENTS PRIOR TO SOLAR CYCLE 19

In an attempt to identify solar proton events prior to the 19th solar cycle, Svestka (1966) interpreted vertical ionospheric sounding data during polar cap absorption (PCA) events, and compiled a list of PCA events probably associated with solar proton events between 1938 and 1955. In this work, he comments on the validity of each event, possible associated source solar flare and inferred solar flares. In an attempt to extend back further in time, we suggest a method of identifying periods of major proton fluences in the vicinity of the Earth, based upon the occurrence of major geomagnetic storms associated with episodes of solar activity across the solar disk.

We have previously argued (Smart & Shea 1989; Shea & Smart 1990a) that the shock-accelerated events (the July 1959 and the August 1972 episodes being outstanding examples) result in large particle populations observed at the Earth. Using the geomagnetic index of Ap* > 150 as a proxy for identifying major solar proton events for the past three solar cycles, we successfully identified 90% of the major fluence events for the period, 1955–1986. In other words, direct correspondence exists between a major geomagnetic storm and a major solar proton fluence event. (The Ap* value, derived by Allen (1982), is the 24-hour running mean of the 3-hourly Ap value. Because the onset of geomagnetic disturbances is not always at 00 UT, and because most daily indexes are based on the 24-hour UT day, the Ap* values are an indication of the most severe 24-hour period of a geomagnetic disturbance.)

The good association between the presence of enhanced solar particle flux at the Earth and strong magnetic disturbances associated with solar flare episodes near the solar central meridian reflects the common source function, (*i.e.*, solar activity). In fact, the presence of these particles, in association with episodes of solar activity as the source region crosses the solar disk, is reliable enough to be used as a predictor of geomagnetic disturbances. Although the technique described in the following paragraphs might identify many of the major fluence events, it cannot be used to postulate proton events that might have been associated with flares having source locations greater

than ~45° from central meridian. Major proton events from west-limb solar activity similar to that of 23 February 1956, 4 May 1960 and 29 September 1989 would have to be inferred from other techniques.

From the geomagnetic records (Mayaud 1973), we can determine the dates of major geomagnetic disturbances for the past century. As a first approximation, one can assume that a major flare within ± 45° of solar central meridian, followed within a day or two by a major geomagnetic disturbance, probably produced a solar particle event at the Earth. However, it is not possible to assemble a consistent record of these events over the past century, because the systematic flare-patrol records, organized by the International Astronomical Union, did not commence until January 1934.

In applying this "geomagnetic disturbance inference technique" to the "known" proton events prior to 1956, we have tested the procedure against the Svestka (1966) probable proton event list, which includes the four known ground-level events prior to 1956. For these associations, we used the probable flare location (Svestka 1966; Cliver *et al.* 1982), the aa* values and the sudden commencement lists of Mayaud (1973), and the Ap* values (Allen, personal communication 1989). From a combination of these records, we were able to associate all but three "strong" PCA events in Svestka's (1966) list with geomagnetic activity, and those three exceptions were events associated with possible source flare positions beyond ± 45° of solar central meridian. Two of these "strong" PCA events were solar cosmic-ray ground-level events (7 March 1942 and 19 November 1949) emanating from source flares near the western limb of the sun, and were not associated with strong geomagnetic activity. Neither would the 23 February 1956 event be identified by this technique, because it was associated with a flare at 80° W, and was not associated with a major geomagnetic storm.

Conclusion

Using the list of significant solar proton events from 1954 to 1986, we have found that the large fluence events at the Earth are usually associated with a sequence of solar activity near the central meridian of the sun and associated geomagnetic storms. This same phenomenon is true for the major events of the present solar cycle. From these results, we have suggested a method of identifying periods when major solar proton fluence events may have occurred throughout the past century. For this method, we use the geomagnetic field records and whatever solar observations are available. We emphasize that this method will not identify major proton events from flares on the western hemisphere of the Sun, because these flares typically do not usually generate a subsequent geomagnetic disturbance. We feel that this method can be further refined using other records of solar activity, such as the measurement of nuclides in polar ice cores.

References

Allen, J. 1982 Some commonly used magnetic activity indices: Their derivation, meaning and use. In *Proceedings of a Workshop on Satellite Drag*, NOAA, ERL, Boulder, Colorado: 114–134.

Cliver, E. W., Kahler, S. W., Shea, M. A. and Smart, D. F. 1982 Injection onsets of ~2 GeV protons, ~1 MeV electrons, and ~100 keV electrons in solar cosmic ray flares. *Astrophysical Journal* 260: 362–370.

Feynman, J., Armstrong, T. P., Dao-Gibner, L. and Silverman, S. 1990 New interplanetary proton fluence model. *Journal of Spacecraft and Rockets* 27(4): 403–410.

Flückiger, E. O., Smart, D. F. and Shea, M. A. 1986 A procedure for estimating the changes in cosmic ray cutoff rigidities and asymptotic directions at low and middle latitudes during periods of enhanced geomagnetic activity. *Journal of Geophysical Research* 91(A7): 7925–7930.

Goswami, J. N., McGuire, R. E., Reedy, R. C., Lal, D. and Jha, R. 1988 Solar flare protons and alpha particles during the last three solar cycles. *Journal of Geophysical Research* 93(A7): 7195–7205.

Levy, E. H., Duggal, S. P. and Pomerantz, M. A. 1976 Adiabatic Fermi acceleration of energetic particles between converging interplanetary shock waves. *Journal of Geophysical Research* 81(1): 51–59.

Lingenfelter, R. E. and Ramaty, R. 1970 Astrophysical and geophysical variations in C14 production. *In* Olsson, I. U., ed., *Radiocarbon Variations and Absolute Chronology*. Proceedings of the 12th Nobel Symposium. New York, John Wiley & Sons, 513–537.

Mayaud, P. N. 1973 A Hundred Year Series of Geomagnetic Data 1868–1967. *IAGA Bulletin* 33. Paris, IUGG Publication Office.

McKinnon, J. A. 1987 *Sunspot Numbers 1610–1986 Based on the Sunspot Activity in the Years 1610–1960*. UAG-95, NOAA, National Geophysical Data Center, Boulder, Colorado.

Shea, M. A. and Smart, D. F. 1990a A summary of major solar proton events. *Solar Physics* 127: 297–320.

_____1990b Solar proton events – review and status. *In* Thompson, R. J., Cole, D. G., Wilkinson, P. J., Shea, M. A., Smart, D. F. and Heckman, G. R., eds., *Solar-Terrestrial Predictions*. Proceedings of a Workshop at Leura, Australia. NOAA, Boulder, Colorado: 213–225.

Smart, D. F. and Shea, M. A. 1989 Solar proton events during the past three solar cycles. *Journal of Spacecraft and Rockets* 26(6): 403–415.

Svestka, Z. 1966 Proton flares before 1956. *Bulletin of the Astronomical Institute of Czechoslovakia* 17(5): 262–270.'

[RADIOCARBON, VOL. 34, NO. 2, 1992, P. 263–270]

ON A PLAUSIBLE PHYSICAL MECHANISM LINKING THE MAUNDER MINIMUM TO THE LITTLE ICE AGE

ELIZABETH NESME-RIBES and ANDRE MANGENEY

CNRS, Observatoire de Paris, 92195 Meudon-Cedex, France

ABSTRACT. To understand better the Earth's climate, we need to know precisely how much radiation the Sun generates. We present here a simple physical mechanism describing the convective processes at the time of low sunspot activity. According to this model, the kinetic energy increased during the Maunder Minimum, causing a decrease of the solar radiation that was sufficient to produce a little Ice Age.

INTRODUCTION

Much effort has been made to find the signature of solar activity in the Earth's atmospheric records (see a summary of recent work by Labitske & Van Loon 1990). Evidence for a statistically significant 11-year periodicity in various atmospheric indices is increasing. However, the time sequence (a few 11-year solar cycles) is usually too short, so that some aliasing effect may result (Teitelbaum & Bauer 1990). Further, we are lacking a physical interpretation of the link between the 11-year solar cycle and the properties of the Earth's atmosphere.

Maunder (1894) reported some relation between long series of solar cycles and climatic events. In particular, a severe cold period was coincident with decreased sunspot activity during the second half of the 17th century. Although the coincidence is intriguing, the relation remains to be established.

In this paper, we offer a plausible mechanism linking the Maunder Minimum to the coincident mini-Ice Age. Our understanding of the Maunder Minimum is based on observations of the present solar cycle as well as on historical data. We shall first summarize our present knowledge about the 11-year solar cycle.

THE 11-YEAR SOLAR CYCLE: PRESENT KNOWLEDGE

During the course of the 11-year solar cycle, the Sun's magnetic field oscillates between a poloidal component, which is dominant at sunspot minimum, and toroidal components, a manifestation known as the "butterfly diagram" of the active regions.

For the α-ω dynamo to hold, two ingredients are required: 1) non-uniform rotation that produces the toroidal field from the poloidal field; 2) some convective motions that regenerate the poloidal field through the "α" effect (Roberts & Stewartson 1974).

Several solar phenomena are related to the solar magnetic cycle:

1. Large-scale circulation in the form of "azimuthal rolls" has been discovered (Ribes & Mein 1984; Ribes & Bonnefond 1990). These giant rolls are cycle-dependent, and are at their maximum, three per hemisphere, in the ascending phase of the cycle. Their upper and lower borders run along 60° and 35°, respectively. After the sunspot maximum, there are two rolls in each hemisphere, with edges at 15°–20°. No rolls are visible any longer at sunspot minimum. Periods of strong solar activity favor the two-roll configuration (Ribes & Bonnefond 1990). One interesting property of the rolls is that they modulate the surface rotation (Ribes, Mein & Mangeney 1985).

2. Helioseismological studies have given some insight into the internal rotation of the Sun (Brown & Morrow 1987). The convective zone (from 0.7 $R_\odot$ up to the surface) exhibits the same latitudinal rotation throughout, whereas the radiative zone (below 0.6 $R_\odot$) rotates like a solid body.
3. The apparent solar diameter varies during the solar cycle, reaching minimum at the time of the sunspot maximum (Laclare 1987). This has been confirmed independently from the frequency shift of acoustic oscillations through the solar cycle (see Fossat *et al.* (1987) for a summary of observations).
4. The total irradiance monitored by ACRIM (on board the Solar Maximum Mission Satellite) varies, and is maximum when the sunspot number is maximum (Willson & Hudson 1991). The changes in the apparent solar diameter and total irradiance observed during cycle 21 (1975–1986) are 2.10^{-4} and 10^{-3}, respectively.

One astrophysical question of interest is the relation between these various observations.

In the framework of the (α-ω) dynamo, the toroidal field is produced from the poloidal field by a shear in the angular velocity. Such a shear exists at the interface between the radiative and the convective zones (Brown & Morrow 1987). Further, a positive shear of the angular velocity is confined to the surface latitude belt of $\pm$ 30°, thus being responsible for the distribution of active regions through the solar cycle, "the butterfly diagram" (Ribes 1990a; Belvedere, Proctor & Lanzafame 1991). The amplitude of the surface differential rotation, which varies from one 11-yr cycle to the other, might reflect the strength of the sunspot cycles. Then, the azimuthal rolls could be the regulator of the internal positive shear and, thus, of the surface rotation.

It is likely that large-scale circulation in the convective zone contributes to the energy transport from below, leading to a structural change in the solar envelope (diameter and luminosity). On the one hand, though sunspots and bright faculae may easily explain the short-term fluctuations present in the total solar irradiance, there must be some phenomenon to account for the 11-yr trend (Willson & Hudson 1991). On the other hand, the good anticorrelation between apparent diameter and solar constant data suggests that the azimuthal roll pattern might be the cause of the trend present in both apparent diameter and solar constant data (Ribes & Laclare 1988). The modulation of the surface rotation can be used as a tracer of the thermal response caused by periodic emergence of magnetic fields. In this context, the Maunder Minimum, characterized by a lack of sunspots, gives a first-order constraint to the models.

THE MAUNDER MINIMUM: OBSERVATIONAL DATA

The Maunder Minimum is a well-documented period. A unique, 50-year record of solar observations has been made at the Observatoire de Paris. Philippe La Hire (1718) observed and recorded the solar diameter over the period, 1683 to 1718, using the same instrument, thus preserving the homogeneity of the data set. His observations have been analyzed (Ribes, Ribes & Barthalot 1987; Ribes *et al.* 1990; Ribes 1990b), and several facts have been noted:

1. The apparent solar diameter expanded, mainly when there were few sunspots, *i.e.*, between 1683 to 1700, and then slowly came back to normal after 1705. We know that 17th-century optics were poor, and systematically enlarged the apparent diameter. However, Ribes *et al.* (1990) estimated a 0.2% increase of the apparent radius from La Hire's 36 years of homogeneous observations, and calibrated these observations with the solar diameter as derived from the solar eclipse timed by Halley, in 1715. Moreover, the observed apparent diameter exhibits a strong 11-yr modulation, despite the little sunspot activity. Some variability, of magnetic origin, is also present in the abundance of cosmo-

genic isotopes, such as ^{14}C (Kocharov 1986) and ^{10}Be (J. Beer, personal communication). The similarity in the variability of the apparent solar diameter and the cosmogenic isotope abundance indicates that the solar envelope responds to the cyclic magnetic fields. If one accepts that the observed changes of the apparent diameter are "*in situ*," the Sun's luminosity might have changed as well.

2. About 100 sunspots were observed during the second half of the Maunder Minimum, and these were confined within the latitude range of ± 18°. The rate of the surface rotation has been obtained by measuring the displacement of these sunspots in their transit across the solar disk. Ribes, Ribes and Barthalot (1987) found that the surface rotation was much more differential than it is now: the equatorial rate was 2% smaller, and the rate at 18° latitude was 6% smaller than at present. In other words, the 18° latitude belt had the same rotation rate as the present 30° latitude belt.

CONVECTIVE PATTERN DURING THE MAUNDER MINIMUM

The model we develop here consists of estimating the contribution of the large-scale convection to the solar luminosity. We make two assumptions:

1. The large-scale rolls inferred from the meridional circulation have a depth comparable to their width, which is the depth of the convective zone (Ribes & Laclarė 1988).
2. We assume that the large-scale convective pattern is the main cause of the modulation of the surface sunspot rotation through the Coriolis forces. In particular, we neglect the Lorentz forces in the dynamic equations; this assumption is supported by the fact that the observed large-scale magnetic field is weak (Hoeksema 1991).

We shall make some comments related to these assumptions. The physical conditions for exciting large-scale modes of convection, the rolls, can be achieved in the convective zone, as suggested by the presence of rolls. The critical Rayleigh number from which the large-scale convective mode develops is reached under the action of the magnetic field on the turbulent (small-scale) plasma.

The Rayleigh number, which measures the importance of the buoyancy force relative to the stabilizing effects of diffusion, is proportional to the temperature gradient and to the depth of the convective layers, and is inversely proportional to the thermal diffusivity, χ, and the kinematic viscosity, ν. In the presence of magnetic field, one usually believes that convection is inhibited, reducing χ and ν. If large-scale convective rolls are thus decoupled from small-scale turbulent plasma, one can imagine a way to reach the critical Rayleigh number for large-scale convection, denoted hereafter as $Ra_{c,r}$: the small-scale (and stronger field) decreases χ and ν, thus increasing $Ra_{c,r}$; the larger the magnetic field, the larger the number of rolls. This explains, qualitatively at least, the change of the roll pattern from no roll (or a single roll per hemisphere) at sunspot minimum up to a three-roll pattern when the sunspot activity reaches its maximum.

We shall examine whether this model is able to estimate the change of solar luminosity through the 11-yr cycle and for longer cycles, of the Maunder Minimum type. In the present paper, we apply our model to the Maunder Minimum, leaving the 11-yr cycle for a separate study.

In principle, the large-scale convection pattern can be derived from the meridional motions of sunspots. The magnitude of the flow is of the order of 10 to 15 m s^{-1}, which was not easily measurable with 17th century sunspot observations. However, the surface rotation profile was strongly modulated in the second half of the 17th century, suggesting that giant convective motions did exist.

A simple equation in which the Coriolis force is balanced by the turbulent diffusivity, in an incompressible fluid, can be obtained from the azimuthal component of the momentum conservation

$$\frac{\partial}{\partial t}\left\{\frac{\delta\Omega}{\Omega_0}\right\} + 2\left\{\frac{w}{r} + \frac{v\cos(\theta)}{r\sin(\theta)}\right\} = \frac{1}{t_R}\frac{\delta\Omega}{\Omega_0} \tag{1}$$

where Ω_0 is the equatorial rotation without meridional circulation, $\delta\Omega$ the deviation from this rotation rate, w and v the vertical and horizontal components of the meridional circulation, r and θ the radial coordinate and the colatitude, and t_R the viscous damping time, $\sim l^2/\nu$, $l \sim 0{\cdot}3R_\odot$ being a typical scale of the circulation pattern, and $\nu \sim 10^{12}$–10^{13} cm^2s^{-1} the turbulent viscosity; with these typical parameters, t_R is a few years. A number of effects have been neglected in this equation, for example, the Lorentz force due to the magnetic field, an assumption which would not really be justified if the magnetic field were larger than a few thousands gauss. However, because we aim only to illustrate the basic consequences of a meridional circulation, we shall neglect all effects besides the Coriolis force and the viscosity. The best justification for doing this is that the order of magnitude for the differential rotation one expects from this balance

$$\frac{\delta\Omega}{\Omega_0} \sim \frac{t_R}{R_\odot} v_{circ}$$

is comparable to what is observed, if any credit is given to the standard estimates of the turbulent viscosity.

To keep with the level of sophistication of Equation (1), we do not study a fully self-consistent problem, but, rather, we consider a steady state with a prescribed meridional circulation in a spherical shell of inner and outer radii, R_1 and R_2, $l = R_2 - R_1$.

We introduce a velocity potential $\Psi(r,\theta)$ such that

$$\frac{1}{\sin(\theta)}\frac{\partial}{\partial\theta}\sin(\theta)\frac{\partial}{\partial\theta}\Psi = -\frac{\partial r^2 w}{\partial r} \tag{2}$$

$$v = \frac{1}{r}\frac{\partial\Psi}{\partial\theta}\,. \tag{3}$$

In the particular model we consider here

1. $\Psi(r,\theta) = H(r)F(\theta)$, with H(r) having the simplest form compatible with the conditions, $w(R_1) = w(R_2) = 0$

$$H(r) = -\frac{V_c}{R_2 l}\left\{4r^2 - 3r(R_1 + R_2) + 2R_1R_2\right\} \tag{4}$$

(V_c being a typical meridional velocity).

2. $F(\theta)$ is a superposition of a small number of even Legendre polynomials of $x = \cos(\theta)$, so that the meridional circulation is symmetric about the equator

$$F(\theta) = \text{constant} \pm (P_2(x) + \lambda P_4(x) + \mu P_6(x)) \,. \tag{5}$$

The value of the constant is irrelevant.

This form of the velocity potential produces a pattern of symmetric meridional cells, with the number of cells depending on the value of the parameters, λ and μ. Figure 1 shows an example of such a pattern. In the steady state, the differential rotation pattern at the surface ($r = R_2$) obtained from equation (1) is

$$\frac{\delta\Omega}{\Omega_0} = \frac{t_R V_c}{R_2}\{f(\lambda,\nu,\theta)\} \tag{6}$$

in which f is a superposition of even Legendre polynomials, with coefficients depending on λ and μ.

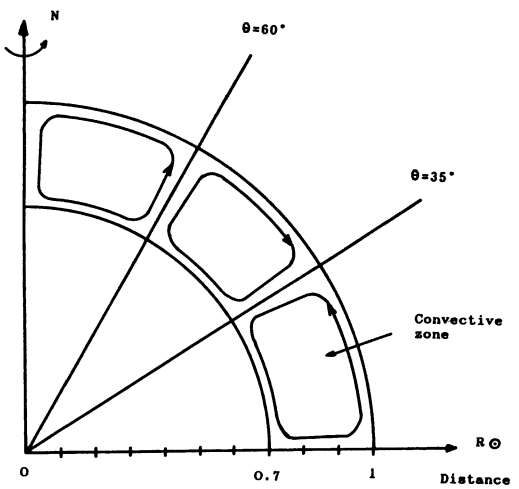

Fig. 1. μ = 1.4; λ = 1.2; Three-cell meridional circulation corresponding to the ascending phase of the solar cycle 21 (1976–1986)

On the other hand, observations of the differential rotation can be fitted with a combination of Legendre polynomials providing Ω, V_c, λ and μ, parameters that characterize the meridional flow. For the Maunder Minimum, the best polynomial fit to the observations gives one roll per hemisphere, with

$$\Omega_0 \sim 13.98\text{deg/day}, \tag{7}$$

and

$$V_c \sim 0{\cdot}3\frac{R_\odot}{t_R} \,. \tag{8}$$

Ω_0 is of the order of the rotation rate of the radiative interior. For comparison, the same fit for 1984, near sunspot minimum, also gives one roll per hemisphere, with

$$\Omega_0 \sim 14{\cdot}4\text{deg/day}, \tag{9}$$

and

$$V_c \sim 0.7\frac{R_\odot}{t_R} \quad . \tag{10}$$

In 1979, near sunspot maximum, there are three rolls per hemisphere, with

$$\Omega_0 \sim 13{\cdot}45\text{deg/day}, \tag{11}$$

and

$$V_c \sim 0{\cdot}07\frac{R_\odot}{t_R} \quad . \tag{12}$$

If the viscous damping time, τ_R, is a few years, the convective velocities deduced from the solar rotation modulation were ranging from 10 ms^{-1} for the Maunder Minimum and the year, 1984, to 1 ms^{-1} for the sunspot maximum of 1979.

How do we relate these variations in V_c to luminosity variations?

One possible line of argument is:

At the base of the convective zone, the flux is constant over the time scales under consideration. On the other hand, the partitioning between large and small scale of motions in the convective zone may change with time. In particular, the energy flux going into large-scale motions can be estimated as:

$$E = M_c V_c^2 / \tau_{conv},$$

where M_c is the mass of the convective zone (10^{31} g). If the observed meridional flow traces deep convective rolls, one can estimate τ_{conv}, the turnover convective time of the roll (ratio between the depth of the convective zone (2.10^8 m) and the meridional velocity (~10m s^{-1})), to be of the order of one year. Thus, the kinetic energy excess is 10^{30} ergs s^{-1}, *i.e.*, 0.1 times the observed change of solar irradiance, suggesting that the efficiency of the thermal driving of the large-scale convection is of the order of 0.1. Our mechanism explains the inverse correlation between V_c and the δ L, as observed.

To obtain more accurate estimates of the luminosity variations, solar envelope models are needed. This will be done in a separate study.

Conclusion

We have shown that a single-roll pattern is capable of reducing the surface rotation in a way shown by the 17th-century observations of the surface rotation. Such a pattern persisted over a period of several decades, at the time of low sunspot activity. The convective velocity associated with the roll is almost an order of magnitude larger than the velocity of the rolls in 1979, at sunspot maximum. We can speculate that the increase of the energy stored in the large-scale convection results in a decrease of solar luminosity, if a constant energy flux is assumed at the base of the convective zone. For the present 11-yr cycle, the solar irradiance changes by one part per thousand between solar maximum and solar minimum. A similar decrease in solar irradiance can be deduced during periods of low sunspot activity, such as the Maunder Minimum. The decrease of luminosity

might have been larger: some time intervals of almost 10 years were characterized by a complete lack of sunspots. So, one conjectures that the convective instability threshold for large-scale rolls had not been reached, causing a more drastic luminosity decrease. The present study does not model this. However, the conservative estimate of the solar irradiance decrease of at least 0.3 Watt m^{-2} at the top of the Earth's atmosphere and persisting over several decades, could account for some climatic changes.

The solar luminosity decrease inferred from the large-scale circulation in the convective zone is corroborated by the reported expansion of the solar diameter during the Maunder Minimum (Ribes *et al.* 1990). No satisfactory mechanism explains the observed anticorrelation between apparent diameter and solar irradiance (see Spruit 1991 for a review of the mechanisms). The expansion of the apparent solar diameter was strongly modulated with an 11-yr periodicity, at least during the period spanned by the Paris observers. The expansion was up to two arcseconds every ten years, and fell to a much smaller value five years later. The modulation exhibits the same characteristics as the present modulation of the apparent diameter, except that the amplitude was ten times larger. We have no measure of the solar output at that time. However, if the ratio between solar irradiance and apparent radius (a ratio of five for the previous 11-yr solar cycle) were the same during the Maunder Minimum, it would correspond to a maximum reduction of 0.1 to 1.10^{-2} of the solar output, at a rhythm of ten years. This would result in a mean variation of the solar constant of 0.5% over several decades. Such a solar radiation forcing corresponding to a decrease of one Watt m^{-2} at the top of the Earth's atmosphere is sufficient to produce a little Ice Age (H. Le Treut, personal communication).

Acknowledgments

Spectroheliograms have been digitized with a digital microphotometer developed and operated by the CNRS/INSU and located at the Observatoire de Paris.

References

Belvedere, G., Proctor, M. R. E. and Lanzafame, G. 1991 The latitude belts of solar activity as a consequence of a boundary-layer dynamo. *Nature* 350: 481–483.

Brown, T. M. and Morrow, C. A. 1987 Depth and latitude dependance of solar rotation. *Astrophysical Journal* 314: L21–L26.

Fossat, E., Gelly, B., Grec, G. and Pomerantz, M. 1987 Search for solar p-mode frequency changes between 1980 and 1985. *Astronomy and Astrophysics* 177: L47–L48.

Hoeksema, J. T. 1991 Large-scale solar and heliospheric magnetic fields. *Advanced Space Research* 11(1): 15–24.

Kocharov, G. E. 1986 Cosmic ray archeology, solar activity and supernova explosions. *Proceedings of the Joint Varenna-Abustumani International School and Workshop on Plasma Astrophysics*. USSR, Ed. ESA SP-25: 259–270.

Labitske, K. and Van Loon, H. 1990 Associations between the 11-year solar cycle the Quasi-biennial oscillation and the atmosphere: A summary of recent work. *Philosophical Transactions of the Royal Society of London* A330: 577–589.

Laclare, F. 1987 Sur les variations du diametre du Soleil observées à l'astrolabe solaire du C.E.R.G.A. *Comptes Rendus de l'Académie des Sciences* 305(2): 451–454.

La Hire, P. 1683–1718 Archives de l'Observatoire de Paris D2: 1–10.

Maunder, R. W. 1894 A prolonged sunspot minimum. *Knowledge* 17(106): 173–176.

Ribes, E. 1990a Longs cycles d'activité solaire. *In* Benest, D. and Froschle, C., eds., *Le Soleil, Une Étoile et Son Domaine, École de Goutelas*: 357–373.

Ribes, E. 1990b Astronomical determinations of the solar variability. *Philosophical Transactions of the Royal Society of London* 330: 487–497.

Ribes, E. and Bonnefond, F. 1990 Magnetic tracers, a probe of the solar convective zone. *Geophysical Astrophysical Fluid Dynamics* 55: 241–261.

Ribes, E. and Laclare, F. 1988 Toroidal convective rolls in the Sun: A challenge to theory. *Geophysical Astrophysical Fluid Dynamics* 41: 171–180.

Ribes, E. and Mein, P. 1984 Search for giant convective cells from the analysis of Meudon spectroheliograms. *In* Muller, R., ed., *Proceedings of the European Astronomical Meeting*. Toulouse: 283–288.

Ribes, E., Mein, P. and Mangeney, A. 1985 A large-scale meridional circulation in the convective zone. *Nature* 318: 170–171.

Ribes, E., Merlin, Ph., Ribes, J.-C. and Barthalot, R. 1990 Absolute periodicities in the solar diameter derived from historical and modern data. *Annales Geophysicae* 7(4): 321–330.

Ribes, E., Ribes, J.-C. and Barthalot, R. 1987 Evidence for a larger Sun with a slower rotation during the seventeenth century. *Nature* 326: 52–55.

Roberts, P. H. and Stewartson, K. 1974 On finite amplitude convection in a rotating magnetic system. *Philosophical Transactions of the Royal Society of London* A277: 287–315.

Spruit, H. 1991 Theory of solar luminosity and solar diameter variations. *In* Sonett, C. and Giampapa, M., eds., *The Sun In Time.* Tucson, The University of Arizona Press: 118–158.

Teitelbaum, H. and Bauer, P. 1990 Stratospheric temperature eleven years variations: Solar influence or stroboscopic effect. *Annales Geophysicae* 8: 239–242.

Willson, R. C. and Hudson, H. 1991 The Sun's luminosity over a complete solar cycle. *Nature* 351: 42–44.

[RADIOCARBON, VOL. 34, NO. 2, 1992, P. 271–276]

A TANDEM MASS-SPECTROMETRIC METHOD OF COSMOGENIC ISOTOPE ANALYSIS

A. K. PAVLOV, V. T. KOGAN

A. F. Ioffe Physico-Technical Institute, Academy of Sciences, Polytechnicheskaya 26
St. Petersburg 194021 Russia

and

G. Y. GLADKOV

St. Petersburg State Technical University, Polytechnicheskaya 29, St. Petersburg 195251 Russia

ABSTRACT. We propose an original method for analysis of low-concentrations of stable and long-lived radioactive nuclides. We discuss the parameters of the main features of the "Trace" spectrometer (a multicharged-ion laser source, a highly sensitive time-of-flight mass spectrometer, a charge-exchange chamber and a mass spectrometer for positive and negative single-charged ion analysis). We also compare these features with conventional AMS devices.

INTRODUCTION

We describe here the setup of our Tandem mass spectrometer, "Trace," which was designed in the Leningrad Physico-Technical Institute and is now under construction. Kocharov *et al.* (1990) discussed the basic operating principles at the Fifth Accelerator Mass Spectrometry (AMS) Conference in Paris. Figure 1 shows the principal layout of the setup, which includes a multicharged ion laser source combined with a highly sensitive time-of-flight (TOF) mass spectrometer and a charge-exchange chamber for the interaction of the ions with energy of about 1 keV/nucleon passing through thin foils or gases. The mass spectrometer can be used for positive and negative single-charged ion analysis. An accelerator of any type can be used as an exit device of the Trace spectrometer for isobar discrimination and noise suppression.

METHODOLOGY

The basic mass-spectrometric problem is the separation of molecular ions with the same masses and isobars from the ions of interest. We resolve this by using an original method based on ideas from AMS.

In the first step, the high-efficiency laser ion source produces the ions with charge $Q > +2$, which are then separated by a TOF mass spectrometer. Because molecular ions with $Q > +2$ are unstable, they are eliminated by the first mass-spectrometer element of our setup. This mass spectrometer is also the separator from the main isotope.

The proportion of the ions in the appropriate charge state produced by the ion source can reach 50%. The total current in these experiments was 10^{-7}–10^{-6} A, and can be increased easily by using a more powerful laser.

The laser source is expected to have a lower background than the standard cesium sputtering source for AMS. This feature is a significant advantage for stable or long-lived radioactive nuclide measurements. We know that the laser source produces ion beams with a very wide spread in angle and energy distribution. Thus, we have designed a new mass spectrometer based on a combination of TOF separation and space focusing by magnetic field. The mass spectrometer shown in Figure 2 can analyze the ions with a wide spread in energy and angle distribution: solid angle – up to 1 sterad; energy – 10–160 eV.

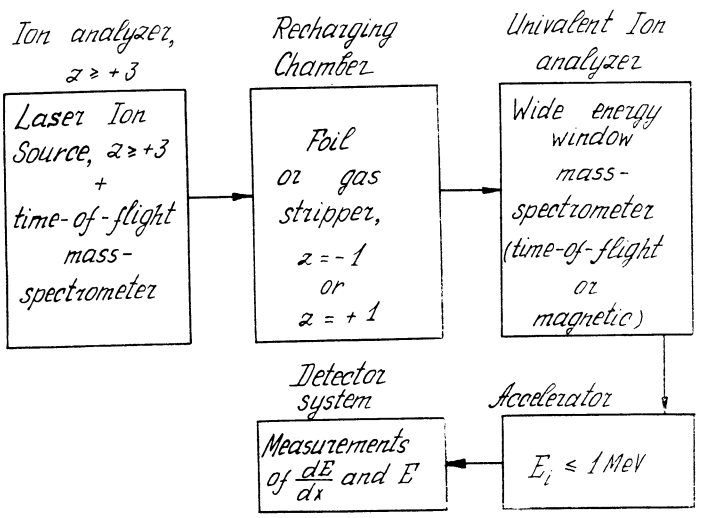

Fig. 1. Block diagram of the Trace setup

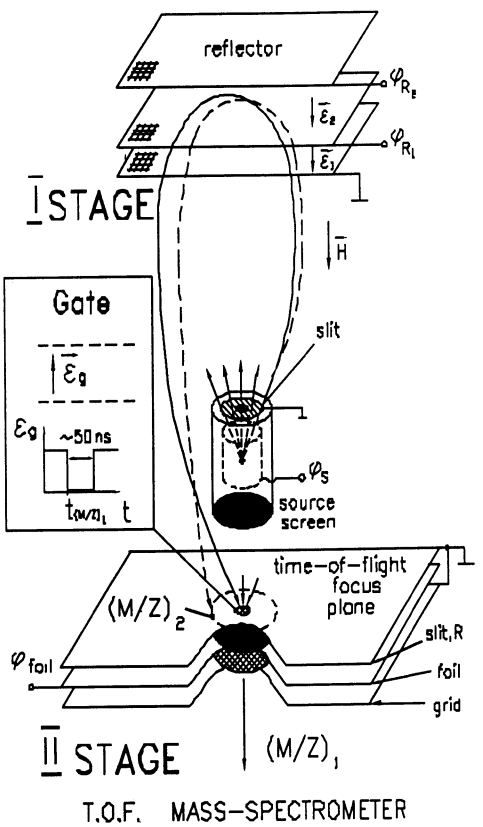

Fig. 2. Magnetic time-of-flight mass spectrometer

In the first step, ions are accelerated up to U = 1 kV, and pass through the first drift region. Then they are reflected by an electrostatic mirror (Smikk & Dubensky 1984) and pass through the second drift region. The total TOF, t, is described as

$$t_f(T) = (M/2z)^{0.5} \cdot (L/T^{0.5} + 4 \cdot T^{0.5}/E)$$
$$T = ezU + t_0 \quad (1)$$

where L = drift length; T_0 = initial ion kinetic energy; E = electric field intensity. This allows us to obtain TOF focusing of ions with different energy on the same plane, for any kind of ion. The mirror consists of two parts for better focusing.

The TOF system is placed in a uniform magnetic field, H, parallel to the electric field in the reflector. Thus, certain mass ions with very wide angles are collected to focus at a point where $t_r = t_f$, and $t_r = (M/z)\,(c/H)$. Other ions are collected in concentric rings of radius, R, on the same plane. An electrostatic gate is placed at the focal point to pass ions under investigation into the recharging chamber.

Results and Discussion

Figures 3 and 4 show the results of our calculations of mass-spectrometric parameters. In the example, the energy window was 150 eV and the TOF mass resolution was equal to 600. Figure 4 shows the Monte-Carlo calculation results of scattered ion background. Screens installed in strategic parts of the mass spectrometer can decrease scattering, because scattered ions can hit the thin foil only from a few regions of the electrostatic mirror.

In the next step, ions with energy of about 1 keV/nucleon pass through the thin foil. Ions with positive charge, Q > + 2 are recharged; their charge-state distribution after the foil depends on their velocity and the foil chemical composition only. For the ion velocity, V = 10^7 cm/s, the efficiency

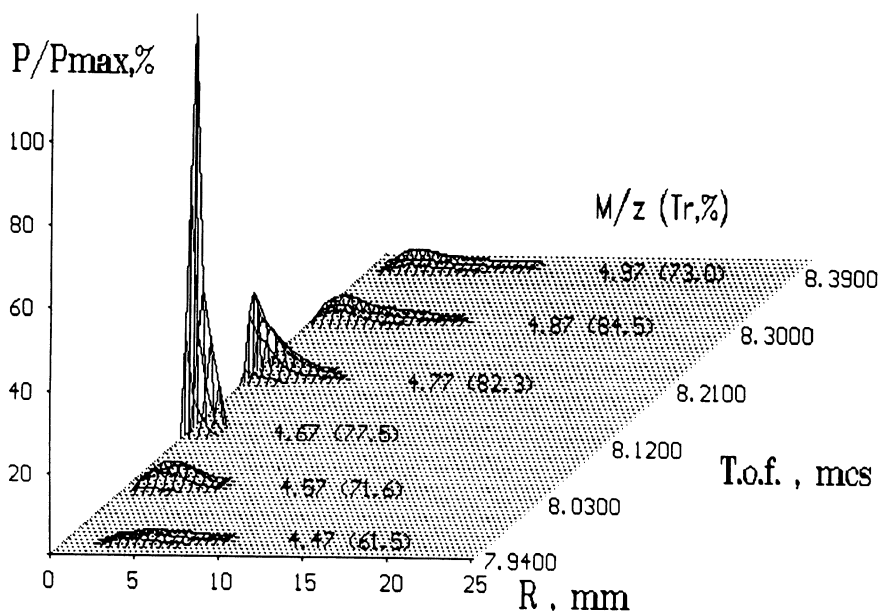

Fig. 3. Transmission and mass resolution of ion beams

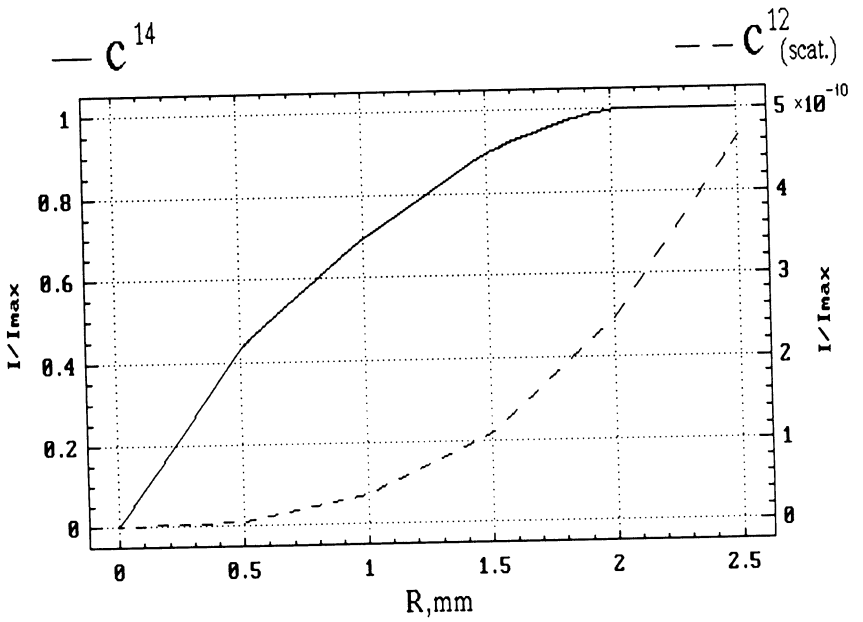

Fig. 4. Scattering ions intensity on the surface of thin foil

of the negative ion production can be from 1% to 10% for ^{14}C, ^{26}Al, ^{36}Cl, ^{129}I, *etc.* (Fig. 5) (Shima, Mikumo & Tawara 1986). For some isotopes, stable negative ions of their isobars do not exist (*e.g.*, ^{14}N - ^{14}C, ^{26}Mg - ^{26}Al pairs). Thus, the subsequent mass spectrometric stage should totally exclude these isobars.

Another method can be used if foil does not efficiently produce stable negative ions (^{10}Be, ^{41}Ca, ^{53}Mn), or stable negative ions of isobars are present (^{36}Cl - ^{36}S, ^{59}Ni - ^{59}Co, *etc.*). This method uses the cross-section difference of the recharging process for multicharged ions on gases, *e.g.*, H_2 or He. Our calculations show that the Be3+ - Be+ cross-section is ten times less than B^{3+} - B^{+}. Thus, about 10% of Be ions in the 3+ state would pass the gas chamber, in contrast to about 10^{-6} of B^{3+} and the selectivity of the step would reach 10^5.

For the ^{36}Cl - ^{36}S isobar pair selection, the negative ion detachment can be used efficiently (Berkovits *et al.* 1990). The pulsed ion beam makes it possible to use the time coincidence of laser and ion pulses, and thus, to overcome the main problem of using this technique: low efficiency of laser pulses interaction with a continuous ion beam.

The Trace spectrometer is free from the process producing the ions with the same mass/charge ratio by recharging, which are possible in AMS, for example,

$$^{12}C_3^- \rightarrow {}^{12}C^+$$
$$^{36}Cl^- \rightarrow {}^{36}Cl^{3+}$$

where the molecule $^{12}C_3^-$ can be a background for ^{36}Cl. Such a process is impossible in Trace due to the reversal recharging method (from positive to negative).

A mass spectrometer of any type (TOF, magnetic or combined) can be used in the next step. It has

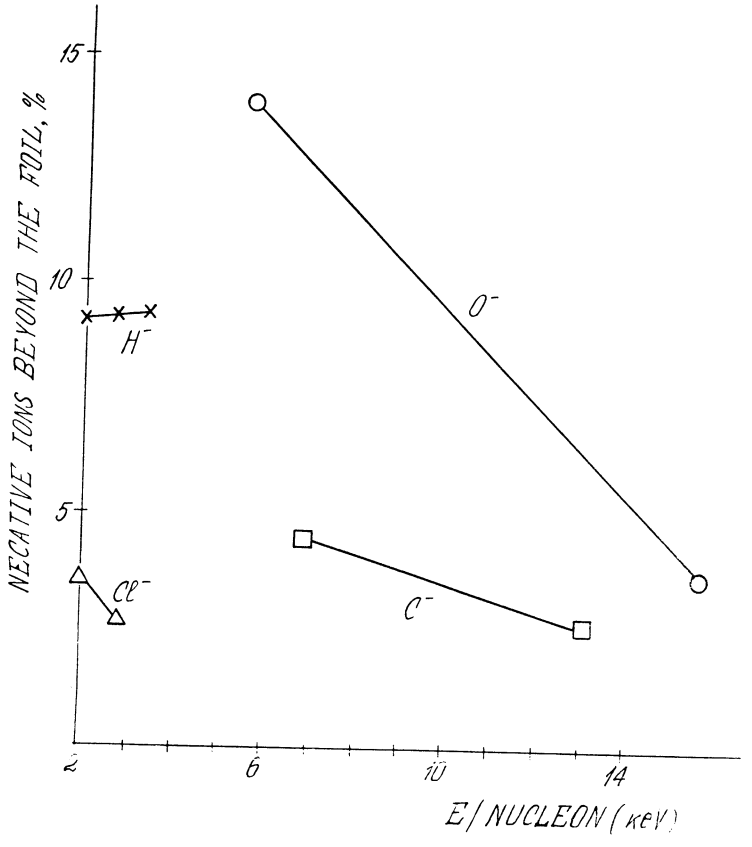

Fig. 5. Production of negative ions beyond the foil

to operate in an ion-energy range of some tens of keV, instead of an MeV range for AMS second mass spectrometers. This peculiarity is advantageous for heavy and very heavy nuclide analysis.

We have also designed another mass-spectrometric scheme based on TOF techniques only (Fig. 6). It is based on a Tandem TOF mass spectrometer with spherical reflectors. This reflector shape allows us to obtain very high sensitivity as a consequence of ion collection from the solid-angle spread to a focus point. Mass resolution is equal to 125 in the first unit and 20 in the second unit, for an energy window of 20–160 eV. Construction of both schemes is now in progress.

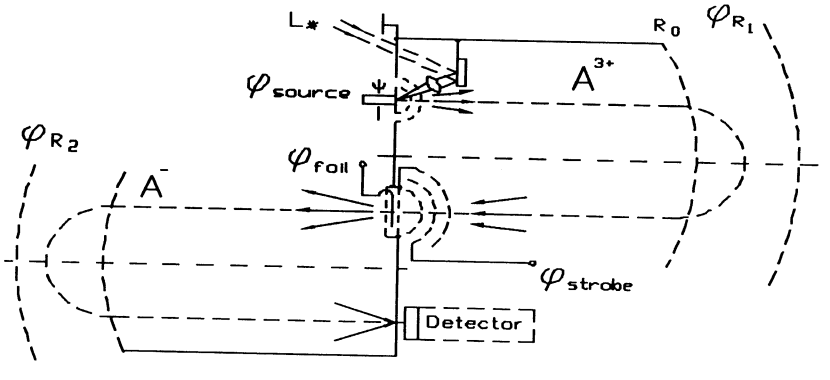

Fig. 6. Time-of-flight mass spectrometer with the spherical mirror

The opportunity of TOF operating control on all spectrometer units allows us to reduce the background level – the random noise component and the component produced by the scattered ions. The Trace spectrometer can also be used as an effective injector for any type of accelerator, as its ion beam has a pulse form and low intensity (10^3–10^5) ions/s.

REFERENCES

Berkovits, D., Boaretto, E., Hollos, G. Kutschera, W. Naaman, R., Paul, M. and Vager, Z. 1990 Study of laser interaction with negative ions. *In* Yiou, F. and Raisbeck, G. M., eds., Proceedings of the 5th International Conference on Accelerator Mass Spectrometry. *Nuclear Instruments and Methods* B52: 384–383.

Kocharov, G., Kogan, V., Konstantinov, A. and Pavlov, A. 1990 The possibilities of cosmogenic isotopes investigation by means of mass-spectrometrical methods. *In* Yiou, F. and Raisbeck, G. M., eds., Proceedings of the 5th International Conference on Accelerator Mass Spectrometry. *Nuclear Instruments and Methods* B52: 384–386.

Shima, K. Mikumo, T. and Tawara, H. 1986 *Atomic Data and Nuclear Data Tables* 34: 57.

Smikk, D. V. and Dubensky, B. 1984 Mirror of mass-reflectron. *Journal of Technical Physics* 54: 912–916 (in Russian).

The Faculty of Mathematics and Natural Sciences of Kiel University Announces the Following Vacancy:

PROFESSOR OF PHYSICS (C3)
and
DIRECTOR OF THE AMS LABORATORY
for
CARBON DATING AND ISOTOPE RESEARCH

The appointee is expected to take part in the planning and establishment of a new Accelerator Mass Spectrometer Laboratory for nuclear dating and isotope research, with the aim of dating samples in Geosciences and Archaeology, using the ^{14}C and ^{10}Be methods.

Duties will include teaching in the research field of the AMS laboratory. Close cooperation with other institutes of Kiel University and with external research groups is expected.

The applicant should have experience in AMS methods and in teaching at the university level. Kiel University welcomes women to apply. Disabled candidates are particularly encouraged to submit applications.

Applications including a curriculum vitae, list of publications and detailed information on the scientific career should be sent **before October 15, 1992** to:

Dekan der Mathematisch-Naturwissenschaftlichen Fakultät der
Christian-Albrechts-Universität zu Kiel
Olshausenstrasse 40
2300 Kiel 1
Federal Republic of Germany

RADIOCARBON
1993 PRICE LIST

New Calibration Issue (Vol. 35, No. 1, 1993)	$ 40.00
Proceedings of the 14th International Radiocarbon Conference (Vol. 34, No. 3, 1992)	$ 65.00
Proceedings of the International Workshop on Intercomparison of ^{14}C Laboratories (Vol. 32, No. 3, 1990)	$ 40.00
Proceedings of the 13th International Radiocarbon Conference (Vol. 31, No. 3, 1989)	$ 60.00
Proceedings of the 12th International Radiocarbon Conference (Vol. 28, Nos. 2A & 2B, 1986 – available separately at $30.00 each)	$ 60.00
Proceedings of the 11th International Radiocarbon Conference (Vol. 25, No. 2, 1983)	$ 50.00
Proceedings of the 10th International Radiocarbon Conference (Vol. 22, Nos. 2 & 3, 1980)	$ 60.00
Vol. 35, Nos. 1–3, 1993 (includes NEW Calibration Issue)	**$105.00/vol. Inst.* $ 73.50/vol. Ind. $ 36.75/vol. Stud.****
Vol. 34, Nos. 1–3, 1992 (includes Proceedings)	$105.00/vol. Inst. $ 73.50/vol. Ind.
Vol. 33, Nos. 1–3, 1991	$ 94.50/vol. Inst. $ 63.00/vol. Ind.
Vol. 32, Nos. 1–3, 1990 (includes Glasgow Proceedings)	$ 94.50/vol. Inst. $ 63.00/vol. Ind.
Vol. 31, Nos. 1–3, 1989 (includes Proceedings)	$ 90.00/vol. Inst. $ 60.00/vol. Ind.
Vol. 30, Nos. 1–3, 1988	$ 85.00/vol. Inst. $ 55.00/vol. Ind.
Vols. 15–29, 1973–1987	$ 75.00/vol. Inst.† $ 50.00/vol. Ind.
Vols. 10–14, 1968–1987	$ 50.00/vol.†
Vols. 1–9, 1959–1967	$ 25.00/vol.
Comprehensive Index (1950–1965)	$ 25.00
Single Issue	$ 25.00
Single copy of out-of-print Issue	$ 35.00

SPECIAL PACKAGE OFFER (now includes 9 out-of-print issues):

Full set, Vols. 1–34 (1959–1992) + *free* subscription for 1993!	$650.00
Postage & handling for Package Offer:	
USA	$ 25.00
Foreign	$ 50.00

***Foreign postage on current volumes $ 10.00**
†Plus additional charge for copy of out-of-print issue(s)
Postage & handling will be added to back orders

****New Student Rate** – with student identification and letter from subscribing sponsor.
Back issues available at 1/2 the individual rate.

Archaeometry

The prime research journal for the archaeologist interested in the involvement of the physical sciences in archaeology and art history. Articles are written with the non-specialist in mind while Research Notes provide state-of-the-art specialist reports.

Contents of Vol 34, part 1 (February 1992) include

Price, including postage, of the 1992 volume: Europe £24 sterling; elsewhere US $56. Reduced prices for individuals: Europe £16 sterling; elsewhere US $38. To order: send cheque or credit card details (VISA, ACCESS, MASTER, EURO, AMEX) to the address below. Despatch is by airfreight/surface to Europe, North America and Australia; by surface elsewhere (air rates on application). All back numbers are in stock.

Published twice a year by the Research Laboratory for Archaeology & the History of Art, Oxford University, 6 Keble Road, Oxford OX1 3QJ, UK. FAX No. 0865 273932.

NOTICE TO READERS AND CONTRIBUTORS

Since its inception, the basic purpose of *RADIOCARBON* has been the publication of compilations of ^{14}C dates produced by various laboratories. These lists are extremely useful for the dissemination of basic ^{14}C information.

In recent years, *RADIOCARBON* has also been publishing technical and interpretative articles on all aspects of ^{14}C. We would like to encourage this type of publication on a regular basis. In addition, we will be publishing compilations of published *and unpublished* dates along with interpretative text for these dates on a regional basis. Authors who would like to compose such an article for his/her area of interest should contact the Managing Editor for information.

Other sections recently added to our regular issues include NOTES AND COMMENTS, LETTERS TO THE EDITOR, RADIOCARBON UPDATES and ANNOUNCEMENTS. Authors are invited to extend discussions or raise pertinent questions to the results of scientific investigations that have appeared on our pages. These sections include short, technical notes to relay information concerning innovative sample preparation procedures. Laboratories may also seek assistance in technical aspects of radiocarbon dating. Book reviews are also encouraged as are advertisements.

Manuscripts. Papers may now be submitted on both floppy diskettes and hard copy. When submitting a manuscript, include three hard copies, double-spaced. When the final copy is prepared after review, please provide a floppy diskette along with one hard copy. We will accept, in order of preference, WordPerfect 5.1 or 5.0, Microsoft Word, Wordstar or any IBM word-processing software program. ASCII files, MS DOS and CPM formatted diskettes are also acceptable. The diskettes should be either 3½" (720 k or 1.44 megabytes) or 5¼" (360 k or 1.2 megabytes). Radiocarbon papers should follow the recommendations in INSTRUCTIONS TO AUTHORS (R, 1992, vol. 34, no. 1, p. 177–185). Offprints are available upon request. Our deadline schedule for submitting manuscripts is:

For	*Date*
Vol. 35, No. 2, 1993	January 1, 1993
Vol. 35, No. 3, 1993	May 1, 1993
Vol. 36, No. 1, 1994	September 1, 1993

Half-life of ^{14}C. In accordance with the decision of the Fifth Radiocarbon Dating Conference, Cambridge, England, 1962, all dates published in this volume (as in previous volumes) are based on the Libby value, 5568 yr, for the half-life. This decision was reaffirmed at the 11th International Radiocarbon Conference in Seattle, Washington, 1982. Because of various uncertainties, when ^{14}C measurements are expressed as dates in years BP, the accuracy of the dates is limited, and refinements that take some but not all uncertainties into account may be misleading. The mean of three recent determinations of the half-life, 5730 ± 40 yr, (*Nature*, 1962, vol. 195, no. 4845, p. 984), is regarded as the best value presently available. Published dates in years BP can be converted to this basis by multiplying them by 1.03.

AD/BC Dates. In accordance with the decision of the Ninth International Radiocarbon Conference, Los Angeles and San Diego, California, 1976, the designation of AD/BC, obtained by subtracting AD 1950 from conventional BP determinations is discontinued in *RADIOCARBON*. Authors or submitters may include calendar estimates as a comment, and report these estimates as cal AD/BC, citing the specific calibration curve used to obtain the estimate. Calibrated dates will now be reported as "cal BP" or "cal AD/BC" according to the consensus of the Twelfth International Radiocarbon Conference, Trondheim, Norway, 1985.

Measuring of $\delta^{14}C$. In Volume 3, 1961, we endorsed the notation Δ (Lamont VIII, 1961) for geochemical measurements of ^{14}C activity, corrected for isotopic fractionation in samples and in the NBS oxalic-acid standard. The value of $\delta^{14}C$ that entered the calculation of Δ was defined by reference to Lamont VI, 1959, and was corrected for age. This fact has been lost sight of, by editors as well as by authors, and recent papers have used $\delta^{14}C$ as the observed deviation from the standard. At the New Zealand Radiocarbon Dating Conference it was recommended to use $\delta^{14}C$ only for age-corrected samples. Without an age correction, the value should then be reported as percent of modern relative to 0.95 NBS oxalic acid (Proceedings of the 8th Conference on Radiocarbon Dating, Wellington, New Zealand, 1972). The Ninth International Radiocarbon Conference, Los Angeles and San Diego, California, 1976, recommended that the reference standard, 0.95 NBS oxalic acid activity, be normalized to $\delta^{13}C = -19‰$.

In several fields, however, age corrections are not possible. $\delta^{14}C$ and Δ, uncorrected for age, have been used extensively in oceanography, and are an integral part of models and theories. For the present, therefore, we continue the editorial policy of using Δ notations for samples not corrected for age.

VOL. 34, NO. 2 **RADIOCARBON** 1992

CONTENTS